REGULATION OF INNATE IMMUNE RESPONSES AND FIBROSIS BY SERUM AMYLOID P

A Dissertation

by

NEHEMIAH COX

Submitted to the Office of Graduate and Professional Studies of
Texas A&M University
in partial fulfillment of the requirements for the degree of

DOCTOR OF PHILOSOPHY

Chair of Committee,	Richard H. Gomer
Committee Members,	David P. Barondeau
	James C. Hu
	Steve W. Lockless
Head of Department,	Thomas D. McKnight

May 2015

Major Subject: Biology

Copyright 2015 Nehemiah Cox

ABSTRACT

Fibrosis is caused by scar tissue formation in internal organs and is associated with 45% of deaths in the U.S. Pentraxins are a group of evolutionarily conserved proteins that have profound effects of the innate immune system and regulate the development of fibrosis. The pentraxin Serum Amyloid P (SAP) alleviates fibrosis in mice and two human clinical trials, whereas C-reactive protein (CRP) which resembles SAP exacerbates fibrosis. Surprisingly, these two pentraxins bind the same Fcγ receptors (FcγR) with similar affinities but have opposite effects. In this dissertation, I elucidate the role of FcγR in the regulation of the innate immune system by pentraxins. I find that although FcγR play a role in the regulation of immune cells by SAP, they are not necessary for SAP effects. SAP mainly uses the C-type lectin receptor DC-SIGN to alter immune responses and through its interaction with DC-SIGN SAP differentiates itself from CRP. I also found that a polycyclic aminothiazole DC-SIGN ligand and anti-DC-SIGN antibodies mimic the effects of SAP *in vitro*. In mice, the aminothiazole alleviates acute lung inflammation and pulmonary fibrosis. The aminothiazole alleviates pulmonary fibrosis by upregulating the anti-inflammatory cytokine IL-10 in lung epithelial cells. Together, these results suggest that SAP activates DC-SIGN to regulate the innate immune system differently from CRP, and that the aminothiazole and anti-DC-SIGN antibodies are potential therapeutics for fibrosis.

DEDICATION

I would like to dedicate this dissertation to my family and my imaginary friends who have supported me throughout my studies.

ACKNOWLEDGEMENTS

I would like to thank my committee chair, Dr. Gomer for his support, guidance, and patience throughout my graduate career. I also would like to thank my committee members, Dr. Barondeau, Dr. Hu, and Dr. Lockless for their advice and support throughout the course of this research.

I also want to extend my gratitude to Dr. Jeff Ravetch and Sjef Verbeek who provided us with different mouse strains. A huge thanks to my current and past undergraduates with their contributions to my work including Hannah Strake. Thanks also go to my friends and colleagues and the department faculty and staff for making my time at Texas A&M University a great experience. A special thanks to my former and current lab mates who make each day unique: Dr. Jeff Crawford, Dr. Anu Maharjan, Dr. Jonathan Phillips, Dr. Darrell Pilling, Patrick Suess, Rachel Sterling, Michael White, and Ivy Zheng.

NOMENCLATURE

CRP	C-reactive protein
CRP N32A	Glycosylated C-reactive protein
DC-SIGN	Dendritic Cell-Specific Intercellular adhesion molecule-3-Grabbing Non-integrin
FcγR	Fcγ receptors
FcRγ	Fcε common γ-chain
HEK293	Human embryonic kidney cells
IFN-γ	Interferon γ
IL-8	Interleukin 8
IL-10	Interleukin 10
iNOS	Inducible nitric oxide synthase
ITAM	Immunoreceptor tyrosine-based activation motif
NPTX1	Neuronal Pentraxin 1
NPTX2	Neuronal Pentraxin 2
NPTXR	Neuronal Pentraxin receptor
PBMC	Peripheral blood mononuclear cells
PTX3	Pentraxin 3
SAP	Serum Amyloid P
SAP-f	Alexa Fluor 647-labeled SAP
SAP (NA)	Desialylated SAP

TGF-β	Tumor growth factor β
TNF-α	Tumor Necrosis Factor α

TABLE OF CONTENTS

Page

ABSTRACT ii

DEDICATION iii

ACKNOWLEDGEMENTS iv

NOMENCLATURE v

TABLE OF CONTENTS vii

LIST OF FIGURES x

LIST OF SUPPLEMENTAL FIGURES xii

LIST OF TABLES xiii

CHAPTER I INTRODUCTION AND LITERATURE REVIEW 1

Regulation of neutrophil function by SAP 2
SAP binds to neutrophils to regulate their function 2
SAP inhibits neutrophil spreading 3
Indirect effects of SAP on neutrophils 4
SAP inhibits monocyte to fibrocyte differentiation 5
SAP binds to Fcγ receptors to inhibit fibrocyte differentiation 7
SAP regulates murine macrophage polarization 7
SAP affects macrophages in mouse models 9

CHAPTER II DISTINCT FCγ RECEPTORS MEDIATE THE EFFECT OF SERUM AMYLOID P ON NEUTROPHIL ADHESION AND FIBROCYTE DIFFERENTIATION 13

Summary 13
Introduction 14
Materials and methods 16
PBMC and neutrophil isolation, cell culture, fibrocyte and macrophage differentiation 16
SAP variant expression, purification, size exclusion chromatography, and labeling 17

Page

Neutrophil adhesion assay, macrophage phagocytosis assay, and SAP binding to Zymosan A 18
SAP affinity assays and receptor expression 19
Statistical analysis 20
Results 20
Identification of SAP amino acids that affect neutrophil adhesion 20
Identification of SAP amino acids that affect fibrocyte differentiation 24
Identification of SAP amino acids that affect phagocytosis 24
SAP binds to endogenous FcγRI and FcγRIIa on immune cells 27
SAP binds to FcγRI and FcγRIIa on HEK293 cells 29
FcγRIIa and FcγRIIIb ligation reduces neutrophil adhesion 35
Blocking FcγRI using antibodies abrogates SAP inhibition of fibrocyte differentiation 35
Identification of a novel Fcγ receptor binding site on SAP 38
Discussion 38

CHAPTER III DC-SIGN MEDIATES THE DIFFERENTIAL EFFECTS OF PENTRAXINS ON THE INNATE IMMUNE SYSTEM 45

Summary 45
Introduction 46
Methods 48
Antibodies and reagents 48
Mouse strains 49
Fibrocyte differentiation assay 49
Macrophage polarization assay 50
Recombinant protein expression 50
SDS-PAGE and Western blots 51
SAP desialylation 51
DC-SIGN binding 52
Neutrophil adhesion assay 52
Mouse models of acute lung inflammation and fibrosis 52
Immunohistochemistry and Immunofluorescence 53
PicroSirius red staining 53
Cell viability assay 53
Statistical analysis 54
Results 54
Fcγ receptors do not mediate many of SAP and CRP effects on the innate immune system 54
SAP glycosylation mediates many of the SAP effects on the innate immune system 55

Page

SAP but not CRP binds to DC-SIGN to regulate innate immune cells....58
Compound 1 reduces neutrophil accumulation in the lungs of bleomycin-treated mice....62
Compound 1 alleviates pulmonary fibrosis in mice....63
Interleukin 10 deficient mice are insensitive to the anti-inflammatory effect of compound 1....65
Lung conducting airway epithelial cells express SIGNR-R1 and IL-10....65
Discussion....67

CHAPTER IV CONCLUSIONS AND FUTURE DIRECTIONS....72

Conclusions....72
Future work....76

REFERENCES....79

APPENDIX I NaCl POTENTIATES HUMAN FIBROCYTE DIFFERENTIATION....104

Summary....104
Introduction....105
Materials and Methods....107
PBMC and Monocyte isolation, cell culture, and fibrocyte differentiation assay....107
Salt solutions and SAP purification....108
Immunohistochemistry....108
Adhesion Assay....109
PBMC/Monocyte pulse experiment....109
Adhesion molecules and flow cytometry....110
Statistical analysis....110
Results....111
Additional NaCl can potentiate fibrocyte formation without influencing cell viability....111
25 mM additional NaCl does not influence PBMC adhesion....113
Monocyte to fibrocyte differentiation is potentiated by additional NaCl....117
PBMCs and monocytes are influenced during their adhesion by additional NaCl 117
Sodium nitrate but not sodium gluconate potentiates fibrocyte differentiation....120
NaCl interferes with the ability of serum amyloid p to inhibit fibrocyte differentiation....124
Discussion....126

APPENDIX II SUPPLEMENTAL FIGURES....129

LIST OF FIGURES

Page

Figure 1: SAP inhibits neutrophil recruitment. 6

Figure 2: SAP inhibits fibrocyte formation. 8

Figure 3: SAP inhibits pro-fibrotic macrophages in mice. 12

Figure 4: Some SAP variants have an altered effect on neutrophil adhesion to human fibronectin. 23

Figure 5: Some SAP variants have an altered effect on human fibrocyte differentiation. 25

Figure 6: Amino acids Q128 and E153 on SAP are necessary for SAP-mediated phagocytosis. 26

Figure 7: Alexa Fluor 647-labeled SAP (SAP-f) binds to monocytes and neutrophils. 28

Figure 8: SAP variant binding to FcγRIIa and FcγRI. 31

Figure 9: Estimating the specific binding of WT SAP to FcγRI. 34

Figure 10: Ligating FcγRIIa and FcγRIIIb by antibodies decreases neutrophil adhesion. 36

Figure 11: FcγRI blocking antibodies reduce the effect of SAP on fibrocyte differentiation. 37

Figure 12: Identification of a novel Fcγ receptor binding site on SAP. 39

Figure 13: A model of the SAP effect on monocytes and neutrophils. 44

Figure 14: Fcγ receptors are necessary for some but not all effects of SAP and CRP on neutrophils, monocytes, and macrophages 56

Figure 15: SAP glycosylation regulates neutrophil adhesion, monocyte differentiation, and macrophage polarization 59

Figure 16: DC-SIGN activation affects neutrophils and monocyte-derived cells 61

Page

Figure 17: Compound 1 decreases neutrophil accumulation in the lungs of mice following bleomycin treatment. 64

Figure 18: Compound 1 alleviates pulmonary fibrosis in mice. 66

Figure 19: Interleukin-10 is necessary for the anti-fibrotic effect of compound 1. 68

Figure 20: Murine lung epithelial cells express SIGN-R1 and IL-10. 69

Figure 21: Addition of NaCl to Fibrolife or RPMI based-medium increases fibrocyte differentiation. 112

Figure 22: The elongated cells are fibrocytes. 114

Figure 23: The effect of NaCl on adherent cells after 5 days. 115

Figure 24: NaCl does not influence the adhesion of PBMCs to plastic, plasma fibronectin or collagen I. 116

Figure 25: NaCl directly potentiates the differentiation of monocytes into fibrocytes. 118

Figure 26: The presence of additional NaCl during PBMC adhesion increases fibrocyte differentiation. 119

Figure 27: The presence of additional NaCl during $CD14^+$ monocyte adhesion increases fibrocyte formation. 121

Figure 28: Incubation of PBMCs with additional NaCl does not influence the cell-surface levels of several adhesion molecules. 122

Figure 29: Sodium nitrate and potassium chloride potentiate fibrocyte differentiation. 123

Figure 30: NaCl interferes with the ability of hSAP to inhibit fibrocyte differentiation. 125

LIST OF SUPPLEMENTAL FIGURES

Page

Figure S 1: Identification of neutrophils, monocytes, and lymphocytes. 129

Figure S 2: Alexa Fluor 647-labeled SAP (SAP-f) has no detectable functional defects. 130

Figure S 3: The expression of Fcγ receptors on K562 cells and HEK293 cells. 131

Figure S 4: Fcγ receptors are not necessary for some PTX3 effects on neutrophils and macrophages. 132

Figure S 5: SAP binding to DC-SIGN^{+} HEK293 cells. 133

Figure S 6: SIGN-R1 is necessary for the effect of PTX3 on fibrocyte differentiation. 134

Figure S 7: The effect of anti-human DC-SIGN antibodies on fibrocyte differentiation and macrophage polarization. 135

Figure S 8: Compound 1 inhibits fibrocyte differentiation through SIGN-R1 without causing extensive cell death. 136

Figure S 9: Compound 1 inhibits neutrophil adhesion and fibrocyte differentiation and promotes M2 macrophages in absence of FcγR. 137

Figure S 10: The effect of compound 1 on mouse weights. 138

LIST OF TABLES

Page

Table 1: The effect of SAP variants on monocyte to fibrocyte differentiation. 22

Table 2: Binding of SAP variants to FcγRI and FcγRIIa. 32

CHAPTER I

INTRODUCTION AND LITERATURE REVIEW*

The mammalian immune system is organized into two arms: innate and adaptive immunity. Innate immunity is evolutionary more ancient and constitutes the first line of defense against foreign pathogens (1). In vertebrates, adaptive immunity complements innate immunity and provides immunological memory (2). Pathogen recognition molecules such as pentraxins are at the core of innate immunity (3, 4). Pentraxins recognize evolutionarily conserved pathogen molecules such as C-polysaccharide, regulate complement activation, and bind apoptotic cells, to initiate and synchronize the immune response (4-7).

Pentraxins are a family of conserved proteins that appeared early on during the evolution of innate immunity (8), and have a 200 amino acid long pentraxin domain with a conserved pentraxin signature (HxCxS/TWxS, where x stands for any amino acid) (9). Pentraxins are organized into two groups: the short and the long pentraxins. The short pentraxins are identified by their pentameric structure consisting of 25 kDa monomers and include C-reactive protein (CRP) and Serum Amyloid P (SAP) (for a review on CRP see (10)). The long pentraxins have a N-terminal domain attached to a pentraxin domain, and include PTX3, PTX4, guinea pig apexin, neuronal pentraxin 1 (NPTX1), NPTX2, and neuronal pentraxin receptor (NPTXR) (for reviews see (4, 9, 11, 12)).

---

* Reprinted with permission from *The Journal of Leukocyte Biology*. Cox, N., D. Pilling, and R. H. Gomer. Serum amyloid P: a systemic regulator of the innate immune response. *J Leukoc Biol.* 2014. Epub 2014/05/09. doi: 10.1189/jlb.1MR0114-068R. Copyright © 2009 The Journal of Leukocyte Biology.

The short pentraxins CRP and SAP are pattern recognition molecules secreted by the liver that interact with pathogens and cell debris to promote their removal by macrophages and neutrophils (13). SAP binds to rough lipopolysaccharide, and lack of SAP causes hypersensitivity to laboratory strains of *E. coli* (14). In addition, CRP and SAP interact with components of the complement pathway to regulate complement activation (15, 16). However, the regulation of the innate immune system by SAP is not limited to its effects on the complement pathway and phagocytosis. SAP directly binds to monocytes, neutrophils, and macrophages to modify their activation and alter their differentiation to modulate the immune response.

Regulation of neutrophil function by SAP

At the onset of inflammation, neutrophils are recruited to the damaged tissue where they release reactive oxygen species and promote clearance of pathogens and cell debris. This recruitment is mediated by cytokines, tissue damage, complement activation, and changes in adhesion receptors on the surface of endothelial cells (17-19). The migration and activation of neutrophils is tightly regulated by factors expressed and secreted by endothelial cells and macrophages (17). However, factors present in plasma also affect neutrophils (17).

SAP binds to neutrophils to regulate their function

One circulating factor that regulates neutrophil accumulation in tissues is SAP (20). SAP binds to human and murine neutrophils and decreases TNF-α and IL-8-

induced neutrophil binding to extracellular matrix components (20, 21). SAP also reduces TNF-α induced human neutrophil adhesion to endothelial cells (22). One possible mechanism underlying the effect of SAP on neutrophils involves SAP binding to, and thus potentially blocking, the adhesion receptor L-selectin on neutrophils (22). This is supported by the observation that adding anti-L-selectin antibodies to human neutrophils decreases their binding to umbilical vein endothelial cells (22) A second possible mechanism involves SAP binding to Fcγ receptors (FcγR) on neutrophils (23-25). Fcγ receptors are best known for binding IgG, and in humans include the activating receptors FcγRI, FcγRIIa, FcγRIIIa, FcγRIIIb, and the inhibitory receptor FcγRIIb (26, 27). FcγRIIa and FcγRIIIb are expressed at high levels on human neutrophils, and activation of FcγRIIa by SAP results in the phosphorylation of the immunoreceptor tyrosine-based activation motif (ITAM) in the cytosolic region of FcγRIIa (28). ITAM activation can then lead to conformational changes in adhesion receptors on neutrophils via inside-out signaling (29). Much remains to be investigated about the effects of SAP on neutrophils, and most likely this effect involves a variety of receptors including Fcγ receptors and L-selectin.

SAP inhibits neutrophil spreading

In addition to decreasing neutrophil adhesion, SAP also decreases human neutrophil spreading, a necessary step for cell polarization and migration (20, 30-33). Paradoxically, SAP does not influence human neutrophil migration in response to fMLP in a Boyden chamber (20). This inconsistency may be due to the differences in the

adhesion receptors used during neutrophil migration on matrix proteins and after stimulation with chemotactic stimuli in a Boyden chamber. On fibronectin, neutrophils use the β1 (VLA-4 and VLA-5) integrins to migrate, whereas in an uncoated Boyden chamber, β2 (CD11b/CD18) integrins are the key adhesion receptors (34, 35). SAP may act as a chemoattractant of human neutrophils, although this finding has not been replicated (21). Alternatively, it is possible that the timing of stimuli (i.e. SAP) could determine how neutrophil spreading and migration is influenced.

Indirect effects of SAP on neutrophils

Neutrophils secrete proteases such as elastase to degrade the extracellular matrix and facilitate tissue infiltration (for a review see (36)). SAP but not CRP binds to neutrophil elastase and inhibits its enzymatic activity (37). This can hinder neutrophil extravasation and the secondary damage caused by the proteolytic activity of elastase in tissues (36-40). SAP also induces macrophages to produce the anti-inflammatory cytokine interleukin (IL)-10, which in turn decreases TNF-α and CXCL8 (IL-8) production. This then results in decreased neutrophil recruitment (23, 41-43). These observations suggest that SAP regulates many aspects of neutrophil biology to exert an anti-inflammatory effect, and set a threshold for neutrophil recruitment and activation (Fig. 1). In agreement with this, we have observed that SAP injections can decrease neutrophil accumulation in a mouse model of acute respiratory distress syndrome (20).

SAP inhibits monocyte to fibrocyte differentiation

Monocytes present within the blood are attracted to sites of injury where they differentiate into macrophages, dendritic cells, or fibrocytes (44, 45). Fibrocytes are spindle-shaped fibroblast-like cells, and at least in part, mediate tissue repair and fibrosis (for a review see (45)). Fibrocytes have been detected in human pathological conditions including pulmonary fibrosis, keloid scars, asthma, chronic kidney disease, and nephrogenic systemic fibrosis (45-49). In addition to contributing to the mass of fibrotic lesions, fibrocytes promote angiogenesis, which can then promote the growth of the lesion, and secrete TGF-β, which activates resident fibroblasts (50). Fibrocyte differentiation is regulated by several factors including cytokines, toll like receptor ligands, semaphorins, and hyaluronic acid (45, 51-53). We found that when human, mouse, or rat peripheral blood mononuclear cells (PBMCs) were cultured in serum-free media, some of the cells became fibrocytes after 3-5 days (54). The fibrocytes did not appear during this timeframe when serum was present (54). We purified the fibrocyte differentiation inhibitor from human serum and identified it as SAP (54). When PBMCs were cultured in serum that was depleted of SAP, fibrocytes rapidly appeared, indicating that SAP is the main endogenous inhibitor of fibrocyte differentiation in the blood. In agreement with this, we observed that depleting SAP from dermal wounds in pigs can facilitate fibrocyte differentiation and scar tissue formation (55). We also tested whether SAP could inhibit fibrocyte differentiation and fibrosis in bleomycin-induced lung fibrosis (56). We found that SAP injections led to reduced numbers of fibrocytes in the

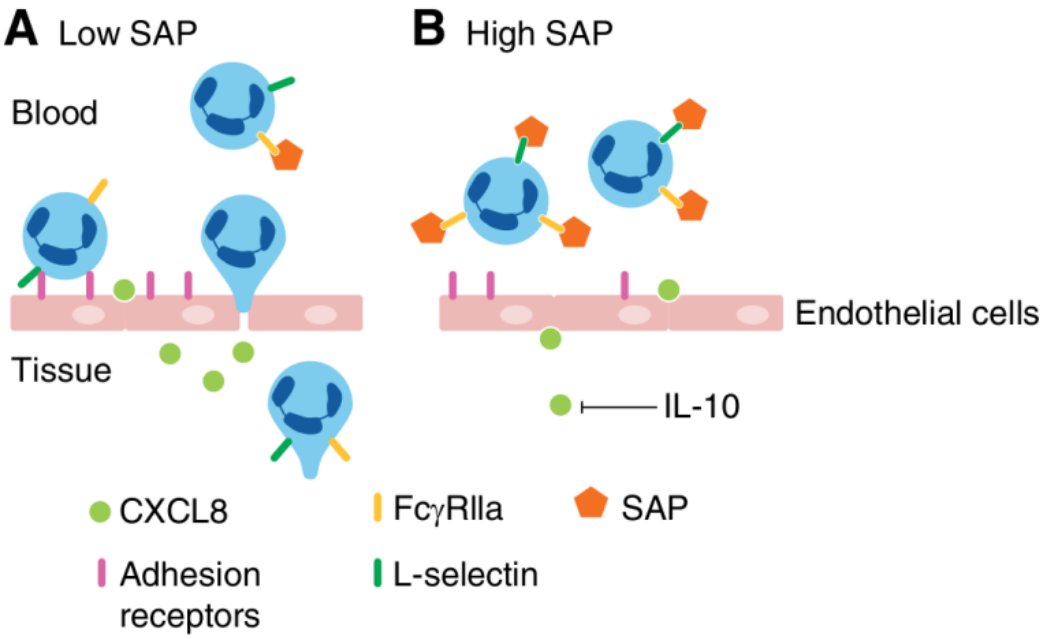

Figure 1: SAP inhibits neutrophil recruitment.
A) In response to chemoattractants such as CXCL8, neutrophils begin to migrate into the tissue in a process that involves neutrophil rolling, arrest, and extravasation. All these steps are mediated by adhesion receptors on the endothelial cells and on neutrophils. **B**) In the presence of high levels of SAP, neutrophil recruitment to the tissue is reduced as SAP-induced IL-10 inhibits the secretion of CXCL8. SAP also reduces neutrophil adhesion by preventing L-selectin binding to adhesion receptors on endothelial cells. SAP may further affect neutrophil adhesion by regulating adhesion receptors on neutrophils by inside-out signaling via Fcγ receptors. In addition, SAP reduces neutrophil migration by inhibiting neutrophil spreading and elastase activity.

lungs and reduced fibrosis in rats and mice, and that delaying SAP injections until inflammation and fibrosis was already apparent could also reduce symptoms (56).

SAP binds to Fcγ receptors to inhibit fibrocyte differentiation

SAP inhibits fibrocyte differentiation in part by binding to Fcγ receptors (57). In support of this, we have found that cross-linked but not monomeric IgG inhibits fibrocyte differentiation, and that blocking the signal transduction pathway of the Fcγ receptors with pharmacological inhibitors blocks the ability of both SAP and cross-linked IgG to inhibit fibrocyte differentiation (58). In mice, deletion of the Fcε common γ-chain (FcRγ), which is necessary for FcγRI and FcγRIIIa signaling, significantly reduces sensitivity to SAP (23, 57, 59). However, deletions of FcγRIIb, FcγRIII, and FcγRIV do not affect sensitivity to SAP (57). We found similar results using siRNA knockdowns of human receptors (57). However, in all these conditions, SAP still caused some inhibition of fibrocyte differentiation (23, 57), indicating the presence of unknown SAP receptors on monocytes. These observations suggest that SAP in part uses FcγRI and FcRγ to inhibit fibrocyte differentiation (Fig. 2).

SAP regulates murine macrophage polarization

Macrophages are considered one of the most important innate effector cells (for reviews see (60-62)). Macrophages can be classified into the classically activated

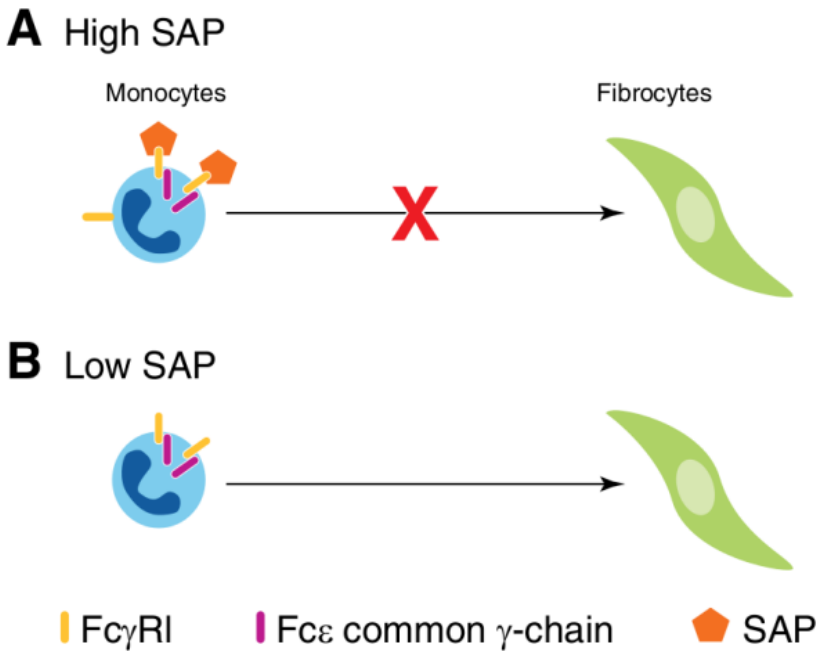

Figure 2: SAP inhibits fibrocyte formation.
A) When SAP is present in the tissue, as is the case in early inflammation, SAP binds to FcγRI to inhibit fibrocyte differentiation. Deletion of the FcγRI or the Fcε common γ-chain significantly reduces the inhibitory effect of SAP. **B**) At late stages of inflammation when SAP levels are low, monocytes differentiate into fibroblast-like cells called fibrocytes. Fibrocytes then secrete extracellular matrix components such as collagen and extracellular modifying enzymes to restore the architecture of the damaged tissue.

macrophages (M1) and the alternatively activated macrophages (M2) (60, 63). M1 macrophages are induced in response to TNF-α, IFN-γ, and specific Toll-like receptor. M2 is a general term for several overlapping macrophage subsets which are induced in response to IL-4, IL-10, IL-13, and SAP (23, 60, 64).The role of M2 macrophages in the agonists (60, 64). The classically activated M1 macrophages modulate host defense against intracellular pathogens, tumor cells, and tissue debris, but are also responsible for tissue damage associated with their release of reactive oxygen species (60, 63, 65-67). immune system is highly dependent on the activating stimuli (i.e. IL-10 vs IL-4) and the environmental context. The alternatively activated M2 macrophages can be classified into three main groups: immuno-regulatory macrophages, pro-fibrotic/wound-healing macrophages, and tumor associated macrophages (60, 63, 68, 69). The hallmark of immuno-regulatory macrophages in both humans and mice is high levels of the anti-inflammatory cytokine IL-10 and low levels of the pro-inflammatory cytokine IL-12 (60). Wound-healing macrophages express high levels of IL-10 and IL-12, whereas tumor associated macrophages are identified by their secretion of angiogenic factors (60, 68).

SAP affects macrophages in mouse models

In a mouse model of systemic lupus erythematosus, macrophages in the kidneys have elevated expression of IL-10, iNOS, and TNF-α (64). IL-10 is a marker for M2 macrophages, whereas iNOS and TNF-α are typically associated with M1 macrophages (60, 64). When the mice were injected with SAP, the expression of the M2 markers IL-

10 and arginase 1 in the kidney macrophages was increased, while the levels of the M1 markers iNOS and TNF-α decreased (64). This change in gene expression involved the phosphatidylinositol 3-Kinase/Akt–ERK signaling pathway, and indicates a shift towards an immuno-regulatory phenotype in macrophages (64).

In mouse models of renal fibrosis, SAP injections decreased expression of the M1 markers Mip2a and IL-1β, and the pro-fibrotic M2 markers CCL17 and CCL22 on renal macrophages (23, 60). These changes were accompanied by a significant increase in the levels of IL-10 (23). In IL-10 and FcRγ knockout mice, the effects of SAP on renal fibrosis was reduced (23). Together, these observations suggest that SAP in two different models of renal injuries polarizes macrophages toward an immuno-regulatory phenotype.

In TGF-β-driven mouse models of pulmonary fibrosis, SAP alleviates fibrosis in part through its effect on macrophages (70, 71). In this model of pulmonary fibrosis, SAP injections decreased M2 markers while increasing the M1 marker CXCL10 on pulmonary macrophages (60, 70). This is in stark contrast to the role of SAP in renal injuries, where it promotes immuno-regulatory macrophages and decreases M1 macrophages. This inconsistency may be attributed to differences that exist in the milieu of kidneys and lungs. In support of this, similar to TGF-β driven pulmonary fibrosis, SAP attenuated M2 macrophage activation in the spore-induced allergic airway disease of mice (60, 72). Furthermore, in spore-induced allergic airway disease, SAP injections increased expression of the M1 marker IFN-γ in lung macrophages while not significantly altering levels of the immuno-regulatory marker IL-10 (72). Together, these

observations suggest that SAP has a significant role in regulating macrophage polarization, but the outcome is tissue dependent (Fig. 3).

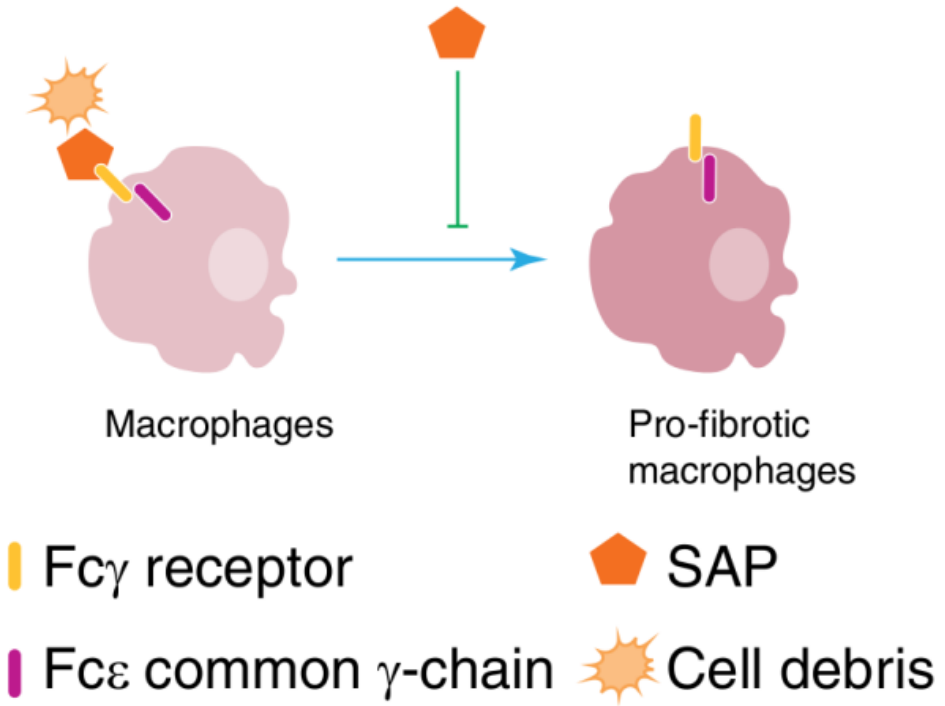

Figure 3: SAP inhibits pro-fibrotic macrophages in mice.
SAP attenuates pro-fibrotic macrophages in renal and pulmonary injuries of mice in an FcRγ-mediated manner. SAP also opsonizes cell debris to promote their removal by macrophages.

CHAPTER II

DISTINCT FCγ RECEPTORS MEDIATE THE EFFECT OF SERUM AMYLOID P ON NEUTROPHIL ADHESION AND FIBROCYTE DIFFERENTIATION*

Summary

The plasma protein Serum Amyloid P (SAP) reduces neutrophil adhesion, inhibits the differentiation of monocytes into fibroblast-like cells called fibrocytes, and promotes phagocytosis of cell debris by macrophages. Together, these effects of SAP reduce key aspects of inflammation and fibrosis, and SAP injections improve lung function in pulmonary fibrosis patients. SAP functions are mediated in part by Fcγ receptors, but the contribution of each Fcγ receptor is not fully understood. We found that amino acids Q55 and E126 in human SAP affect human fibrocyte differentiation and SAP binding to FcγRI. E126, K130, and Q128 affect neutrophil adhesion and SAP affinity for FcγRIIa. Q128 also affects phagocytosis by macrophages and SAP affinity for FcγRI. All the identified functionally significant amino acids in SAP form a binding site that is distinct from the previously described SAP-FcγRIIa binding site. Blocking FcγRI with an IgG blocking antibody reduces the SAP effect on fibrocyte differentiation, and ligating FcγRIIa with antibodies reduces neutrophil adhesion. Together, these results

---

* Reprinted with permission from *The Journal of Immunology*. Cox, N., D. Pilling, and R. H. Gomer. Distinct fcgamma receptors mediate the effect of serum amyloid p on neutrophil adhesion and fibrocyte differentiation. *J Immunol.* 2014;193(4):1701-8.

Copyright © 2013 The American Association of Immunologists, Inc. http://www.jimmunol.org/

suggest that SAP binds to FcγRI on monocytes to inhibit fibrocyte differentiation, and binds to FcγRIIa on neutrophils to reduce neutrophil adhesion.

Introduction

Aberrant scar tissue formation is the hallmark of fibrosing diseases such as end-stage kidney disease, liver cirrhosis, pulmonary fibrosis, and congestive heart disease (45, 73, 74). The inappropriate scar tissue in fibrosis ultimately leads to organ failure and/or death. Fibrosing diseases are associated with 45% of deaths in the US (73, 75).

Serum Amyloid P component (SAP) is a pentameric protein that belongs to the pentraxin family of evolutionarily conserved proteins. Pentraxins also include C-reactive protein (CRP) and the long pentraxin PTX3 (11). SAP, CRP, and PTX3 all have regulatory roles in the immune system (4, 9, 76). Injections of SAP inhibit inflammation and fibrosis in mouse models of pulmonary fibrosis, ischemic cardiac fibrosis, and renal fibrosis (20, 23, 56, 77), and in a phase 1b clinical trial, SAP injections appear to improve lung function in pulmonary fibrosis patients (78).

At the onset of tissue damage and inflammation, neutrophils are recruited to the tissue in response to chemokines such as CXCL2 and CXCL8 (IL-8) to remove pathogens and/or cell debris via phagocytosis (17). This migration and activation of neutrophils is tightly regulated by factors expressed and secreted by endothelial cells, macrophages and other cell types (17). When this regulation is compromised, the elevated influx of neutrophils and recruitment of other immune cells by activated neutrophils can cause severe organ damage and fibrosis (17, 40, 79). SAP binds

neutrophils to inhibit their spreading and adhesion to components of extracellular matrix and endothelial cells (20, 80). Injections of SAP decrease the infiltration of neutrophils into the lungs following bleomycin insult in mice (20). However, the mechanism for this function is not well understood.

Following neutrophil migration into the inflammation site, $CD14^+$ monocytes enter and differentiate into macrophages and fibrocytes (45). Fibrocytes are $CD45^+$ collagen I^+ fibroblast-like cells that share characteristics of both hematopoietic and stromal cells (81). Fibrocytes are found in healing dermal wounds and some fibrotic lesions, and secrete collagen and enzymes which modify the extracellular matrix (45, 55, 56, 77, 82). SAP inhibits fibrocyte differentiation partly through a group of receptors called Fcγ receptors (23, 25, 57, 59, 83). These receptors bind IgG and consist of FcγRI, FcγRIIa, FcγRIIb, FcγRIIIa, and FcγRIIIb (84). We have previously shown that FcγRI is one of the receptors responsible for the effect of SAP on fibrocyte differentiation in both humans and mice (57). SAP also binds the IgA receptor FcαRI (85).

In addition to modifying neutrophil adhesion and monocyte differentiation, SAP can also enhance phagocytosis of cell debris by professional phagocytes such as macrophages (24, 25). The SAP pentamer forms a flat disk, and binds to bacteria and cell debris on one surface, and to Fcγ receptors on the other surface, to promote phagocytosis by cells (25). Previous studies have implicated FcγRI as the key receptor for SAP-induced phagocytosis, but the precise role of each Fcγ receptor in this process is unclear (24, 25).

In this report, we examined how SAP interacts with Fcγ receptors to regulate different aspects of the immune system. We found that SAP inhibits fibrocyte differentiation and promotes phagocytosis by macrophages through FcγRI, while it reduces neutrophil adhesion via FcγRIIa. Using site-directed mutagenesis we determined that although the same site on SAP affects monocytes, macrophages, and neutrophils, it is possible to affect specific SAP functions without altering the other functions in an appreciable way. In addition, we identified a novel Fcγ receptor binding site that is distinct from the site previously identified in a co-crystal structure of SAP and FcγRIIa (83).

Materials and methods

PBMC and neutrophil isolation, cell culture, fibrocyte and macrophage differentiation

Human peripheral blood was collected into heparin tubes (BD Bioscience, San Jose, CA) from healthy adult volunteers who gave written consent and with specific approval from the Texas A&M University human subjects Institutional Review Board. Peripheral blood mononuclear cells (PBMC) were isolated from the blood using Ficoll-Paque Plus (GE Healthcare Biosciences, Piscataway, NJ), as described previously (86). PBMCs were cultured in Fibrolife (LifeLine Cell Technology, Walkersville, MD) defined serum-free medium (SFM) in the presence or absence of SAP variants as previously described (57). To determine the contribution of each Fcγ receptor to the SAP effect on fibrocyte differentiation, we incubated PBMCs with 5 μg/ml of $F(ab')_2$ fragments of either anti-FcγRI antibody clone 10.1 (mouse IgG1, Ancell, Bayport, MN), anti-FcγRII antibody clone 7.3 (mouse IgG1, Ancell), anti-FcγRIII antibody clone 3G8

(mouse IgG1, Ancell), or a mouse IgG1 isotype control (Ancell) in the presence and absence of SAP. Fibrocytes were identified and counted based on their elongated spindle-shaped morphology in five different 900 μm-diameter fields of view per well (86-88). PBMCs were incubated overnight in RPMI-1640 (Lonza, Allendale, NJ) with 10% fetal bovine serum (Caisson Laboratories, North Logan, UT) to generate macrophages, as described previously (25). Neutrophils were isolated from blood using Lympholyte-poly (Cedarlane Laboratories, Hornby, BC, Canada) following the manufacturer's protocol and resuspended in 2% BSA (fraction V, A3059; Sigma-Aldrich) in RPMI-1640 (20, 89). HEK293 cells (Life Technologies, Grand Island, NY) were cultured in Freestyle (Life Technologies) medium following the manufacturer's protocol. K562 cells (ATCC, Manassas, VA) were grown in RPMI-1640 with 10% fetal bovine serum (Caisson).

SAP variant expression, purification, size exclusion chromatography, and labeling

Starting with the previously described SAP expression vector (57), SAP variants were generated with a QuickChange II Site-Directed Mutagenesis Kit (Agilent Technologies, Santa Clara, CA) following the manufacturer's protocol, and the DNA sequences of the constructs were verified. SAP variants were expressed in HEK293 cells as described previously and then purified by affinity purification (57). Briefly, cell supernatants from the SAP-expressing HEK293 cells were clarified by centrifugation at 300 x g. 1 M $CaCl_2$ was added to the supernatant to a final concentration of 2 mM, and the cell supernatant was then mixed with 1 ml of a 50% slurry of Sepharose Fast Flow

(GE Healthcare BioSciences, Piscataway, NJ, USA) in 20 mM Tris, 140 mM NaCl, 2 mM $CaCl_2$, pH 7.4 for 1 h. The Sepharose beads were collected and washed 3 times with 15 ml wash buffer (20 mM Tris, 300 mM NaCl, 2 mM $CaCl_2$, pH 7.4). Bound protein was eluted overnight at 4°C with 20 mM Tris, 140 mM NaCl, 50 mM EDTA, pH 7.4. The eluted protein was then buffer exchanged into 20 mM sodium phosphate buffer pH 7.4 (57). The purified SAP was assayed by size exclusion chromatography using a Superose 12 (GE Healthcare Life Sciences, Piscataway, NJ) column on an AKTA chromatography system (GE Healthcare Life Sciences) as previously described (57). Purified SAP was labeled using Alexa Fluor 647-NHS (Life Technologies) following the manufacturer's protocol.

Neutrophil adhesion assay, macrophage phagocytosis assay, and SAP binding to Zymosan A

Neutrophils were incubated with 80 nM (10 μg/ml) of wildtype (WT) or mutated SAP, and their binding to human plasma fibronectin (Trevigen, Gaithersburg, MD) was assessed as previously described (20). To determine the effect of Fcγ receptor ligation on neutrophil adhesion, neutrophils were incubated with 5 μg/ml of either anti-FcγRI antibody clone 10.1 (mouse IgG1, eBiosciences), anti-FcγRII antibody clone Clkm-5 (mouse IgG1, Millipore, Billerica, MA), anti-FcγRII antibody clone FUN-2 (mouse IgG1, Biolegend), anti-FcγRII antibody clone AT10 (mouse IgG1, Abcam, Cambridge, MA), anti-FcγRIII antibody clone 3G8 (mouse IgG1, Biolegend), or a mouse IgG1 isotype control (Biolegend). Phagocytosis of FITC-conjugated Zymosan A bio-particles

(Life Technologies) by macrophages was assayed as described previously (25). To measure the binding of SAP to Zymosan A bio-particles, we first quenched the fluorescence of FITC-conjugated Zymosan A with 2% Trypan blue in PBS for 20 minutes and then incubated the quenched Zymosan A bio-particles with 240 nM (30 μg/ml) of WT SAP or mutant SAP in 20 mM Tris, 140 mM NaCl, 2 mM $CaCl_2$ for 1 hour. The bio-particles were then washed, and bound SAP was detected by staining with anti-SAP antibody clone 5.4A (Millipore) and goat anti-mouse Alexa Fluor-647 (Life Technologies) on an Accuri C6 flow cytometer (BD Bioscience).

SAP affinity assays and receptor expression

FcγRI and Fcε common γ-chain (FcRγ) cDNA (PSI:Biology-materials repository, Tempe, AZ) (90, 91) were ligated into the pCMV6-AC-His vector (OriGene, Rockville, MD) and then transfected into HEK293 cells using jetPRIME (Polyplus, New York, NY) following the manufacturer's protocol. FcγRIIIb plasmid was obtained from the PSI:Biology-materials repository and transfected into HEK293 cells. K562 cells, which express FcγRIIa, were used to measure the affinity of SAP for FcγRIIa (92). The binding of fluorescently labeled WT SAP or mutant SAP to cells was then measured as previously described using an Accuri C6 flow cytometer (25). When measuring SAP binding to HEK293 cells expressing FcγRI or FcγRIIIb, mock transfected HEK293 cells were used to estimate the non-specific binding. K562, HEK293, $FcγRI^+$ HEK293, and $FcγRIIa^+$ HEK293 cells were stained for FcγRI (Cone 10.1, eBiosciences), FcγRII (Clone FUN-2, Biolegend), and FcγRIII (Clone 3G8, Biolegend) to determine the

expression of the indicated receptor by flow cytometry (87). Leukocytes stained for CD3 (Biolegend), CD14 (Biolegend), CD15 (Biolegend), CD19 (Biolegend), CD45 (Biolegend), FcγRI (Clone 10.1, eBiosciences), FcγRII (Clone FUN-2, Biolegend), and FcγRIII (Clone 3G8, Biolegend) were assayed by flow cytometry to determine the presence of different immune cell populations as previously described (87, 88, 93).

Statistical analysis

Data was analyzed by ANOVA (with Dunnett's post test) or t-test when appropriate using Prism software (GraphPad software, San Diego, CA). Data were fit to the appropriate model of binding as determined by F-tests. Normality was tested using Shapiro-Wilk and D'Agostino-Pearson omnibus tests when applicable.

Results

Identification of SAP amino acids that affect neutrophil adhesion

We previously made site-directed mutations of human SAP at amino acids that interact with human FcγRIIa in a SAP-FcγRIIa co-crystal structure (83), and observed that changes to these amino acids had no significant effect on the ability of SAP to inhibit fibrocyte differentiation (57). To better understand the interaction of SAP with Fcγ receptors, we compared the amino acid sequence of human SAP to the related pentraxin CRP. SAP and CRP have 51% sequence identity and similar crystal structures, but have different affinities for Fcγ receptors and different roles in the immune system (4, 23, 24, 83). Thus, the sequence differences can be used to identify structurally and

functionally significant amino acids. Of the amino acids that were different between SAP and CRP, we mutated only the ones that were exposed on the surface of SAP (83). E153, which is at the interface between SAP monomers, was also mutated in an attempt to destabilize the pentameric protein and introduce functional defects. We then expressed all the generated SAP variants in HEK293 cells. All the SAP variants eluted at 10-12 ml from a Superose 12 size exclusion chromatography column, indicating the absence of aggregates larger than pentamers, and the absence of free monomers (Table 1 and Fig. 4A). We subsequently tested the ability of these variants to decrease neutrophil adhesion, inhibit fibrocyte differentiation, and promote phagocytosis. In addition, we examined the binding of these variants to Fcγ receptors.

We first examined the ability of our SAP variants to reduce neutrophil adhesion to human fibronectin. We screened 29 SAP variants for their ability to reduce neutrophil adhesion and then based on our preliminary data focused on 13 of the examined variants (data not shown). These 13 SAP variants were screened at 80 nM (10μg/mL) (Fig. 4B). We chose this concentration because it was close to the IC_{50} (67 ± 7 nM) of SAP for reducing neutrophil adhesion (Fig. 4C) and hence allowed us to detect both increases and decreases in the SAP effect on neutrophils. Following our screen, we observed that SAP variants E126A and Q128A had increased inhibitory effect on neutrophil adhesion compared to WT SAP (Fig. 4B). SAP variant K130V conversely had a significantly reduced inhibitory effect on neutrophil adhesion (Fig. 4B).

SAP Variants	Multimerization state	Hill Coefficient	IC_{50} (nM ± SEM)
WT SAP	Pentameric	1.8 ± 0.1	2.9 ± 0. 3
H19A	Pentameric	1.8 ± 0.1	1.1 ± 0.1
N21A	Pentameric	2.2 ± 0.2	2.5 ± 0.5
I23G	Pentameric	0.9 ± 0.1	1.2 ± 0.7
T24A	Pentameric	2.6 ± 1.2	5.3 ± 1.7
E27A	Pentameric	0.7 ± 0.1	1.6 ± 0.8
Q31A	Pentameric	1.9 ± 0.2	2.9 ± 1.1
Q55A	Pentameric	1.1 ± 0.2	1.5 ± 0.5 *
G56A	Pentameric	2.1 ± 0.1	4.4 ± 2.8
V68A	Pentameric	3.8 ± 1.4 *	2.8 ± 0.5
K87A	Pentameric	1.7 ± 0.7	1.6 ± 0.8
S101A	Pentameric	0.8 ± 0.5	5.4 ± 0.2
E126A	Pentameric	0.8 ± 0.1	8.1 ± 1.0 *
Q128A	Pentameric	2.7 ± 0.3 *	2.5 ± 0.6
P129A	Pentameric	1.4 ± 0.4	2.9 ± 0.8
K130V	Pentameric	1.6 ± 0.2	1.1 ± 0.2 *
Y140A	Pentameric	3.1 ± 1.1	4.3 ± 1.3
K143A	Pentameric	16.4 ± 10.3	2.7 ± 1.1
R146A	Pentameric	1.1 ± 0.5	5.4 ± 1.4
E153A	Pentameric	3.3 ± 1.5	19.2 ± 5.7 *
P165A	Pentameric	1.1 ± 0.4	4.4 ± 0.3
S171A	Pentameric	1.5 ± 0.3	2.9 ± 0.5
Y173A	Pentameric	2.4 ± 0.2	4.9 ± 1.1
Q174A	Pentameric	1.3 ± 0.1	6.9 ± 1.2
N189A	Pentameric	1.9 ± 0.7	3.3 ± 0.2
R193A	Pentameric	3.3 ± 1.6	1.8 ± 0.9
I23A-Q55A	Pentameric	1.1 ± 0.1	1.9 ± 0.5
I23A-K130V	Pentameric	0.7 ± 0.4	13.6 ± 7.4
Q55A-K130V	Pentameric	3.3 ± 2.5	4.7 ± 3.2
I23A-Q55A-K130V	Pentameric	1.2 ± 0.3	6.6 ± 2.1

Table 1: The effect of SAP variants on monocyte to fibrocyte differentiation. PBMCs were incubated with different concentrations of the indicated SAP variant as shown in Figure 2. After 5 days, the cells were stained and the fibrocyte counts for each SAP variant were used to estimate the IC_{50} and the Hill coefficient for inhibition of fibrocyte differentiation. Pentamerization was assessed using a Superose 12 size exclusion chromatography column. The SAP variants were considered pentameric if they eluted at 10-12 ml. Values are IC_{50} or Hill coefficient ± SEM, n=3-10. The data for SAP variants S171A, Y173A, and Q174A were taken from (21). * indicates $p < 0.05$ by t-test when compared to the wildtype (WT) SAP.

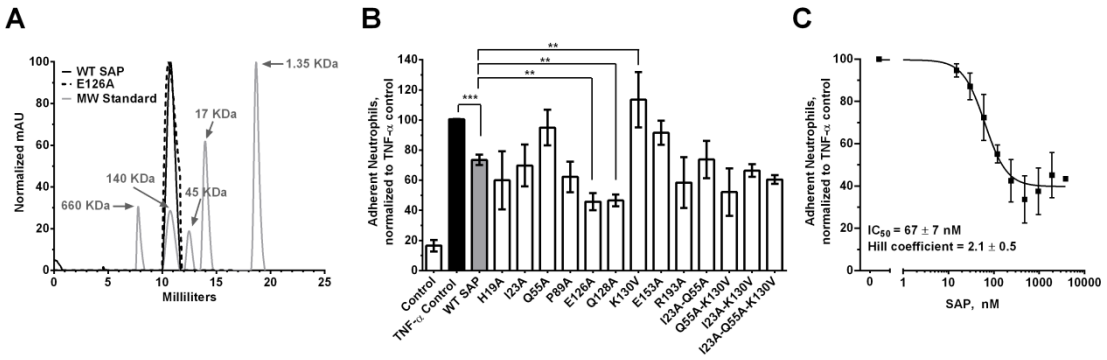

Figure 4: Some SAP variants have an altered effect on neutrophil adhesion to human fibronectin.

A) A representative plot indicating that both WT SAP and K87A variant are pentameric. **B**) Human neutrophils were incubated with 80 nM (10 μg/ml) of the indicated SAP variants. Following the initial incubation with SAP, the neutrophils were transferred to a fibronectin coated plate and were then activated by the addition of TNF-α. After 30 minutes, the non-adherent neutrophils were removed and the remaining cells were stained and counted. **C**) Human neutrophils were incubated with increasing concentrations of WT SAP to estimate the IC_{50} of SAP for reducing neutrophil adhesion. The data were fit to a sigmoidal dose response curve with variable Hill coefficient. Values are adherent neutrophils normalized to the TNF-α control ± SEM, n=3-7. ** represents $p<0.01$ and *** represents <0.001 by t-test.

Identification of SAP amino acids that affect fibrocyte differentiation

Since SAP inhibits fibrocyte differentiation, we also screened the 29 SAP variants for their ability to inhibit the differentiation of monocytes into fibrocytes (Table 1) (54, 57, 86, 87). Using PBMCs from a variety of donors, we observed 1200 to 3100 fibrocytes per 10^5 PBMCs. Because of this variability, fibrocyte counts were normalized to the no-SAP control, as described previously (57, 86, 94). WT SAP inhibited fibrocyte differentiation with an IC_{50} of 2.9 ± 0.3 nM, similar to previously published data (54, 57). 25 out of the 29 variants tested did not significantly alter the ability of SAP to inhibit fibrocyte differentiation (Table 1). Compared to wildtype SAP, variants Q55A and K130V were more effective at inhibiting fibrocyte differentiation whereas variants E153A and E126A had reduced activity (Fig. 5 and Table 1). In addition, we observed significant changes in the Hill coefficient of SAP variants V68A and Q128A compared to WT SAP (Table 1). This change could be due to alterations in SAP variant binding to Fcγ receptors and/or how these variants activate the receptors.

Identification of SAP amino acids that affect phagocytosis

SAP enhances phagocytosis of pathogens and cell debris through Fcγ receptors (24, 25). However, the exact receptor and amino acids involved are unknown. We first screened the 29 SAP variants for their ability to enhance phagocytosis and then based on our preliminary data focused on 13 variants (data not shown). The 13 SAP variants were screened at 240 nM (30μg/mL, physiological concentration in the human plasma) for

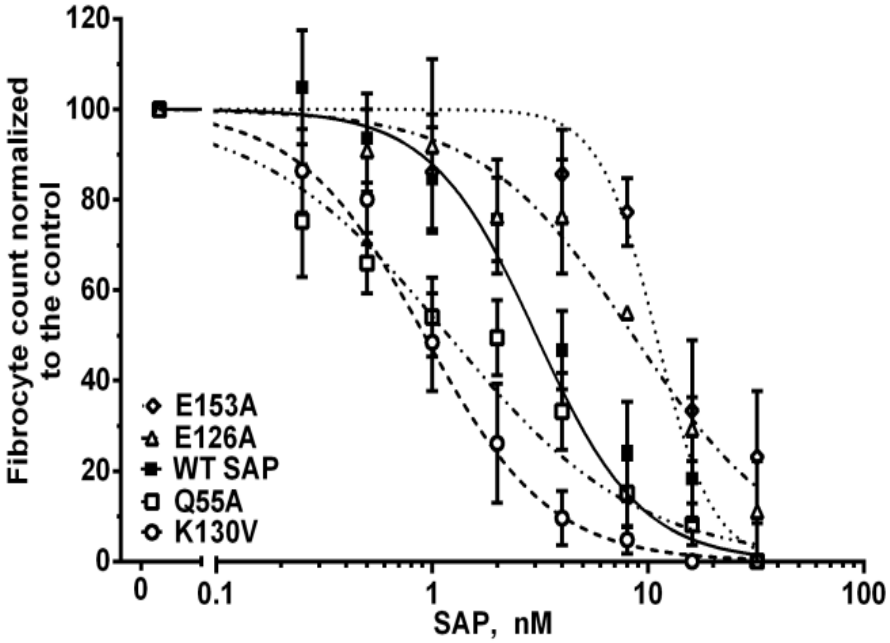

Figure 5: Some SAP variants have an altered effect on human fibrocyte differentiation.

PBMCs were incubated for 5 days in the presence of WT SAP or SAP variants. Compared to WT SAP, the SAP variants K130V and Q55A were more effective inhibitors of fibrocyte differentiation, whereas E126A and E153A had reduced activity. Values are fibrocyte count normalized to the no-SAP control ± SEM, n=3-5. The data were fit to sigmoidal dose response curves with variable Hill coefficients. The absence of error bars indicates that the error was smaller than the plot symbol.

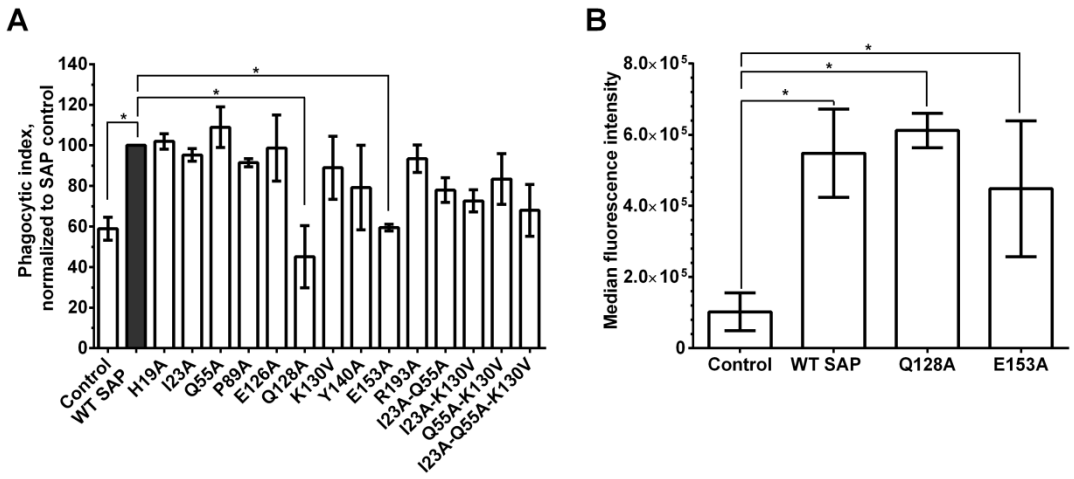

Figure 6: Amino acids Q128 and E153 on SAP are necessary for SAP-mediated phagocytosis.

A) FITC-labeled Zymosan A bio-particles were incubated in the presence of WT SAP or SAP variants and then added to monocyte-derived macrophages. After 1 hour, the free bio-particles were removed and the number of phagocytized particles was counted. The phagocytic index was estimated as the number of bio-particles engulfed by 100 macrophages. Values are means of the phagocytic index normalized to the WT SAP ± SEM, n=3-6. **B**) The binding of WT, Q128A, and E153A SAP to Zymosan A was detected using an anti-SAP antibody and flow cytometry. Values are mean ± SEM, n=3. * represents $p<0.05$ by t-test.

their ability to promote phagocytosis of Zymosan A bio-particles by macrophages (Fig. 6A). 11 of the SAP variants examined did not significantly alter the ability of SAP to enhance phagocytosis (Fig. 6A). Compared to WT SAP, SAP variants Q128A and E153A had significantly reduced ability to promote phagocytosis by macrophages (Fig. 6A). We then measured the binding of WT, Q128A and E153A SAP to Zymosan A bio-particles to determine if these SAP variants had deficiencies in binding the bio-particles. Compared to WT SAP, we found no statistically significant differences in the binding of Q128A or E153A to Zymosan A (Fig. 6B). Together, this indicates that SAP variants Q128A and E153A have defects in binding and/or activating Fcγ receptors to promote phagocytosis of Zymosan A.

SAP binds to endogenous FcγRI and FcγRIIa on immune cells

Much of the work done on SAP binding to Fcγ receptors has focused on SAP binding to recombinant Fcγ receptors or to receptors expressed on non-human cells such as COS-7 and NIH-3T3 (23, 25, 83). This is problematic because the affinity of Fcγ receptors for their ligands is sensitive to the receptor glycosylation state and the presence of intracellular signaling proteins (26, 95-97). Therefore to identify functionally significant receptors in the SAP response, we examined the binding of SAP to endogenous Fcγ receptors on human immune cells and to receptors expressed on the human-derived cell line HEK293. We used fluorescently labeled WT SAP (SAP-f) to measure the binding to different peripheral blood cell populations as identified by their flow characteristics and receptor expression (Fig. S1). We tested the activity of SAP-f on

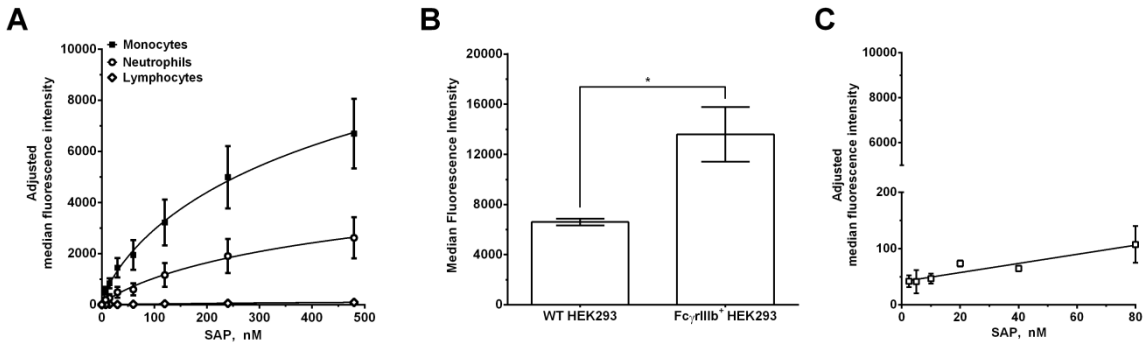

Figure 7: Alexa Fluor 647-labeled SAP (SAP-f) binds to monocytes and neutrophils. **A**) SAP-f was incubated with isolated leukocytes and then subjected to flow cytometry. Neutrophils, monocytes, and lymphocytes were identified based on forward scatter and side scatter as in Figure **S2**. Autofluorescence values were subtracted from the total binding values. Curves are fits of the resulting data to models of one-site binding with variable Hill coefficient. **B**) WT HEK293 cells and HEK293 cells expressing Fcγ RIIIb were incubated with 20 µg/ml of human IgG-Alexa Fluor 488 and then subjected to flow cytometry to determine if the expressed receptor is functional and therefore binds IgG. Values are mean ± SEM, n=3. * represents $p<0.05$ by t-test. **C**) HEK293 cells expressing FcγRIIIb were incubated with SAP-f and then subjected to flow cytometry to measure SAP binding. Mock transfected cells were used to estimate the non-specific binding, which was then subtracted from the total binding. Values are adjusted median fluorescence intensity ± SEM, n=3. The data were fit to a line. The absence of error bars indicates that the error was smaller than the plot symbol.

neutrophils, monocytes, and macrophages and observed no functional defects compared to unlabeled SAP (Fig. S2). When SAP-f was incubated with leukocytes, we observed no binding to the lymphocyte population (Fig. 7A). Since B cells (~5 % of lymphocytes) express FcγRIIb (84), and NK cells (~5-10% of lymphocytes) express FcγRIIIa (84), this suggests that SAP does not bind to these receptors under our experimental conditions. However, SAP-f did bind to monocytes and neutrophils (Fig. 7A). Monocytes express FcγRI, FcγRIIa, and some FcγRIIIa (Fig. S1) (20, 88). This indicates that SAP could be binding to any or all of the Fcγ receptors on monocytes. As NK cells express FcγRIIIa, and we did not detect binding of SAP-f to NK cells, this suggests that SAP binds to FcγRI and/or FcγRIIa on monocytes. Neutrophils express FcγRIIa and FcγRIIIb (Fig. S1) (20, 88). When we incubated SAP-f with FcγRIIIb^{+} HEK293 cells, we did not detect any appreciable binding although the receptor was functional as determined by human IgG binding (Fig. 7B and C and Fig. S3). This then suggests that SAP binds to FcγRIIa on neutrophils. We observed more SAP biding to monocytes than to neutrophils, and we hypothesize that this is likely due to the presence of FcγRI on monocytes (Fig. 7A). Together, our data indicates that SAP-f binds to endogenous FcγRI and FcγRIIa on monocytes and neutrophils but not to FcγRIIb, FcγRIIIa, and FcγRIIIb (Fig. 7).

SAP binds to FcγRI and FcγRIIa on HEK293 cells

Following our initial binding assays using human immune cells, we investigated the binding of our SAP variants to FcγRI and FcγRIIa. Of the 29 SAP variants, we chose

6 that had altered functions as measured by neutrophil adhesion assays, fibrocyte differentiation assays, and macrophage phagocytosis assays. The 6 SAP variants were fluorescently labeled and then incubated with K562 cells to measure the binding to FcγRIIa. The only known receptor that binds SAP on the surface of K562 cells is FcγRIIa ((92) and Fig. S3). WT SAP bound to FcγRIIa with a K_d of 19.7 ± 3.4 nM (Fig. 8A and Table 2). Previous measurements of the K_d for SAP binding to FcγRIIa range from 0.29 nM to 1.4 μM (23, 25, 83). As previously described, these inconsistencies are most likely caused by the method of receptor expression and how the K_d was estimated (26). Of the 6 SAP variants tested, compared to WT SAP, E126A, Q128A, and K130V had significant differences in their binding to FcγRIIa (Fig. 8A and Table 2). These changes in affinity correlate with the ability of these SAP variants to reduce neutrophil adhesion. Variants E126A and Q128A have a higher affinity for FcγRIIa and have an increased inhibitory effect on neutrophil adhesion (Table 2 and Fig. 7). Conversely, variant K130V has a decreased affinity for FcγRIIa and has a reduced inhibitory effect on neutrophil adhesion to fibronectin (Table 2 and Fig. 7). In addition, variant E126A has a Hill coefficient of 3.3 ± 0.5, indicating cooperativity in SAP E126A-FcγRIIa binding. This cooperatively is absent from the other SAP variants as their Hill coefficient is not significantly different from the 1.2 ± 0.2 we measured for WT SAP. One possible explanation for this increased Hill coefficient is self-aggregation of SAP E126A following binding to cells. This would then manifest as an increase in the maximal binding (B_{max}) of SAP E126A to cells. However, the SAP E126A B_{max} was

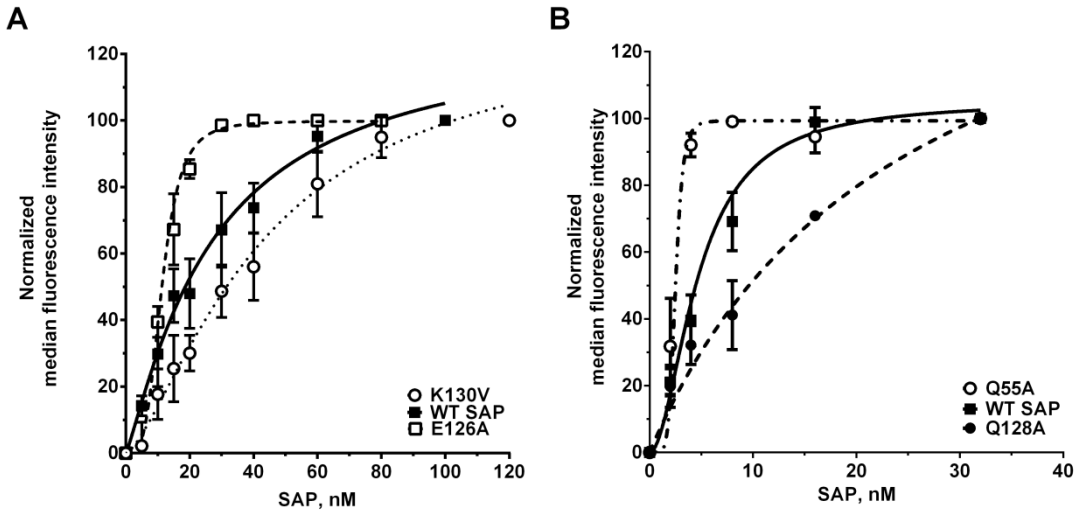

Figure 8: SAP variant binding to FcγRIIa and FcγRI.
A) K562 cells, which express FcγRIIa, were incubated with fluorescently-labeled SAP variants. The cells were then washed and the binding of the labeled SAP to the cells was measured by flow cytometry. **B**) HEK293 cells expressing FcγRI were incubated with fluorescently-labeled SAP variants and then binding was measured by flow cytometry. Mock transfected cells were used to estimate the non-specific binding. Median fluorescence intensity values were normalized to the intensity value of the highest SAP concentration. Values are normalized mean ± SEM, n=3-5. Curves are fits to models of one-site binding with variable Hill coefficient. The absence of error bars indicates that the error was smaller than the plot symbol.

SAP Variants	FcγRI K_d (nM ± SEM)	Hill coefficient	FcγRIIa K_d (nM ± SEM)	Hill coefficient
WT SAP	4.6 ± 0.8	2.1 ± 0.6	19.7 ± 3.4	1.2 ± 0.2
I23G	9.8 ± 5.8	1.1 ± 0.4	25.2 ± 9.8	1.5 ± 0.4
Q55A	2.6 ± 0.1 ***	6.7 ± 0.2 ***	22.3 ± 3.3	1.7 ± 0.2
E126A	36.9 ± 2.8***	0.9 ± 0.1	11.9 ± 0.6 *	3.3 ± 0.5 *
Q128A	24.7 ± 6.0 *	0.9 ± 0.1*	11.9 ± 2.1 *	2.3 ± 0.6
K130V	4.5 ± 0.7	3.7 ± 1.9	43.7 ± 8.7 *	1.4 ± 0.4
E153A	5.3 ± 0.6	3.2 ± 0.9	27.8 ± 1.4	4.7 ± 0.9

Table 2: Binding of SAP variants to FcγRI and FcγRIIa.
HEK293 cells expressing FcγRI were incubated with Alexa Fluor 647-labeled SAP variants. The cells were then washed and the binding of the labeled SAP to the cells was measured by flow cytometry. Mock transfected cells were used to estimate the non-specific binding. K562 cells were used to measure the binding of SAP variants to FcγRIIa. Values are mean ± SEM, n=3-6. * indicates $p < 0.05$ and *** indicates $p < 0.001$ by t-test when compared to the corresponding wildtype (WT) control.

69.7 ± 10.8 % of WT SAP (mean ± SEM, p not significant by t-test), indicating that SAP E126A was not aggregating on the surface of cells. To measure the binding of our 6 SAP variants to FcγRI, we used FcγRI$^+$ HEK293 cells (Fig. S3). The FcγRI$^+$ HEK293 cells were co-transfected with FcRγ, as this intracellular protein is necessary for FcγRI localization to the cell membrane (98). The mock transfected cells were used to estimate the non-specific binding (Fig. 9). WT SAP bound to FcγRI with a K_d of 4.6 ± 0.8 nM and a Hill coefficient of 2.1 ± 0.6 (Table 2). This affinity matches the previously published K_d of 4.3 nM (23). The Hill coefficient of greater than 1 for the SAP-FcγRI interaction suggests cooperativity, and could indicate FcγRI receptor-receptor interactions. Compared to WT SAP, variants Q55A, E126A, and Q128A had significant changes in their affinity for FcγRI (Fig. 8B and Table 2). However, we did not observe any significant changes in the B_{max} values of Q55A (105 ± 36.7 % of WT SAP), E126A (123.9 ± 45.2), and E128A (110.9 ± 14.4) when binding to FcγRI. All the changes in affinity observed for Q55A, E126A, and E128A correlate with the ability of these variants to inhibit fibrocyte differentiation. Variant Q55A has a higher affinity for FcγRI and increased inhibitory effect on fibrocyte differentiation (Table 1 and Table 2). SAP variant E126A has decreased affinity for FcγRI and has reduced inhibitory effect on fibrocyte differentiation (Table 1 and Table 2). The decrease in affinity of Q128A variant for FcγRI does not alter the IC_{50} of SAP for fibrocyte differentiation but it does abrogate enhancement of phagocytosis by macrophages (Fig. 9A and Table 1). Additionally, the decrease in affinity of SAP Q128A for FcγRI significantly increases

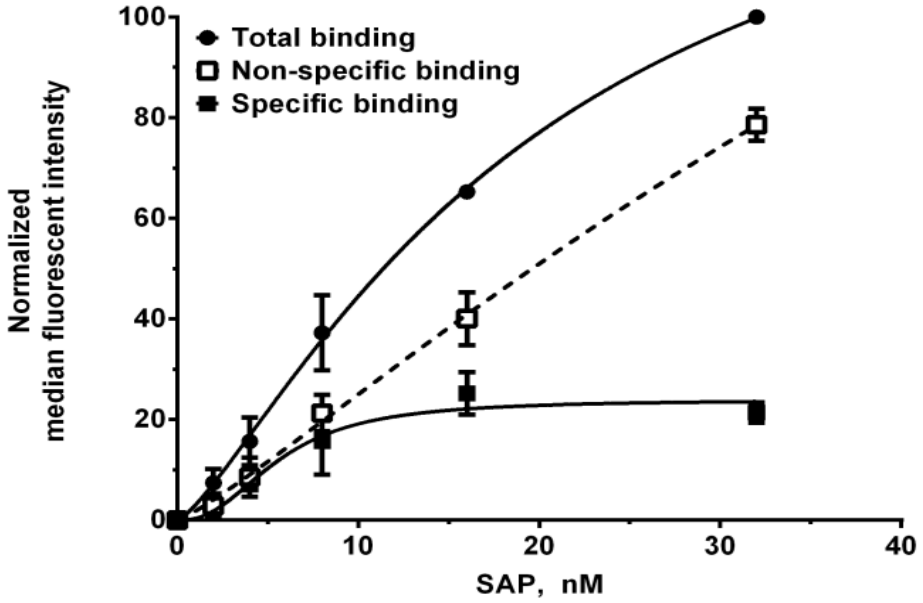

Figure 9: Estimating the specific binding of WT SAP to FcγRI.
HEK293 cells expressing FcγRI were incubated with Alexa Fluor 647-labeled WT SAP (SAP-f) as in Table 2. The cells were then washed and the binding of SAP-f to the cells was measured by flow cytometry. The specific binding was estimated by subtracting the binding of SAP-f to mock transfected cells from FcγRI expressing cells. The values were normalized to the median fluorescence intensity of SAP total binding at 32 nM. Values are mean ± SEM, n=3. The absence of error bars indicates that the error was smaller than the plot symbol.

the Hill coefficient from 1.8 ± 0.1 in WT SAP to 2.7 ± 0.3 in our fibrocyte differentiation assay (Table 1). This indicates that although the IC_{50} is not altered by this mutation, Q128 still plays a role in inhibition of fibrocyte differentiation by SAP. Together, our data indicates that SAP binds to FcγRIIa on neutrophils to reduce neutrophil adhesion and to FcγRI on monocytes to inhibit fibrocyte differentiation.

FcγRIIa and FcγRIIIb ligation reduces neutrophil adhesion

Our analysis of SAP variant binding to FcγRI and FcγRIIa indicates the significance of FcγRIIa in SAP reduction of neutrophil adhesion. To corroborate this finding, we investigated the effect of antibody-mediated ligation of FcγRI, FcγRIIa, and FcγRIIIb on neutrophil adhesion. Mouse IgG1 and the anti-FcγRI antibody clone 10.1 had no effect on neutrophil adhesion (Fig. 10). However, 2 of 3 anti-FcγRIIa antibodies and an anti-FcγRIIIb antibody tested decreased neutrophil adhesion (Fig. 10). The anti-FcγRII antibody clone AT10 is a blocking antibody and reduces IgG binding to FcγRII, but in our assay it had no effect on neutrophil adhesion. Together, this indicates that SAP binds FcγRIIa to decrease neutrophil adhesion, and that FcγRIIIb ligation by antibodies can also reduce neutrophil adhesion to fibronectin.

Blocking FcγRI using antibodies abrogates SAP inhibition of fibrocyte differentiation

SAP variant binding to FcγRI and the functional data on fibrocyte differentiation suggests a critical role for FcγRI in mediating the SAP effect on fibrocytes. To test this

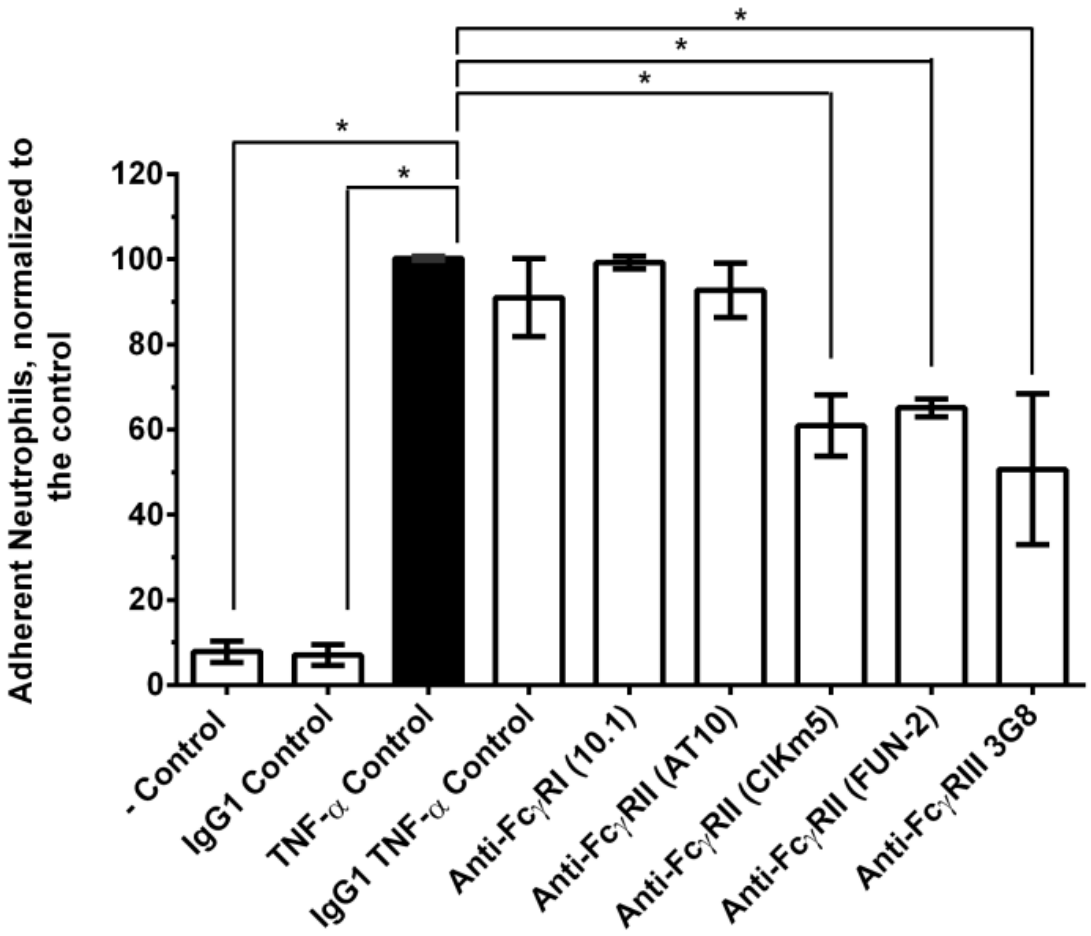

Figure 10: Ligating FcγRIIa and FcγRIIIb by antibodies decreases neutrophil adhesion.

Neutrophils were incubated with the indicated anti-Fcγ receptor antibodies to assess the effect of Fcγ receptor ligation on neutrophil adhesion to fibronectin as described in Figure **4**. Values are adherent neutrophils normalized to the TNF-α control, mean ± SEM, n=3. * indicates $p<0.05$ by t-test.

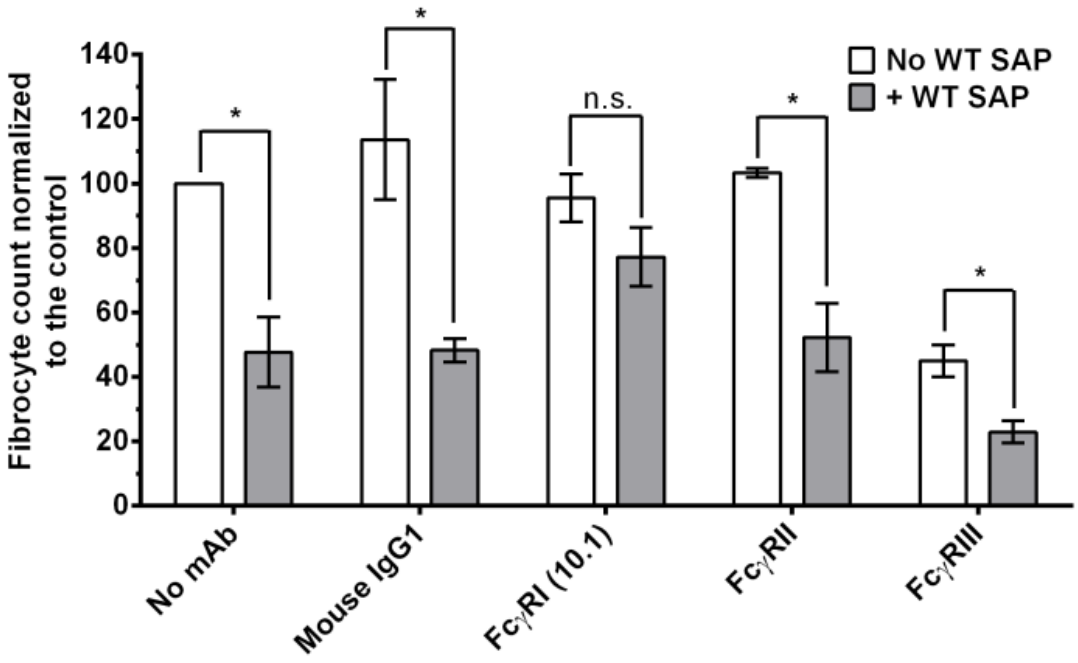

Figure 11: FcγRI blocking antibodies reduce the effect of SAP on fibrocyte differentiation.

PBMCs were incubated with $F(ab')_2$ fragments of anti-Fcγ receptor antibodies in the presence or absence of WT SAP to determine their effect on SAP-mediated inhibition of fibrocyte differentiation. Values are fibrocyte count normalized to the control ± SEM, n=4. * represent $p < 0.05$ by t-test; n.s. indicates not significant.

hypothesis, we incubated PBMCs with $F(ab')_2$ fragments of anti-FcγRI, anti-FcγRII, and anti-FcγRIII antibodies in the presence or absence of WT SAP. The anti-FcγRII and anti-FcγRIII antibodies used in this experiment do not discriminate between the different FcγRII or FcγRIII isoforms (99). However, they do block IgG binding to all FcγRII or FcγRIII receptors (99). Mouse IgG1, anti-FcγRII, and anti-FcγRIII antibodies had no effect on the inhibitory effect of SAP on fibrocyte differentiation (Fig. 11). However, the $F(ab')_2$ fragment of anti-FcγRI antibody clone 10.1 reduced the ability of SAP to inhibit fibrocyte differentiation (Fig. 11). This indicates that SAP binds to FcγRI to inhibit fibrocyte differentiation.

Identification of a novel Fcγ receptor binding site on SAP

Following our functional assays, we mapped all the mutated amino acids onto the SAP structure (Fig. 12A). Excluding amino acid E153, all the functionally significant amino acids form a distinct binding site on the surface of SAP (Fig. 12B and 12C). This novel binding site is different from the previously identified FcγRIIa binding site (Fig. 12B and (25)). The position of this novel binding site on SAP may allow for the binding of multiple Fcγ receptors.

Discussion

The pentraxin Serum Amyloid P (SAP) is an anti-fibrotic agent that inhibits aberrant scar tissue formation by regulating neutrophils, monocytes, and macrophages (20, 23, 25, 64, 100). All SAP functions appear to be mediated partly through Fcγ

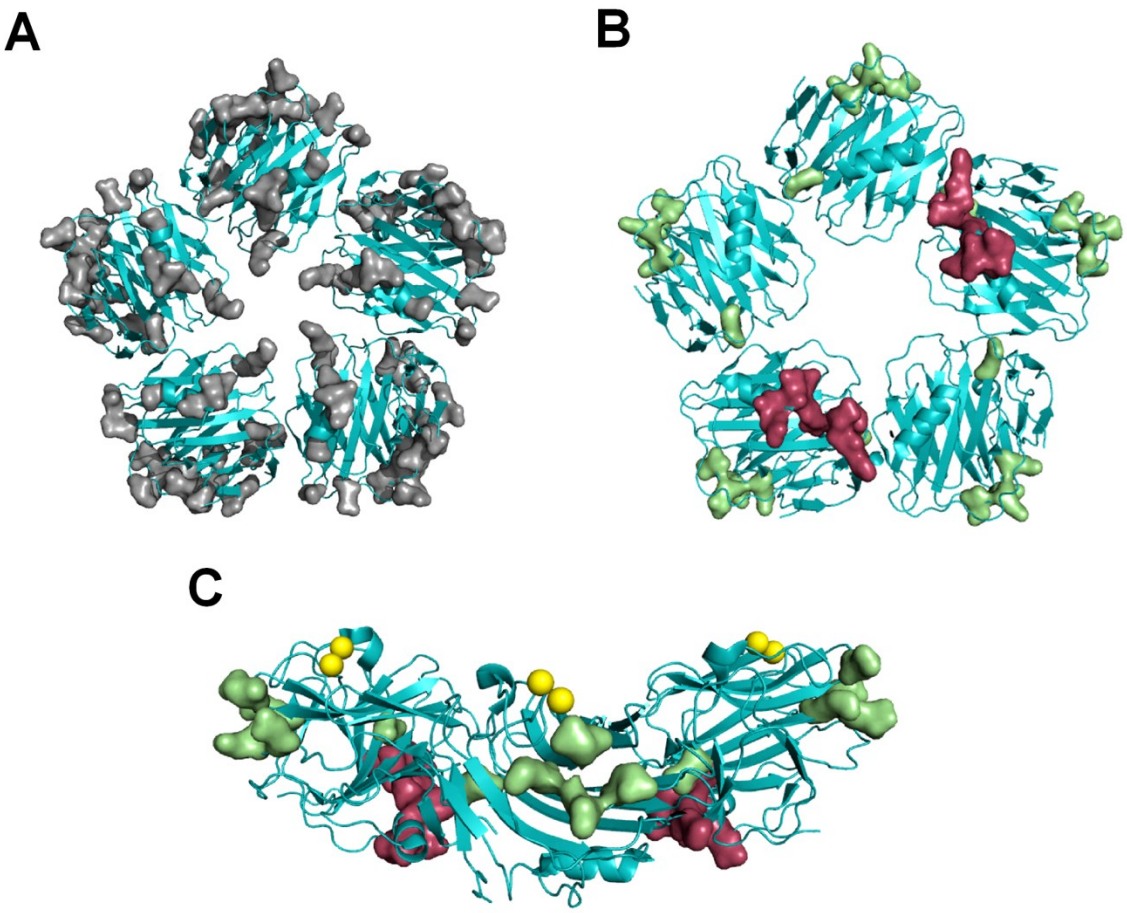

Figure 12: Identification of a novel Fcγ receptor binding site on SAP.
A) Mutated amino acid residues are indicated by molecular surface representation (gray) on the SAP structure. **B**) The functionally significant amino acid residues (green) are distinct from the previously identified FcγRIIa binding site (red). **C**) When E153 is excluded; the remaining functionally significant amino acid residues form a distinct binding site. The yellow spheres represent the two calcium ions bound to SAP.

receptors (23, 57, 58). As there are multiple Fcγ receptors on neutrophils, monocytes, and macrophages, we determined how each receptor contributed to different SAP function. We found through site-directed mutagenesis that SAP binds to FcγRI on monocytes to inhibit fibrocyte differentiation and to FcγRIIa on neutrophils to reduce adhesion to fibronectin. In addition, we identified a novel Fcγ receptor binding site on SAP.

Mutations in SAP that affect binding to FcγRIIa significantly change the ability of SAP to reduce neutrophil adhesion to fibronectin. Similar to SAP, ligating FcγRIIa by anti-FcγRII antibodies decreases neutrophil adhesion. This suggests that SAP binds to FcγRIIa to decrease cell adhesion. The activation of FcγRIIa results in the phosphorylation of the immunoreceptor tyrosine-based activation motif (ITAM) in the cytosolic region of this receptor (29). ITAM phosphorylation is implicated in inside-out signaling and regulation of adhesion molecules (29). This then suggests that FcγRIIa activation can reduce adhesion of neutrophils to fibronectin by regulating adhesion molecules on neutrophils. Additionally, ligating FcγRIIIb by an anti-FcγRIII antibody reduces neutrophil adhesion to fibronectin, suggesting that ligands of FcγRIIIb such as immunoglobulin could also regulate neutrophil adhesion to fibronectin.

Mutations in SAP that affect binding to FcγRI significantly alter the ability of SAP to inhibit fibrocyte differentiation. In addition, blocking FcγRI with an IgG blocking antibody reduces the SAP effect on fibrocyte differentiation. Together, this suggests that although there are multiple Fcγ receptors on monocytes, SAP activates

FcγRI to inhibit fibrocyte differentiation. This is in agreement with our previous results where we observed that siRNA knock down of FcγRI in humans results in decreased inhibitory effect of SAP on fibrocyte differentiation (57), and that cross-linking FcγRI with antibodies can mimic the inhibitory effect of SAP on fibrocyte differentiation (101). Here, we have identified a FcγRI binding site on each SAP monomer, suggesting that SAP can cross-link multiple Fcγ receptors (Fig. 12). Together, this suggests a role for FcγRI cross-linking in SAP inhibition of fibrocyte differentiation.

SAP appears to promote phagocytosis of bio-particles such as Zymosan A through FcγRI (Table 2 and (24). However, not all SAP variants with alteration in FcγRI binding have defects in phagocytosis. For instance, variant E126A has a ~ 10 fold reduction in affinity for FcγRI and defects in inhibiting fibrocyte differentiation, but has no deficiencies in promoting phagocytosis. This suggests that a SAP opsonized bio-particle activates FcγRI to promote phagocytosis in a manner that is distinct from how SAP activates FcγRI to inhibit fibrocyte formation. This is supported by the fact that FcγRI mediated phagocytosis is Syk-kinase dependent but inhibition of fibrocyte differentiation by SAP is Syk-kinase independent (58, 102-104). It is also possible that SAP binding to FcγRI is sufficient to promote phagocytosis irrespective of changes in SAP-FcγRI affinity. Alternatively, it is feasible that Q128A and E153A modulate Zymosan A phagocytosis by altering macrophage activation. However, SAP opsonized Zymosan A particles were incubated with macrophages for a short time (60 minutes),

which would not allow for significant alteration in macrophage activation and phenotype.

In surface plasmon resonance experiments, SAP binds to all of the Fcγ receptors (23, 83). However, we observed that SAP only binds to endogenous FcγRI and FcγRIIa on immune cells. This inconsistency can be explained by the differences in the glycosylation state of the receptors and/or the lack of some intracellular signaling components (26). FcγRIIIa is a highly glycosylated receptor in humans. Modifying FcγRIIIa glycosylation changes its affinity for IgG and perhaps SAP (26). FcγRI and FcγRIIIa in humans interact with an intracellular protein called Fcε common γ-chain (FcRγ) (26, 98). The absence of FcRγ alters the affinity of FcγRI and FcγRIIIa for IgG in humans (26, 98). This can potentially alter SAP binding to FcγRI and FcγRIIIa. Together, this suggests that the SAP affinity for Fcγ receptors is dependent on the modification of these Fc receptors and the interactions they make prior to binding SAP.

Our findings indicate that it is possible to mimic specific SAP functions by targeting particular Fcγ receptors (Fig. 13). For instance, activation of FcγRIIa by antibodies or small molecules could be used to decrease neutrophil adhesion and hence reduce neutrophil accumulation in lungs of patients suffering from acute respiratory distress syndrome or cystic fibrosis. Similarly, blocking SAP binding to FcγRI might promote fibrocyte differentiation and wound healing. In addition, our results suggest that altering the SAP sequence could improve its ability to inhibit fibrocyte differentiation

and/or reduce neutrophil adhesion. This could lead to the development of a more potent SAP anti-fibrotic.

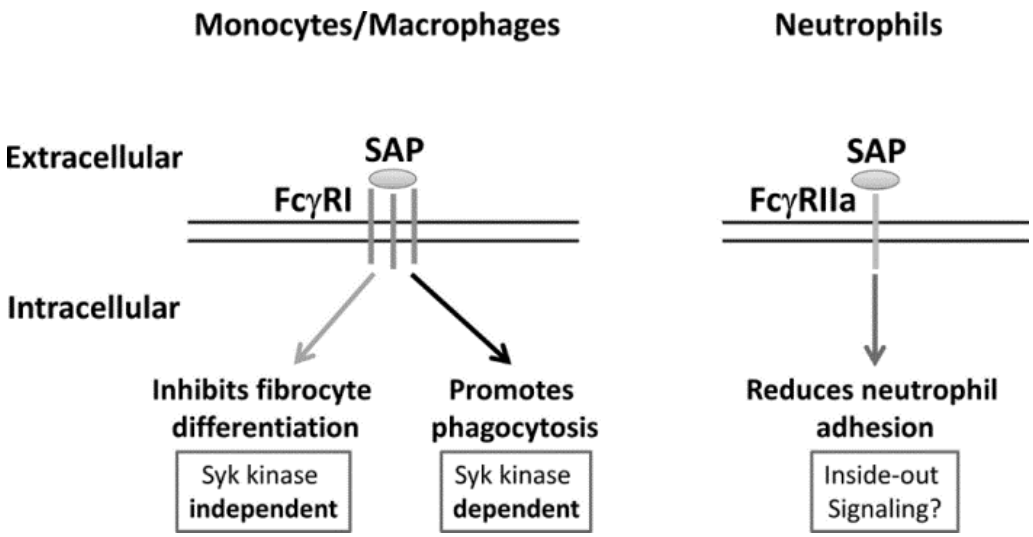

Figure 13: A model of the SAP effect on monocytes and neutrophils.
SAP cross-links FcγRI to inhibit fibrocyte differentiation in a Syk kinase independent manner. SAP also binds FcγRI to promote phagocytosis of zymosan A by macrophages. However, this pathway is Syk kinase dependent. SAP binds to FcγRIIa which then phosphorylates the ITAM domain of FcγRIIa. This then regulates adhesion molecules on the surface of neutrophils and decrease neutrophil adhesion.

CHAPTER III

DC-SIGN MEDIATES THE DIFFERENTIAL EFFECTS OF PENTRAXINS ON THE INNATE IMMUNE SYSTEM

Summary

Fibrosis is caused by scar tissue formation in internal organs and is associated with 45% of deaths in the U.S. Two closely related human serum proteins, Serum Amyloid P (SAP) and C-reactive protein (CRP), strongly affect fibrosis. In multiple animal models, and in Phase 1 and Phase 2 clinical trials, SAP suppresses several aspects of the innate immune system to reduce fibrosis, whereas CRP appears to potentiate fibrosis. However, SAP and CRP bind the same Fcγ receptors (FcγR) with similar affinities, and why SAP and CRP have opposing effects is unknown. Here we report that a glycosylation on SAP that is not present on CRP binds the receptor DC-SIGN (SIGN-R1) to suppress the innate immune system, and that FcγR are not necessary for SAP function. A polycyclic aminothiazole DC-SIGN ligand and anti-DC-SIGN antibodies mimic SAP effects *in vitro*. In mice, the aminothiazole reduces neutrophil accumulation in a model of acute lung inflammation, and at 0.001 mg/kg alleviates pulmonary fibrosis by increasing levels of the immunosuppressant IL-10. DC-SIGN (SIGN-R1) is present on mouse lung epithelial cells, and SAP and the aminothiazole potentiate IL-10 production from these cells. Our data suggest that SAP activates DC-SIGN to regulate the innate immune system differently from CRP, and that the aminothiazole and anti-DC-SIGN antibodies are potential therapeutics for fibrosis.

Introduction

Fibrosing diseases such scleroderma, pulmonary fibrosis, and renal fibrosis are caused by aberrant scar tissue formation in internal organs and are associated with 45% of deaths in the U.S. (73). At a fibrotic lesion, monocytes leave the blood, enter the tissue, and differentiate into cells such as macrophages and fibrocytes (45). Fibrocytes and macrophages then secrete extracellular matrix (ECM) proteins, ECM modifying enzymes, and/or cytokines such as IL-4 to promote scar tissue formation and fibrosis (71, 82, 105, 106).

Pentraxins are a family of highly conserved secreted proteins that have a profound effect on the development of fibrosis and regulation of the innate immune system (10, 11, 107). The pentraxin Serum Amyloid P (SAP) reduces neutrophil activation and recruitment (20, 108), inhibits the differentiation of monocytes into fibroblast-like cells called fibrocytes(54, 56, 108), and promotes IL-10-secreting macrophages (23, 64, 70). In animal models and two human trials (23, 56, 59, 71, 78, 109), injections of SAP decrease fibrosis indicating that SAP has a dominant effect on a disease that is mediated in part by the innate immune system. Conversely, the closely-related pentraxin C-reactive protein (CRP) has a pro-inflammatory effect and promotes fibrosis (110-112). Human serum CRP levels increase up to a thousand fold during infection and inflammation (113), and elevated serum CRP is the best biomarker for inflammatory diseases (10). However, under some conditions, CRP decreases inflammation, indicating that much remains to be understood about this molecule (10, 114). In contrast to SAP and CRP, which are produced by hepatocytes, Pentraxin 3

(PTX3) is produced by macrophages, neutrophils, endothelial cells, epithelial cells, and fibroblasts (3). PTX3 is associated with inflammation in humans, but in mice appears to be pro-inflammatory in some models and limits inflammation in other models (115). Despite the strong effects of pentraxins on the innate immune system and fibrosis (10, 107), little is known about their mechanism of action. For instance, pentraxins such as SAP and CRP appear to bind the same Fcγ receptors (FcγR) with similar affinities (11, 83, 108), but they generally have opposite effects. What causes this functional difference is not known.

Dendritic cell-specific intercellular adhesion molecule-3-grabbing non-integrin (DC-SIGN/CD209) is a C-type lectin found on dendritic cells, macrophages, and monocytes (116, 117). DC-SIGN mainly binds to mannosylated and fucosylated proteins (116, 117). In humans, there is a single DC-SIGN receptor, whereas mice have eight DC-SIGN orthologs called SIGN-R1-8 (118). SIGN-R1 most closely resembles DC-SIGN (118). DC-SIGN and SIGN-R1 also bind sialylated proteins such as IgG (sIgG) (117). Both sIgGs and SAP have α(2→6)-linked terminal sialic acids on the protein surface, and both sIgGs and SAP alleviate inflammation in mice (107, 117, 119).

In this report, we show that in absence of all the FcγR, neutrophils, monocytes and macrophages still respond to SAP, indicating that SAP uses other receptors. For SAP, we show that one of the other receptors is DC-SIGN. A small-molecule DC-SIGN ligand mimics the effects of SAP. This ligand shows efficacy in murine models of acute lung inflammation and pulmonary fibrosis. In contrast to SAP, we find that CRP requires the Fc□R to regulate neutrophils and IL-10 secretion from macrophages, but not to

increase ICAM-I^{+} macrophages. This suggests that there are additional CRP receptors that regulate macrophage polarization. Our findings suggest the presence of a novel pentraxin target that accounts for some of the functional difference between SAP and CRP, and which might be useful as a therapeutic target to regulate the innate immune system.

Methods

Antibodies and reagents

Mouse anti-human CD209 antibody clone H200 was obtained from Santa Cruz Biotechnology (Dallas, TX). Mouse anti-human CD209, CD163, and ICAM-I antibodies, anti-mouse CD206, ICAM-I, CD11b, Ly6G, CD45, and rat IgG1 isotype control antibodies, and biotinylated IL-10 (JES5-16E3) were from Biolegend (San Diego, CA). Anti-mouse CD11c was from MBL (Woburn, MA). Anti-mouse SIGN-R1 (22D1) and Armenian hamster isotype control were from eBioscience (San Diego, CA). Anti-mouse Epcam-1 antibody was from Abcam (Cambridge, MA). Anti-rat Dylight 488 and anti-Armenian hamster biotin-conjugated antibodies were from Novus (Littleton, CO). Alexa Fluor 488-anti-rabbit antibodies and IgG-free albumin were from Jackson ImmunoResearch (West Grove, PA). Streptavidin-Alexa Fluor 647, Alamar Blue cell viability reagent, and Alexa Fluor 647-NHS were from Life Technologies (Grand Island, NY). Human GM-CSF, mouse M-CSF, and mouse IL-13 were from Biolegend Inc. Sambucus Nigra lectin, streptavidin-alkaline phosphatase, and Vector Red alkaline phosphatase substrate kits were from Vector (Burlingame, CA). The CRP cDNA

expression plasmid was a kind gift from Dr. Jeff Crawford (Baylor College of Medicine, Houston, TX) and the DC-SIGN cDNA expression plasmid was from the NIH AIDS reagent program (Germantown, MD). SAP and bleomycin were from EMD Millipore (Billerica, MA). CRP was from Fitzgerald Industries (North Acton, MA) and PTX3 from R&D systems (Minneapolis, MN). Neuraminidase (Cat # N2876) and DMSO were from Sigma-Aldrich (St. Louis, MO). Compound 1 (Cat#5931866) was purchased from ChemBridge (San Diego, CA).

Mouse strains

C57/BL6 and IL-10-null mice (120) were obtained from Jackson laboratories (Bar Harbor, ME). FcγR quad-null (121) and SIGN-R1-null (117) mice were a kind gift from Dr. Jeffery Ravetch (Rockefeller University, New York, NY). All animals were used in accordance with National Institutes of Health guidelines and with a protocol approved by the Texas A&M University Institutional Animal Care and Use Committee.

Fibrocyte differentiation assay

Human blood was collected into heparin tubes (BD Bioscience, San Jose, CA) from adult volunteers who gave written consent and with specific approval from the Texas A&M University human subjects Institutional Review Board. PBMCs were then isolated and cultured to examine human fibrocyte differentiation as described previously (108). Mouse spleen cells were isolated and cultured to assess murine fibrocyte differentiation as previously described (94).

Macrophage polarization assay

Cells were cultured at 37˚C in a humidified incubator with 5% CO_2. Human monocytes were differentiated into macrophages in 200 µl of RPMI-1640 (Lonza, Basel, Switzerland)/10% fetal calf serum (FCS, Seradigm, Randor,PA) for 6 days at a concentration of $0.5x10^6$ cells/ml in a well of an 8 well slide (EMD Millipore). The medium was then replaced with fresh serum-free RPMI-1640 (supplemented with 10 mM HEPES, 2 mM glutamine, 100 U/ml penicillin, 100 g/ml streptomycin, and ITS-3, all from Sigma-Aldrich), containing 3 µg/ml of the indicated pentraxin, 1 µg/ml of the indicated antibody, or 10 pg/ml of compound 1 for 3 days. Subsequently, the cells were dried, fixed and stained as previously described (88). Mouse tibias and femurs were flushed with RPMI-1640 and the cells were washed 3x in PBS. The cells were then resuspended in RPMI-1640/ 10% FCS and 200 µl of $5x10^5$ cells/ml was incubated in each well of an 8 well slide (EMD Millipore). After 1 hour, the medium and non-adherent cells were removed and replaced with fresh RPMI-1640/ 10% FCS/ 10 ng/ml GM-CSF. On day 7, the medium was replaced with serum-free RPMI-1640 containing 10 µg/ml of the indicated pentraxin. After 3 days, cells were dried, fixed and stained.

Recombinant protein expression

The cDNA for human CRP was mutated at residue 32 using a QuickChange II Site-Directed Mutagenesis Kit (Agilent, Santa Clara, CA) and the primer 5' AAGGCGCGCCATGGAGAAGCTGTTG 3'. CRP cDNA was inserted into a pCMV6-AC-His vector (Origene, Rockville, MD) and then expressed in HEK293 cells (Life

Technologies, Grand Island, NY) as previously described (108). CRP and glycosylated CRP were purified using immobilized p-aminophenyl phosphoryl choline beads (Thermo Fisher scientific, Walthan, MA) following the manufacturer's protocol.

SDS-PAGE and western blots

Proteins were diluted in 20 mM sodium phosphate, pH 7.4 to a concentration of 40 μg/ml and then analyzed by SDS-PAGE gels as described previously (54). For Western blotting, p**r**oteins from gels were transferred to polyvinylidene difluoride membranes (Immobilon P; Millipore, Bedford, MA) in Tris/glycine/SDS buffer containing 20% methanol following the manufacturer's protocol. Filters were blocked for 30 minutes at room temperature in Carbo-Free Blocking Solution (Vector). Membranes were then incubated in PBS containing 10 μg/ml of Biotinylated Sambucus Nigra Lectin (Vector) for 30 minutes at room temperature to detect α (2→6)-linked terminal sialic acids following the manufacturer's protocol. Vectastain Elite ABC peroxidase kits (Vector) were used to detect the biotinylated lectin following the manufacturer's protocol. We then used Clarity Western ECL chemiluminescence substrate (Bio-Rad, Hercules, CA) to visualize the peroxidase with a ChemiDoc XRS+ imager (Bio-Rad).

SAP desialylation

SAP (125 KDa) was incubated with neuraminidase (SigmaAldrich) for 2 days at 37°C following the manufacturer's protocol. The desialylated SAP (SAP (NA)) was then

buffer exchanged to 20 mM Tris, pH 7.4 using a 100 KDa filter (EMD Millipore) to remove the 60 kDa neuraminidase.

DC-SIGN binding

The DC-SIGN cDNA expression plasmid was transfected into HEK293 cells (Life Technologies) using Lipofectamine 3000 (SigmaAldrich) following the manufacturer's protocol. After 3 days, the transfected cells were washed twice in 20 mM Tris, 140 mM NaCl, 2mM $CaCl_2$, pH 7.4 and then incubated with Alexa Fluor 647 (Life Technologies) labeled SAP or SAP (NA) in binding buffer (PBS/ 1 mM $MgCl_2$/ 1 mM $CaCl_2$/ 1% IgG-free albumin) at 4°C. After 1 hour, cells were washed 3x in ice cold binding buffer and fluorescence of the cells was measured by flow cytometry as previously described (108). Mock transfected cells were used to estimate the non-specific binding.

Neutrophil adhesion assay

Human and murine neutrophils were isolated from blood and adhesion assays were performed as described previously (20).

Mouse models of acute lung inflammation and fibrosis

C57BL/6 mice (Jackson laboratories) were given an oropharyngeal instillation of 3U/kg of bleomycin (EMD Millipore) to induce acute inflammation and neutrophil recruitment as described previously (20, 89). Pulmonary fibrosis was induced in mice by

instillation of 3U/Kg of bleomycin as described previously (122). Briefly, on day 0 mice were given bleomycin instillation (50µl) or saline (50µl). Mice were then injected with vehicle control (48µl PBS, 2 µl DMSO), SAP (50µg of SAP in 50µl of PBS), or compound 1 (48µl PBS, 2 µl compound 1 in DMSO) at the indicated dose on days 1-2 for acute lung inflammation and days 1-20 for pulmonary fibrosis. On day 3 for the acute lung inflammation model and day 21 for pulmonary fibrosis model, mice were euthanized and the blood, bronchoalveolar lavage fluid (BAL), and the lungs were collected.

Immunohistochemistry and immunofluorescence

BAL cells and lungs were fixed and stained as previously described (56, 88). Immunofluorescence images were acquired with a FluorView FV1000 Confocal Microscope (Olympus, Center valley, PA).

PicroSirius red staining

PicroSirius red staining was performed as described previously (56).

Cell viability assay

Cell viability was assessed with Alamar Blue cell viability reagent (Life Technologies) following the manufacturer's protocol.

Statistical analysis

Data were analyzed by ANOVA (with Holm-Bonferroni posttest) or *t*-test when appropriate using Prism software (GraphPad, San Diego, CA). Statistical significance was defined as $p < 0.05$. Data were fit to the appropriate model of binding as determined by F-tests.

Results

Fcγ receptors do not mediate many of SAP and CRP effects on the innate immune system

SAP and CRP both bind Fcγ receptors (FcγR), but have different effects on the innate immune system (83, 108). To determine the role of FcγR in SAP and CRP function, we examined the effect of these proteins on mouse cells lacking all known FcγR (FcγR quad KO). As previously observed (20, 108), SAP and CRP decreased the adhesion of C57BL/6 neutrophils to fibronectin (Fig. 14A). When added to FcγR quad KO neutrophils, SAP but not CRP, significantly reduced neutrophil adhesion to fibronectin (Fig. 14A).

In addition to reducing neutrophil adhesion, SAP inhibits the differentiation of monocytes into fibroblast-like cells called fibrocytes (54, 108) (Fig. 14B). In the absence of FcγR, SAP reduced but could not completely inhibit fibrocyte differentiation (Fig. 14B). As previously observed (54), CRP had no effect on fibrocyte differentiation (Fig. 14C). The absence of FcγR did not alter this (Fig. 14C).

SAP increases the expression of CD206 (64, 88) on macrophages (Fig. 14D). CRP, however, primarily promotes the inflammatory M1-like phenotype (110) and

increased ICAM-I$^+$ macrophages (Fig. 14E). Both SAP and CRP were able to polarize FcγR quad KO macrophages as determined by CD206 and ICAM-I expression (Fig. 14, D and E). SAP also increased IL-10 secretion from C57BL/6 and FcγR quad KO macrophages (Fig. 14F). In contrast, CRP increased IL-10 secretion from C57BL/6 macrophages but not the FcγR quad KO cells (Fig. 14F). PTX3 uses the FcγR to potentiate fibrocyte differentiation (Pilling et al, manuscript submitted). However in the absence of the FcγR, PTX3 was able to decrease neutrophil adhesion and alter macrophage phenotype, although the PTX3-induced IL-10 secretion by macrophages was absent (Fig. S4). These results indicate that SAP does not require the FcγR to reduce neutrophil adhesion, inhibit fibrocyte differentiation, and polarize macrophages. This suggests the presence of additional SAP receptors. Conversely, CRP requires the FcγR to reduce neutrophil adhesion and promote IL-10 secretion by macrophages, but not to increase ICAM-I$^+$ macrophages. This suggests that some aspects of the CRP effect on macrophages is mediated by an unknown receptor.

SAP glycosylation mediates many of the SAP effects on the innate immune system

CRP has sequence and structural similarity to SAP, and like SAP binds FcγR (10, 107). However, SAP and CRP have different effects on monocyte and macrophage differentiation; for instance while SAP inhibits fibrocyte differentiation (56, 108) and promotes IL-10 secreting macrophages (64, 71), CRP has no effect on fibrocyte differentiation (54) and promotes pro-inflammatory macrophages (110). One possible

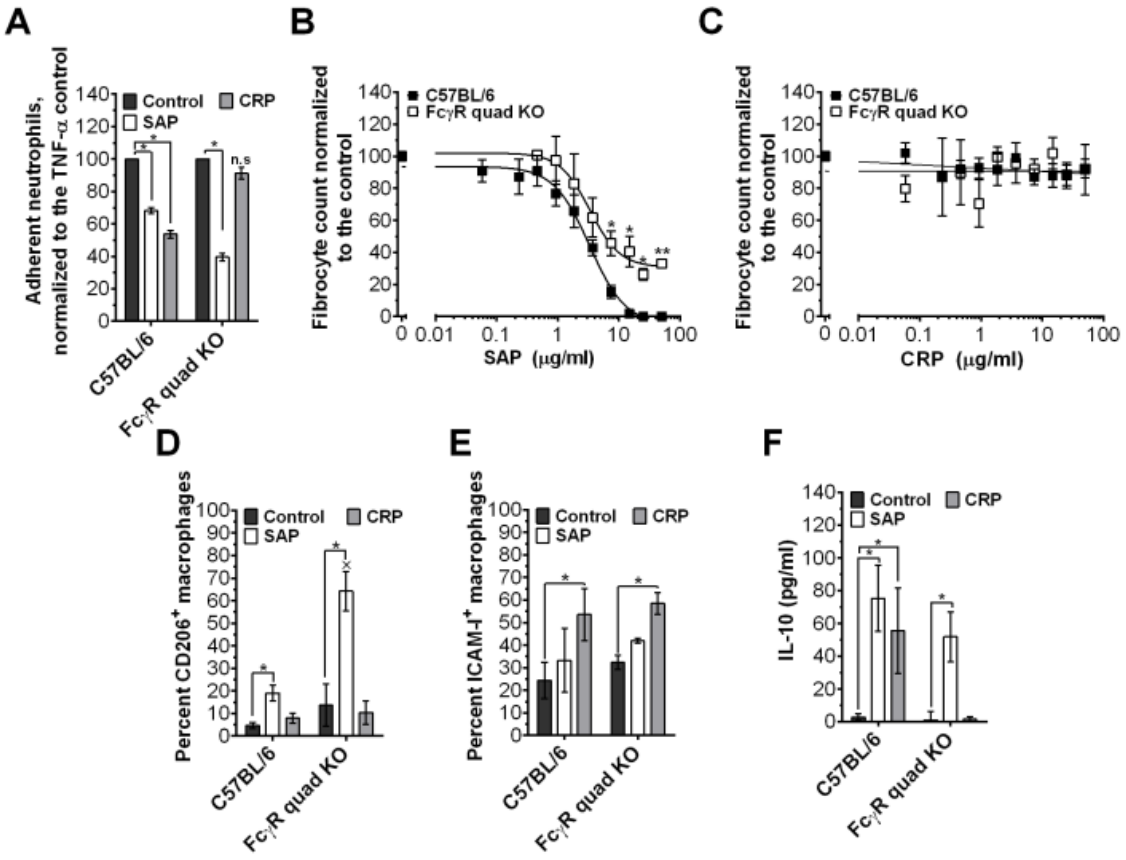

Figure 14: Fcγ receptors are necessary for some but not all effects of SAP and CRP on neutrophils, monocytes, and macrophages.

A) Mouse neutrophils were incubated with 0 (control) or 30 μg/ml of the indicated pentraxin, transferred to a fibronectin coated plate, and then activated with TNF-α. After 30 minutes, neutrophils bound to the plate were stained and counted, n=3. **B,C**) Mouse spleen cells were incubated with the indicated concentrations of pentraxin. After 5 days, the cells were fixed, stained, and fibrocytes were counted, n=3-6. **D,E**) Mouse bone marrow-derived macrophages were polarized for 3 days in serum-free medium containing 0 (control) or 10 μg/ml of the indicated pentraxin. Cells were then fixed and stained for CD206 and ICAM-I, n=3. **F**) Macrophages were polarized as in 1d and then soluble IL-10 levels in the supernatants were measured by ELISA, n=3-8. n.s (not significant relative to the control), **P <0.05* (*t*-test), (**D**) ×*P*<0.05 (*t*-test relative to SAP in C57BL/6). (a-f) Values are mean ± SEM. (**B**) Data were fit to sigmoidal dose response curves with a variable Hill coefficient or (**C**) a line.

reason for this functional difference is sequence divergence between SAP and CRP. However, we previously found that mutating SAP surface amino acid residues that are different between SAP and CRP has only a modest effect on SAP function (108). An alternative cause of this functional difference may be a difference in SAP and CRP glycosylation: SAP is glycosylated at N32 with α(2→6)-linked terminal sialic acids (119), whereas CRP has no glycosylation (119). To determine if the SAP glycosylation affects its function, we enzymatically removed the terminal sialic acids with neuraminidase. The resulting desialylated SAP (SAP (NA)) could no longer be detected on western blots stained with *Sambucus Nigra* lectin, which binds preferentially to α(2→6)-linked terminal sialic acids (Fig. 15, A and B).

SAP and CRP reduce TNF-α induced human neutrophil adhesion to fibronectin (20) (Fig. 15C). Compared to SAP, SAP (NA) had a reduced effect on human neutrophil adhesion and was unable to completely inhibit fibrocyte differentiation when added to human PBMCs and mouse spleen cells (Fig. 15, C, D and E). Conversely, we mutated CRP at position 32 from an alanine to an asparagine to engineer a glycosylated CRP. The mutated CRP (CRP A32N) was glycosylated and had a lower mobility on SDS-PAGE gels compared to CRP (Fig. 15, A and B). Similar to CRP and SAP, CRP A32N reduced human neutrophil adhesion (Fig. 15C). As previously observed (54), CRP had no significant effect on human or murine fibrocyte differentiation (Fig. 15, E and F). However, CRP A32N inhibited fibrocyte differentiation when added to human PBMC or spleen cells from C57BL/6 mice or FcγR quad KO mice (Fig. 15, E and F).

In addition to regulating fibrocyte differentiation, SAP and CRP can polarize macrophages (64, 70, 71). To examine the role of SAP glycosylation on macrophage polarization, we added pentraxins to mouse and human macrophages. SAP and CRP A32N increased the expression of the M2 marker CD206 on mouse bone marrow-derived macrophages (Fig. 15G), while CRP and SAP (NA) increased the expression of the M1 marker ICAM-I (123) (Fig. 15G). We observed a similar trend in human monocyte-derived macrophages, where SAP and CRP A32N increased the expression of the M2 marker CD163 (63) while SAP (NA) and CRP increased the expression of the M1 marker ICAM-I (Fig. 15H). Together, these results indicate that SAP glycosylation is a key mediator of its effect on innate immune cells and can explain the functional differences between SAP and CRP.

SAP but not CRP binds to DC-SIGN to regulate innate immune cells

The α(2→6)-linked terminal sialic acids on sIgG can bind to DC-SIGN to alter IgG responses (117). Since SAP shares the same type of glycosylation as sIgG (119), and SAP and the Fc domain of IgG bind to FcγR , we examined the possibility that SAP might bind to DC-SIGN. We expressed DC-SIGN on HEK293 cells and measured SAP binding to the transfected cells (Fig. 16A and Fig. S5, A and B). We used mock-transfected HEK293 cells to estimate the non-specific binding (Fig. S5). SAP bound to DC-SIGN with a K_D of 2.3 ± 1 μg/ml (19 ± 8 nM) and a Hill coefficient of 0.7 ± 0.3. However, SAP (NA) and CRP did not show detectable binding (Fig. 16A). This suggests that SAP may bind to DC-SIGN through its terminal sialic acids to alter immune

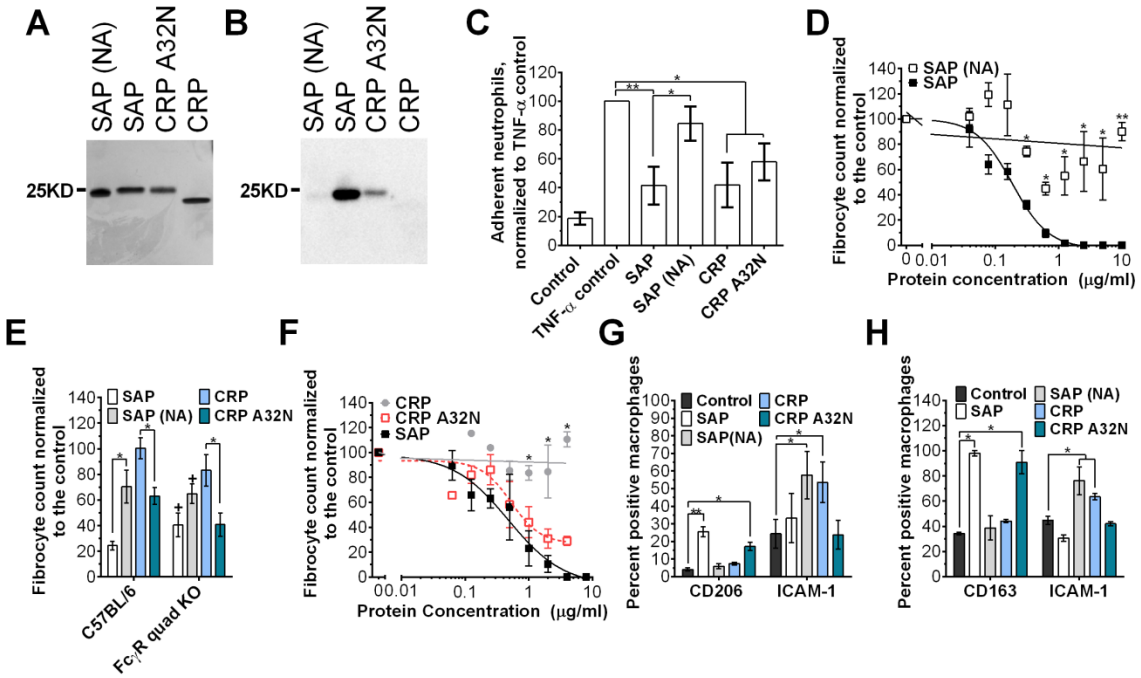

Figure 15: SAP glycosylation regulates neutrophil adhesion, monocyte differentiation, and macrophage polarization.

A) Desialylated SAP (SAP (NA)), SAP, glycosylated CRP (CRP A32N), and CRP were electrophoresed on a SDS-PAGE gel and stained with silver stain. **B**) A western blot of the samples shown in 2a was stained with biotinylated Sambucus Nigra lectin to detect α(2,6)-linked terminal sialic acids. **C**) Human neutrophils were incubated with 0 (control) or 10 μg/ml of the indicated pentraxin, transferred to a fibronectin coated plate, and then activated with TNF-α. The adherent neutrophils were then counted, n=3-5. **D**) Human PBMC were incubated with the indicated concentrations of pentraxins. After 5 days, fibrocytes were counted, n=3-5. **E**) Mouse spleen cells were incubated in the presence or absence of 10 μg/ml of the indicated pentraxin. Fibrocyte counts were normalized to the no-pentraxin control, n=3. **F**) Human PBMC were incubated with the indicated concentrations of pentraxin. After 5 days fibrocytes were counted, n=3-5. **G**) Mouse C57BL/6 bone marrow-derived macrophages were polarized for 3 days in serum-free medium containing 0 (control) or 10 μg/ml of the indicated pentraxins. Cells were then stained for the indicated markers, n=3. **H**) Human monocyte-derived macrophages were polarized by 3 μg/ml of the indicated protein. Macrophages were then stained for the indicated markers, n=3. **P*<0.05, ***P*<0.01 (*t*-test). (**E**) + *P*<0.05 (t-test relative to the no-protein control). (**C-H**) Values are mean ± SEM. (**D-E**) Data were fit to sigmoidal dose-response curves with a variable Hill coefficient or a line where appropriate.

responses. To test this possibility, we examined the effect of SAP on spleen cells from mice lacking the mouse orthologue of human DC-SIGN, SIGN-R1. The absence of SIGN-R1 significantly decreased the inhibitory effect of SAP on fibrocyte differentiation (Fig. 16B). CRP A32N and PTX3 were also unable to alter fibrocyte differentiation from spleen cells of SIGN-R1 deficient mice, suggesting that SIGN-R1 might mediate CRP A32N and PTX3 effects on fibrocyte differentiation (Fig.16C and Fig. S6).

DC-SIGN is expressed on macrophages, dendritic cells, and monocytes (116, 117). We also detected cell-surface DC-SIGN on human neutrophils and a subpopulation of human lymphocytes (Fig. S5C). As the majority of cells expressing DC-SIGN appear to respond to SAP, we examined how DC-SIGN activation by antibodies against the extracellular domain of this receptor can alter neutrophil, monocyte, and macrophage function. Some, but not all, anti-human DC-SIGN antibodies decreased human neutrophil adhesion to fibronectin (Fig. 16D), and inhibited human fibrocyte differentiation with an IC_{50} of 2.4 ± 0.4 μg/ml (Fig. 16E and Fig. S7, A and B). A different subset of anti-DC-SIGN antibodies also altered macrophage phenotype and increase CD163 expression similar to SAP and CRP A32N (Fig. 16F and Fig. S7C).

Antibodies against DC-SIGN may also interact with the FcγR through their Fc region, therefore confounding our observations and resulting in FcγR dependent responses. To rule out this possibility, we used synthetic ligands of DC-SIGN that block the binding of HIV to this receptor (124). Some DC-SIGN ligands have previously been shown to activate DC-SIGN (125). When added to immune cells, a polycyclic

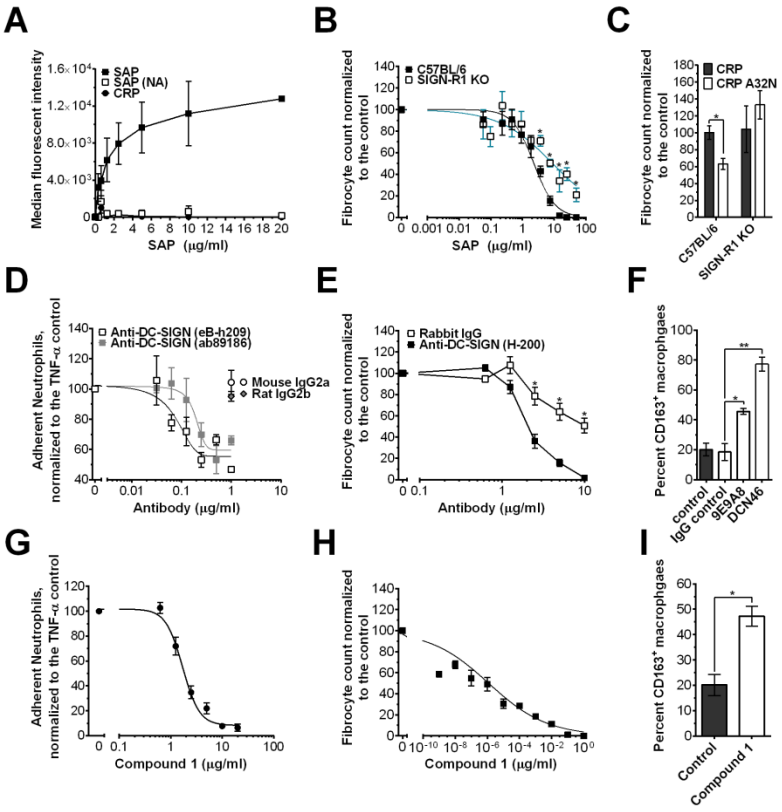

Figure 16: DC-SIGN activation affects neutrophils and monocyte-derived cells. **A**) HEK293 cells expressing DC-SIGN were incubated with fluorescently labeled SAP, CRP, or SAP (NA). The cells were then washed, and the binding of the labeled protein to the cells was measured by flow cytometry. Mock transfected cells were used to estimate the non-specific binding, n=3. **B**) The effect of SAP on fibrocyte differentiation in C57BL/6 and SIGN-R1 deficient mice was assessed, n=3-5. **C**) Mouse spleen cells were incubated in the presence or absence of 10 μg/ml of the indicated pentraxin. Fibrocytes were counted as a percent of the no-pentraxin control, n=3-5. **D**) Human neutrophils were incubated with increasing concentrations of anti-DC-SIGN antibodies and then neutrophil adhesion to fibronectin was assessed, n=3. **E**) Human PBMCs were incubated with the indicated concentrations of a rabbit anti-DC-SIGN antibody or a rabbit isotype control. After 5 days, fibrocytes were counted, n=3-5. **F**) Human monocyte-derived macrophages were polarized with 1 μg/ml of the indicated antibody. Macrophages were then fixed and stained for CD163, n=3. **G**) The effect of compound 1 on human neutrophil adhesion to fibronectin was assessed, n=3. **H**) The effect of compound 1 on human fibrocyte differentiation, n=3. **I**) Macrophage polarization by 10 pg/ml of compound 1 was examined in human monocyte-derived macrophages, n=3. **P*<0.05 (*t*-test). (**A-I**) Values are mean ± SEM. (**A**) Curves are fits to models of one-site binding with variable Hill coefficient where appropriate. (**B,D,G,H**) Data were fit to sigmoidal dose response curves with a variable Hill coefficient.

aminothiazole DC-SIGN ligand (compound 1; shown as compound 4 in Fig. 2 of reference (124)) decreased human neutrophil adhesion (IC_{50} of 1.7 ± 0.3 μg/ml and a Hill coefficient of 2.6 ± 0.2) (Fig. 16G) and inhibited human fibrocyte differentiation (IC_{50} = 1.2 ± 0.4 pg/ml, Hill coefficient = 0.30 ± 0.01) (Fig. 16H) without affecting cell viability below 0.1 μg/ml (Fig S8, A and B). Compound 1 also promoted M2 macrophages as measured by CD163 expression (Fig. 16I). Compound 1 similarly reduced neutrophil adhesion, inhibited fibrocyte differentiation, and promoted M2 macrophages in FcγR quad KO cells (Fig. S9). However, compound 1 did not affect fibrocyte differentiation when added to SIGN-R1 deficient cells (Fig S8C). These data suggest that DC-SIGN activation by antibodies or a synthetic ligand is sufficient to mimic some SAP functions. This SAP-DC-SIGN interaction may also contribute to the differences in SAP and CRP effects on the innate immune system.

Compound 1 reduces neutrophil accumulation in the lungs of bleomycin-treated mice

SAP and PTX3 can regulate neutrophil recruitment in mice (20, 126). To determine if SIGN-R1 activation similarly affects neutrophils in mice, WT mice were given bleomycin to induce acute lung inflammation. We then injected the mice with compound 1 and examined neutrophil accumulation in the lungs. We did not use anti-SIGN-R1 antibodies because they would activate both SIGN-R1 and FcγR, therefore confounding the results. As previously observed (89), oropharyngeal instillation of bleomycin significantly increased the number of $Ly6G^+$ neutrophils in the lungs (Fig. 17). When mice were injected with compound 1 at 0.1 mg/kg on days 1 and 2 after

bleomycin, there was a significant decrease in $Ly6G^+$ cells in the lungs at day 3 compared to the bleomycin control (Fig. 17). Bleomycin treatment also resulted in a significant increase in $CD11b^+$ macrophages and $CD45^+$ immune cells in the bronchoalveolar lavage (BAL) fluid (Fig. 17B). This increase in infiltrating cells was absent when mice were given compound 1 (Fig. 17B). Additionally in the post-BAL lungs, compound 1 reversed a bleomycin-induced decrease in $CD11c^+$ cells (Fig. 17C). However, compound 1 did not alter the number of $CD11b^+$ macrophages in the lungs compared to the bleomycin control (Fig. 17C). Our results indicate that DC-SIGN ligands such as compound 1 can, similar to SAP and PTX3 (20, 126), regulate neutrophil accumulation in mouse lungs following an insult.

Compound 1 alleviates pulmonary fibrosis in mice

Compound 1 alters macrophage phenotype and inhibits fibrocyte differentiation in a manner similar to SAP. As macrophages and fibrocytes are implicated in fibrosing diseases (45, 127), we determined if DC-SIGN activation by compound 1 in a murine bleomycin model of pulmonary fibrosis was sufficient to mimic SAP and alleviate fibrosis. As previously observed (122), oropharyngeal instillation of bleomycin resulted in increased collagen deposition and recruitment of $CD11b^+$ macrophages to the lungs (Fig. 18). Daily injections of compound 1 at doses as low as 0.001 mg/kg significantly decreased collagen deposition in the lungs and improved overall health as indicated by weight change (Fig. 18, A and B and Fig. S10A). In addition, compound 1 significantly reduced the number of $CD11b^+$ macrophages compared to the bleomycin control (Fig.

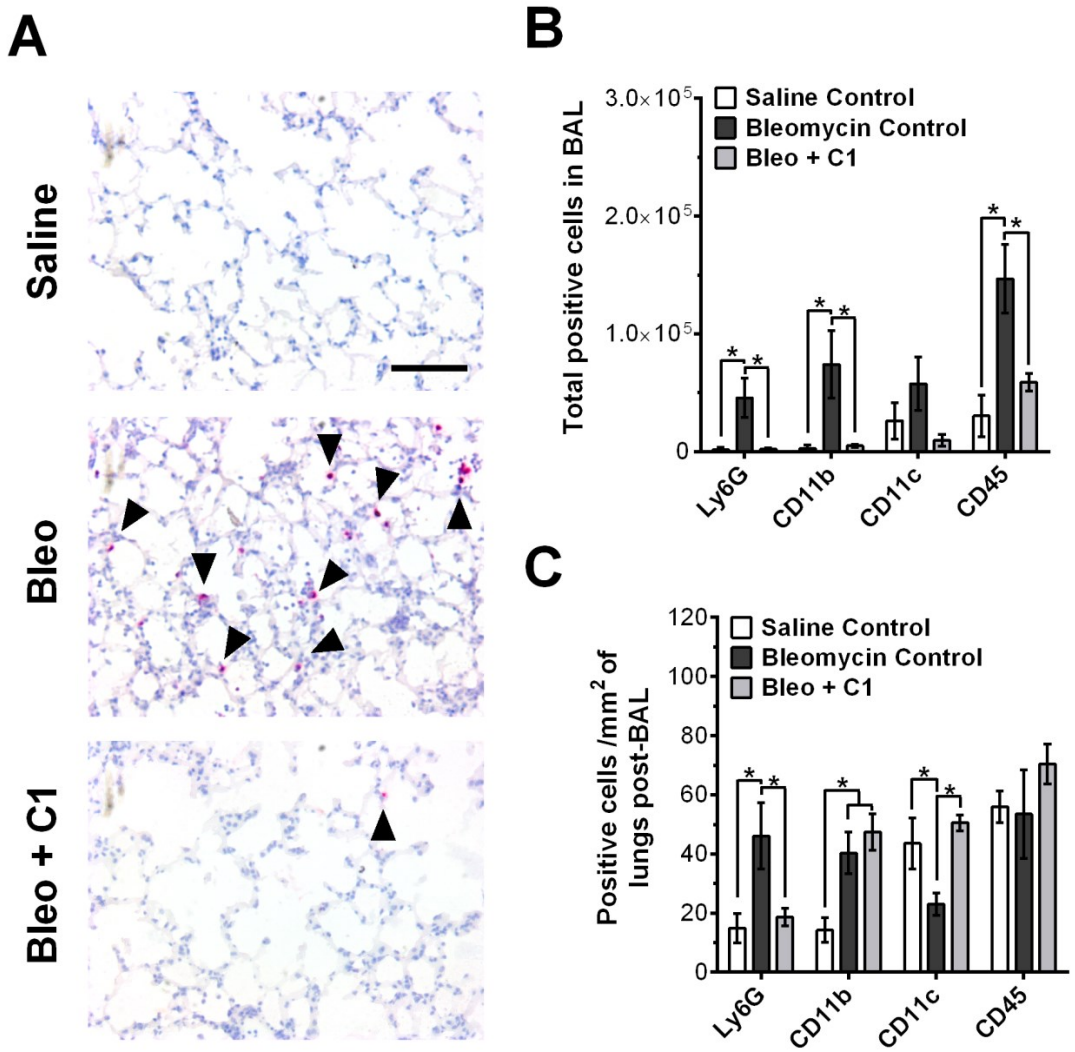

Figure 17: Compound 1 decreases neutrophil accumulation in the lungs of mice following bleomycin treatment.

A) C57BL/6 mice received oropharyngeal bleomycin on day 0 to induce acute respiratory distress syndrome. The control mice received saline. Mice were then treated with intraperitoneal injections of 0.1 mg/kg of compound 1 (C1) or an equal volume of vehicle control on days 1 and 2. On day 3 the mice were euthanized and lungs after BAL were stained for the neutrophil marker Ly6G. Images are representative of 3 independent experiments. Bar is 100 µm. **B**) BAL cells were stained for the indicated markers, n=4. **C**) After collecting the BAL, lungs were stained for the indicated markers, n=4. **P*<0.05 (1-way ANOVA, Holm-Bonferroni posttest). (**B-C**) Values are mean ± SEM.

18, C and D). These data suggest that compound 1, similar to SAP, can alleviate pulmonary fibrosis and inflammation in mice.

Interleukin 10 deficient mice are insensitive to the anti-inflammatory effect of compound 1

Interleukin-10 (IL-10) is an anti-inflammatory cytokine that is released in response to DC-SIGN activation (118). IL-10 is also necessary for the anti-fibrotic effect of SAP in a mouse model of renal fibrosis (23, 64). As compound 1 activates DC-SIGN and mimics some SAP functions, we examined the efficacy of compound 1 on pulmonary fibrosis in IL-10 deficient mice. In IL-10 deficient mice, bleomycin instillation significantly increased collagen deposition and $CD11b^+$ and CD11c+ macrophages in lungs (Fig. 19). Oropharyngeal instillation of bleomycin also resulted in significant decrease in body weight (Fig. S10B). Daily injections of 0.1 mg/kg of compound 1 had no significant effect on collagen deposition, $CD11b^+$ macrophage accumulation, $CD11c^+$ cell accumulation, or body weight in IL-10 deficient mice (Fig. 19 and Fig. S10B). These results suggest that IL-10 is necessary for the anti-fibrotic effects of compound 1 in a mouse bleomycin model of pulmonary fibrosis.

Lung conducting airway epithelial cells express SIGNR-R1 and IL-10

Since compound 1 binds SIGN-R1 to regulate monocyte functions in mice, we examined the expression of this receptor in mouse lungs. We found that SIGN-R1 was expressed on Epcam-1^+ lung epithelial cells and on $CD45^+$ cells (Fig. 20A). To

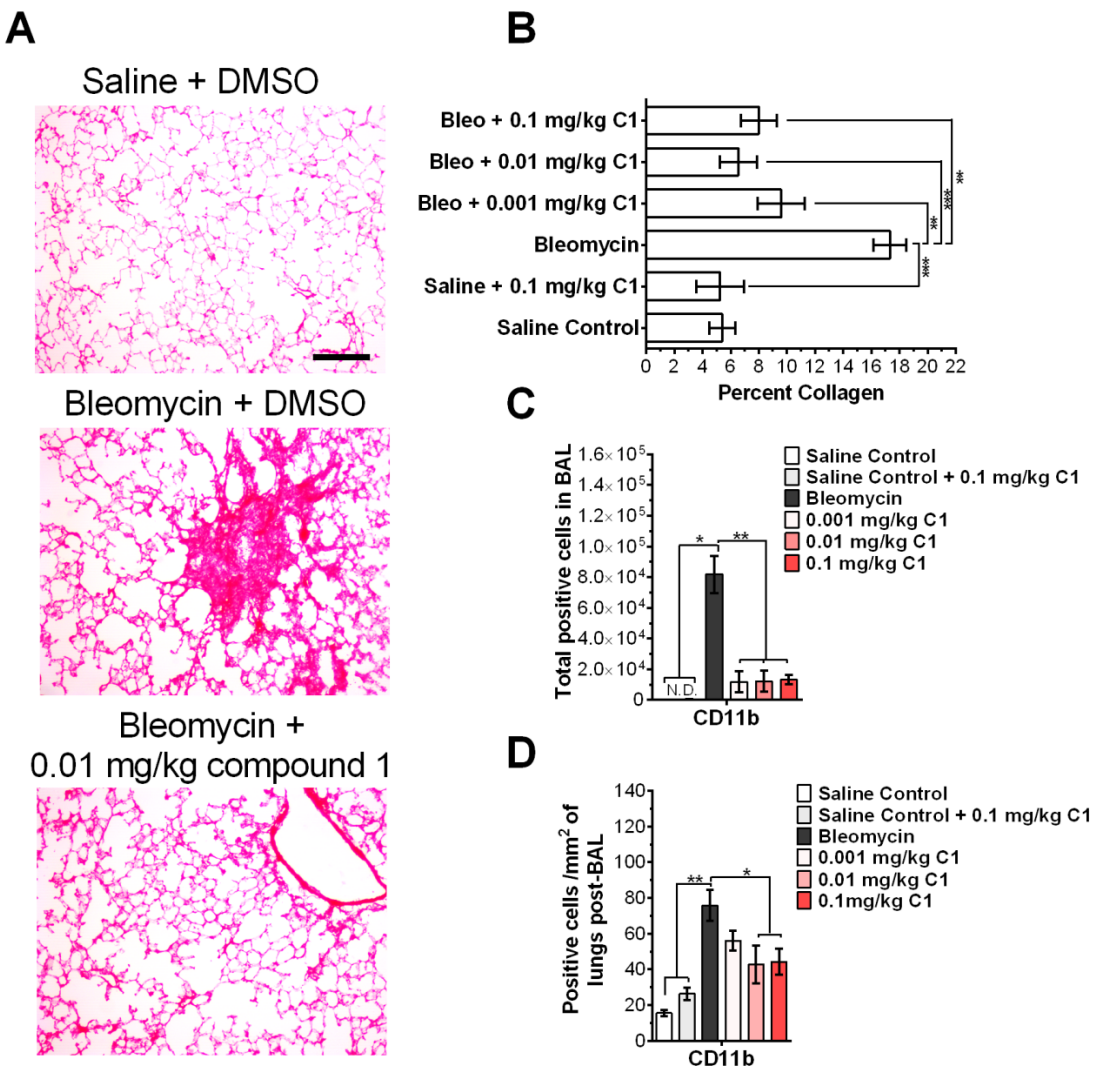

Figure 18: Compound 1 alleviates pulmonary fibrosis in mice.
A) C57BL/6 mice received oropharyngeal bleomycin (Bleo) on day 0 to induce pulmonary fibrosis. Control mice received saline. Mice were then injected with compound 1 (C1) or vehicle control at the indicated dose daily starting on day 1 and ending on day 20. On day 21, mice were euthanized and after collecting BAL fluid, lungs were stained with PicroSirius red to estimate collagen deposition. Images are representative of 3 different experiments. Bar is 200 µm. **B**) Quantification of PicroSirius red staining, n=3. **C**) BAL cell were stained for CD11b, n=3. Rat IgG1 was used as the isotype control. **D**) After collecting BAL, lungs were stained for CD11b, n=3. **P*<0.05, ***P*<0.01, ****P*<0.001(1-way ANOVA, Holm-Bonferroni posttest). (**B-D**) Values are mean ± SEM.

determine the source of IL-10, we stained mouse lungs for Epcam-1, CD45, and IL-10 by immunofluorescence. In saline treated mice, Epcam-1^+ epithelial cells but not $CD45^+$ immune cells expressed detectable levels of IL-10 (Fig. 20, B and C). However when mice were treated with bleomycin, the number of IL-10-expressing epithelial cells (Epcam-1^+) significantly decreased (Fig. 20D). This decrease in IL-10^+ Epcam-1^+ cells was reversed when mice were injected with compound 1 or SAP (Fig. 20D). These results suggest that compound 1 and SAP can bind to SIGN-R1 on Epcam-1^+ epithelial cells to induce IL-10 expression and reduce inflammation.

Discussion

SAP and CRP bind FcγR and regulate the innate immune system and fibrosis (23, 83, 108). In this report, we found that in the absence of all FcγR, SAP still reduces neutrophil adhesion, inhibits fibrocyte differentiation, and alters macrophage phenotype. Conversely, CRP requires FcγR to reduce neutrophil adhesion and promote IL-10 secretion by macrophages, but not to increase ICAM-I^+ macrophages. These results indicate that FcγR mediate only a few aspect of SAP function, but many effects of CRP. These observations suggest the presence of additional pentraxin receptors. We identified an additional SAP receptor as DC-SIGN, found that SAP binds to this receptor through its glycosylation, and observed that a DC-SIGN ligand mimics some SAP functions *in vitro* and in animal models of acute lung injury and pulmonary fibrosis. The DC-SIGN ligand alleviates pulmonary fibrosis in mice through an IL-10 dependent mechanism, with the IL-10 most likely originating from the epithelial cells in the lungs. The effect of

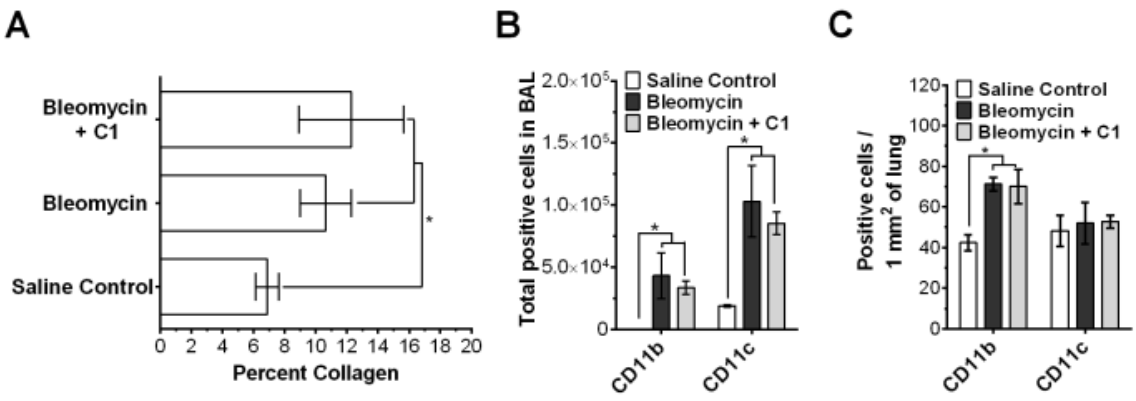

Figure 19: Interleukin-10 is necessary for the anti-fibrotic effect of compound 1. **A**) IL-10 deficient mice were given oropharyngeal bleomycin or saline (control) on day 0. The bleomycin-treated mice were injected with 0.1 mg/kg compound 1 (C1) or an equal volume of vehicle control daily starting on day 1 and ending on day 20. On day 21, mice were euthanized and after collecting BAL fluid, lungs were stained with PicroSirius red to estimate collagen deposition, n=3. **B**) BAL cells were stained for the indicated markers, n=3. Rat IgG1 was used as the isotype control. **C**) After collecting BAL, lungs were stained for the indicated markers, n=3. **P*<0.05 (1-way ANOVA, Holm-Bonferroni posttest). (**A-C**) Values are mean ± SEM.

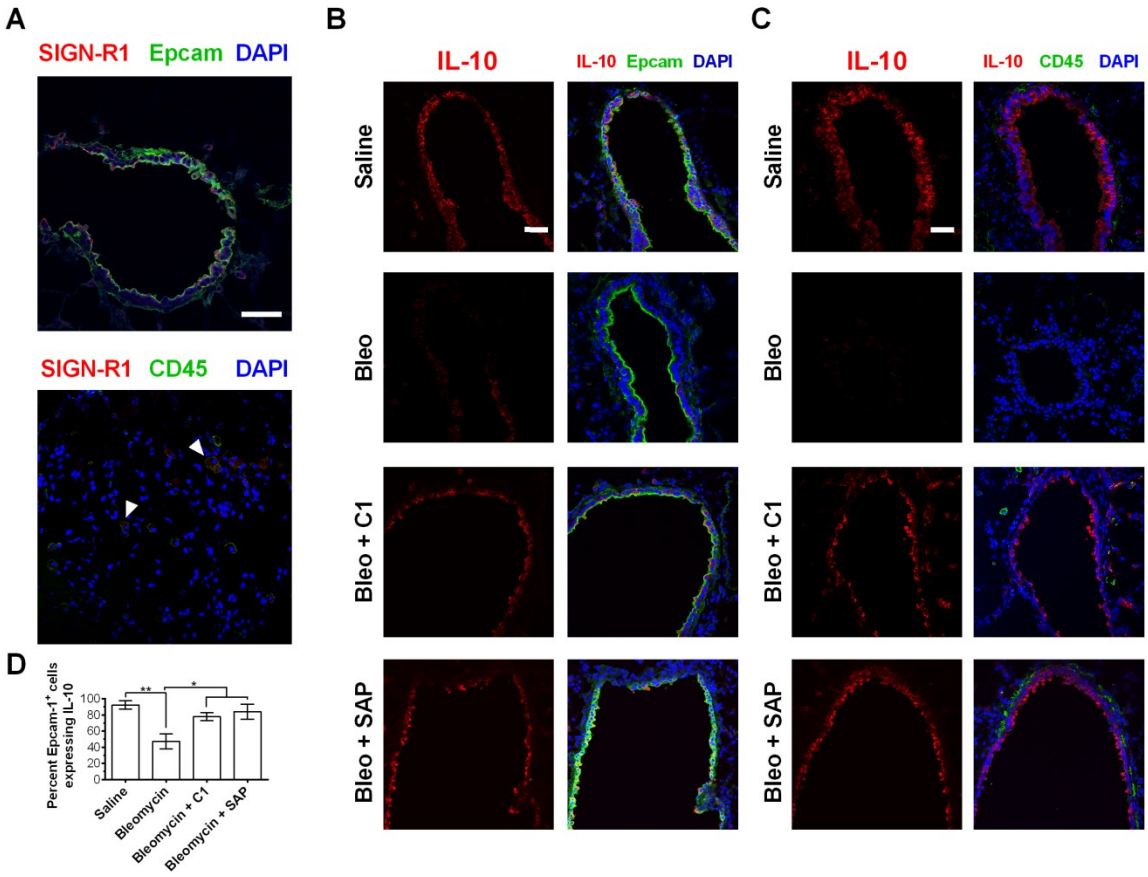

Figure 20: Murine lung epithelial cells express SIGN-R1 and IL-10.
A) Mouse lungs following BAL were stained for the indicated markers. Images are representative of 3 different experiments. Bar is 50 µm. **B**) Mouse lungs were stained for Epcam-1 and IL-10. Images are representative of 3 different experiments. Bar is 50 µm. **C**) The expression of CD45 and IL-10 in mouse lungs post-BAL was assessed by immunofluorescence. Images are representative of 3 different experiments. Bar is 50 µm. **D**) The number of Epcam-1^+ cells expressing IL-10 in mouse lungs after BAL was quantified and compared between different treatment groups, n=3. **P*<0.05, ***P*<0.01, (1-way ANOVA, Holm-Bonferroni posttest). (**D**) Values are mean ± SEM.

CRP on the expression of ICAM-I on macrophages appeared to be independent of FcγR, and since CRP does not bind DC-SIGN, an unknown receptor thus mediates some CRP signaling.

The FcγR have been viewed as the main targets for SAP and CRP in the innate immune system (10, 83). Our data counter this view, as SAP is able to regulate the innate immune cells in absence of all FcγR. In fact, SAP is a more potent polarizer of FcγR deficient macrophages than WT macrophages, suggesting that some of the FcγR may counteract the effect of SAP. In agreement with this, anti-DC-SIGN antibodies, which interact with both FcγR and DC-SIGN, reduced but did not abolish neutrophil adhesion, whereas a DC-SIGN ligand completely abolished this adhesion. A similar trend was observed with SAP, which is a more potent inhibitor of FcγR deficient neutrophil adhesion than WT neutrophils. However, this effect of FcγR appears to be cell-type dependent as both the FcγR and DC-SIGN seem to act cooperatively to inhibit monocyte to fibrocyte differentiation. Both DC-SIGN and FcγR regulate the activity of Src kinases in innate immune cells (84, 128). The antagonism of DC-SIGN and FcγR signaling in some cells, and the cooperativity of DC-SIGN and FcγR signaling in other cells, may thus be due to their differential effects on Src kinases.

Although DC-SIGN/ SIGN-R1 is considered to be primarily expressed by innate immune system cells, the majority of SIGN-R1 staining in mouse lungs was on Epcam-1^+ epithelial cells. These SIGN-$R1^+$ Epcam-1^+ expressed high levels of IL-10. Following a bleomycin insult, at day 21, although there was no appreciable reduction in the number

of Epcam-1+ cells, there was a significant decrease in the number of IL-10^+ Epcam-1^+ cells. IL-10 inhibits apoptosis of epithelial cells (129) and increases the clearance of cell debris (130). As such, up-regulation of IL-10 by SAP or compound 1 may have a protective effect on lungs by limiting tissue damage and inflammatory responses. A similar role has been previously observed for epithelial cell-derived IL-10 in mouse models of inflammatory bowel disease (131). Alternatively, it is possible that IL-10 expression in SIGN-$R1^+$ epithelial cells is a function of their health. However, this is unlikely because our studies in IL-10 deficient mice suggest a critical role for IL-10 in the anti-fibrotic role of compound 1.

Together, our data indicate that SAP binds DC-SIGN/SIGN-R1 to regulate innate immune cells and epithelial cells. Through its interaction with DC-SIGN, SAP distinguishes itself functionally from CRP. This suggests that DC-SIGN/SIGN-R1 is a key regulator of the innate immune system and is thus an interesting therapeutic target. Additionally, the functional interaction of SAP and PTX3 with DC-SIGN suggest that these pentraxins may regulate dendritic cells, and thus possibly the adaptive immune system.

CHAPTER IV

CONCLUSIONS AND FUTURE DIRECTIONS

Conclusions

Fibrosing diseases such scleroderma, pulmonary fibrosis, and renal fibrosis are caused by aberrant scar tissue formation in internal organs and are associated with 45% of deaths in the U.S. (73). The two short pentraxins Serum Amyloid P (SAP) and C-reactive protein (CRP) regulate fibrosis by effecting neutrophils, monocytes, and macrophages (20, 23, 25, 64, 100). All SAP and CRP functions are thought to be mediated through Fcγ receptors which include the FcγRI, FcγRII, and FcγRIII (23, 57, 58). However, despite extensive similarities between SAP and CRP and their comparable affinities for the FcγR, they generally have opposing effects on the innate immune system. What causes these functional differences is not known.

In the work presented in this dissertation, I found through site-directed mutagenesis that SAP effects fibrocyte differentiation and neutrophil adhesion in part by binding FcγRI on monocytes and FcγRIIa on neutrophils. Further experimentation revealed that FcγR are not necessary for SAP effects as in the absence of all FcγR, SAP still reduced neutrophil adhesion, inhibited fibrocyte differentiation, and altered macrophage phenotype. Conversely, CRP required FcγR to reduce neutrophil adhesion and promote IL-10 secretion by macrophages, but not to alter macrophage phenotype. These results indicate that FcγR play a more significant role in CRP responses than in SAP effects providing a potential explanation for the difference in SAP and CRP

function. These observations also indicate the presence of additional SAP and CRP receptors. I identified DC-SIGN as a novel SAP receptor, found that SAP bound to this receptor through its glycosylation, and observed that a DC-SIGN ligand mimics SAP functions *in vitro* and in animal models of acute lung injury and pulmonary fibrosis. The DC-SIGN ligand alleviated pulmonary fibrosis in mice through an IL-10 dependent mechanism, with the IL-10 most likely originating from the epithelial cells in the lungs. Together, the results in this dissertation indicate that SAP binds to DC-SIGN to regulate the innate immune system differently from CRP, and that DC-SIGN ligands and antibodies can be used as novel anti-fibrotic therapies.

The data presented in this dissertation indicate that DC-SIGN is the main mediator of SAP effect while the FcγR play a secondary role. These findings are in stark contrast to the current model of pentraxin function which suggests that SAP and CRP affect the innate immune system mainly through the FcγR. However, despite the apparent contradiction the data presented here does not refute the previous studies on the role of FcγR in SAP signaling. It simply challenges the interpretation of those studies. Previous studies have examined the role of FcγR in SAP function by using Fcε common γ-chain deficient mice that have defects in FcγR signaling (23, 107). The results from these studies were used to suggest a role of FcγR in SAP signaling. However, only two out of the four FcγR use the common γ-chain (84). Furthermore, excluding the FcγR there are additional ~10 receptors that use the common γ-chain for signaling (132). Therefore, *in vivo* studies on γ-chain deficient mice cannot be used to clearly indicate the

role of FcγR in pentraxin response. These studies simply suggest a role for γ-chain dependent signaling in SAP function.

Glycosylated proteins bind DC-SIGN in a Ca^{2+} dependent manner to activate the receptor and initiate a signal transduction pathway that involves the Src family of kinases(118). The activation of Src kinase by DC-SIGN ultimately leads to up-regulation of anti-inflammatory proteins such as IL-10. The FcγR also use the Src family of kinases to affect immune response (84). The convergence of DC-SIGN and FcγR signaling at Src kinases suggest a hypothetical mechanism by which activation of FcγR can alter DC-SIGN signaling. In accordance with this hypothetical DC-SGIN-FcγR cross talk, I observe that in FcγR deficient macrophages, SAP was a more potent polarizer of macrophages suggesting that FcγR signaling may antagonize DC-SIGN activation by SAP. A similar trend was observed with neutrophils where FcγR deficient cells were modestly more sensitive to SAP. Conversely, SAP seems to require both the FcγR and DC-SIGN to completely inhibit fibrocyte differentiation from monocytes. Therefore, although FcγR may not be necessary for SAP responses, the activation of FcγR by SAP may regulate signaling by DC-SIGN.

In this dissertation, I observed that SIGN-$R1^+$ Epcam-1^+ epithelial cells express high levels of IL-10 under non-inflammatory conditions. However, following a bleomycin insult, there was a significant decrease in the number of IL-10^+ Epcam-1^+ cells. IL-10 inhibits apoptosis of epithelial cells (129) and increases the clearance of cell debris (130). As such, up-regulation of IL-10 by SAP or compound 1 (DC-SIGN ligand)

may have a protective effect on lungs by limiting tissue damage and inflammatory responses. A similar role has been previously observed for epithelial cell-derived IL-10 in mouse models of inflammatory bowel disease (131). In agreement with this, in IL-10 deficient mice our DC-SIGN ligand has no anti-fibrotic effect.

DC-SIGN/ SIGN-R1 is considered to be primarily expressed by innate immune cells(118). However, SIGN-R1 staining in mouse lungs revealed that Epcam-1^{+} epithelial cells were the main source of this receptor. In humans, in addition to DC-SIGN which is mainly found on immune cells there is L-SIGN. The C-type lectin L-SIGN has a similar ligand recognition profile to DC-SIGN (118). But, L-SIGN is mainly found on liver endothelial cells and lung cells (118, 133). Hence, SIGN-R1 on mouse lung epithelial cells may be functionally equivalent to L-SIGN and not DC-SIGN in humans.

DC-SIGN/SIGN-R1 is found on the surface of dendritic cells, monocytes, macrophages, neutrophils, lung epithelial cells, and a subpopulation of lymphocytes in the blood ((118) and Fig S5). The observation that SAP binds to DC-SIGN suggest novel targets of this protein in the body. In particular, the presence of DC-SIGN on dendritic cells and .a sub-population of lymphocytes indicates a direct mechanism by which SAP may alter an adaptive immune response. Furthermore, the potential regulation of epithelial cells by SAP is significant as not much is understood about how the immune system regulates the epithelial cells under normal and diseased conditions (134).

This dissertation suggests that despite the current model, FcγR receptors are dispensable for SAP function. SAP primarily uses DC-SIGN/SIGN-R1 to regulate innate immune cells and epithelial cells. Also, through its interaction with DC-SIGN, SAP distinguishes itself functionally from CRP explaining why two closely related proteins have opposite functions. Lastly, the data presented here suggest that DC-SIGN/SIGN-R1 is a key regulator of the innate immune system and is thus an interesting therapeutic target.

Future work

There are number of ways the work in this dissertation can be developed. Some are as followed:

1. In absence of the FcγR, macrophages respond to CRP. However, CRP does not bind DC-SIGN.
    a. Hence, what is the unknown CRP receptor on macrophages?
    b. How does this receptor regulate CRP responses in other cell types?
    c. What happens to immune responses when this CRP receptors in deleted from mice?
2. SAP and PTX3 interact with DC-SIGN.
    a. How do DC-SIGN deficient mice respond to SAP and PTX3?
    b. Does lacking DC-SIGN make the mice more susceptible to fibrosis or autoimmune disorders?

3. DC-SIGN activation has been shown to alleviate a multitude of immune related diseases such as inflammatory bowel disease. How would SAP affect these inflammatory disorders?
4. SAP affects DC-SIGN^{+} epithelial cells in the lungs. A subpopulation of these DC-SIGN+ cells belong to type II alveolar cells that are differentiate and form other epithelial cells. These type II alveolar cells are implicated in lung regeneration and maintenance. How SAP affects the type II epithelial cells will provide valuable insight into how lungs are maintained and how they respond to infections and injuries.
5. FcγR receptors seem to antagonize SAP signaling in mice.
    a. What are the underlying elements that contribute to this effect?
    b. How would mice respond to high levels of SAP in absence of all FcγR receptors?
6. SAP reduces neutrophil adhesion partly through its glycosylation which binds to DC-SIGN.
    a. How does this interaction reduce adhesion?
    b. Is DC-SIGN an adhesion receptor that SAP blocks?
    c. Does DC-SIGN activation lead to downstream events that alter neutrophil responses?
    d. How does SAP reduce neutrophil recruitment in mice?

7. IL-10 is necessary for the anti-fibrotic effect of compound 1. But does IL-10 truly originate from epithelial cells? What would happen if IL-10 is knocked out in epithelial cells vs immune cells?
8. SAP binds to FcγR and DC-SIGN. How would deleting all FcγR and DC-SIGN affect SAP, CRP and PTX3 responses?
9. There are 8 DC-SIGN receptors in mice. Do all bind SAP and contribute to its function?
10. DC-SIGN and FcγR signaling seem to converge on the Src kinases. How do the FcγR and DC-SIGN "talk" to each other?

REFERENCES

1. Janeway, C. A., Jr., and R. Medzhitov. 2002. Innate immune recognition. *Annu Rev Immunol* 20: 197-216.
2. Boehm, T. 2012. Evolution of vertebrate immunity. *Curr Biol:* 22: R722-732.
3. Mantovani, A., S. K. Biswas, M. R. Galdiero, A. Sica, and M. Locati. 2013. Macrophage plasticity and polarization in tissue repair and remodelling. *J Pathol* 229: 176-185.
4. Deban, L., S. Jaillon, C. Garlanda, B. Bottazzi, and A. Mantovani. 2011. Pentraxins in innate immunity: lessons from PTX3. *Cell Tissue Res* 343: 237-249.
5. Tillett, W. S., and T. Francis. 1930. Serological reactions in pneumonia with a non-protein somatic fraction of pneumococcus. *J Exp Med* 52: 561-571.
6. de Haas, C. J., M. E. van der Tol, K. P. Van Kessel, J. Verhoef, and J. A. Van Strijp. 1998. A synthetic lipopolysaccharide-binding peptide based on amino acids 27-39 of serum amyloid P component inhibits lipopolysaccharide-induced responses in human blood. *J Immunol* 161: 3607-3615.
7. Litvack, M. L., and N. Palaniyar. 2010. Review: Soluble innate immune pattern-recognition proteins for clearing dying cells and cellular components: implications on exacerbating or resolving inflammation. *Innate Immun* 16: 191-200.
8. Robey, F. A., and T. Y. Liu. 1981. Limulin: a C-reactive protein from *Limulus polyphemus*. *J Biol Chem* 256: 969-975.

9. Deban, L., B. Bottazzi, C. Garlanda, Y. M. de la Torre, and A. Mantovani. 2009. Pentraxins: multifunctional proteins at the interface of innate immunity and inflammation. *BioFactors* 35: 138-145.

10. Du Clos, T. W. 2013. Pentraxins: Structure, function, and role in inflammation. *ISRN Inflammation* 2013: 379040.

11. Mantovani, A., S. Valentino, S. Gentile, A. Inforzato, B. Bottazzi, and C. Garlanda. 2013. The long pentraxin PTX3: a paradigm for humoral pattern recognition molecules. *Ann N Y Acad Sci* 1285: 1-14.

12. Martinez de la Torre, Y., M. Fabbri, S. Jaillon, A. Bastone, M. Nebuloni, A. Vecchi, A. Mantovani, and C. Garlanda. 2010. Evolution of the pentraxin family: the new entry PTX4. *J Immunol* 184: 5055-5064.

13. Hutchinson, W. L., E. Hohenester, and M. B. Pepys. 2000. Human serum amyloid P component is a single uncomplexed pentamer in whole serum. *Mol med* 6: 482-493.

14. Noursadeghi, M., M. C. Bickerstaff, J. R. Gallimore, J. Herbert, J. Cohen, and M. B. Pepys. 2000. Role of serum amyloid P component in bacterial infection: protection of the host or protection of the pathogen. *Proc Natl Acad Sci U S A* 97: 14584-14589.

15. Mold, C., H. Gewurz, and T. W. Du Clos. 1999. Regulation of complement activation by C-reactive protein. *Immunopharmacology* 42: 23-30.

16. Ying, S. C., A. T. Gewurz, H. Jiang, and H. Gewurz. 1993. Human serum amyloid P component oligomers bind and activate the classical complement

pathway via residues 14-26 and 76-92 of the A chain collagen-like region of C1q. *J Immunol* 150: 169-176.

17. Kolaczkowska, E., and P. Kubes. 2013. Neutrophil recruitment and function in health and inflammation. *Nat Rev Immunol* 13: 159-175.

18. Montecucco, F., S. Steffens, F. Burger, A. Da Costa, G. Bianchi, M. Bertolotto, F. Mach, F. Dallegri, and L. Ottonello. 2008. Tumor necrosis factor-alpha (TNF-alpha) induces integrin CD11b/CD18 (Mac-1) up-regulation and migration to the CC chemokine CCL3 (MIP-1alpha) on human neutrophils through defined signalling pathways. *Cell Sig* 20: 557-568.

19. Leonard, E. J., and T. Yoshimura. 1990. Neutrophil attractant/activation protein-1 (NAP-1 [interleukin-8]). *Am J Respir Cell Mol Biol* 2: 479-486.

20. Maharjan, A. S., D. Roife, D. Brazill, and R. H. Gomer. 2013. Serum amyloid P inhibits granulocyte adhesion. *Fibro Tissue Repair* 6: 2.

21. Galkina, E. V., P. G. Nazarov, A. V. Polevschikov, L. K. Berestovaya, V. E. Galkin, and N. V. Bychkova. 2000. Interactions of c-reactive protein and serum amyloid p component with interleukin-8 and their role in regulation of Neutrophil Functions. *Russ Jour of Immunol* 5: 363-374.

22. Stibenz, D., M. Grafe, N. Debus, M. Hasbach, I. Bahr, K. Graf, E. Fleck, U. Thanabalasingam, and C. Buhrer. 2006. Binding of human serum amyloid P component to L-selectin. *Eur J Immunol* 36: 446-456.

23. Castaño, A. P., S. L. Lin, T. Surowy, B. T. Nowlin, S. A. Turlapati, T. Patel, A. Singh, S. Li, M. L. Lupher Jr, and J. S. Duffield. 2009. Serum amyloid P inhibits

fibrosis through Fc gamma R-dependent monocyte-macrophage regulation *in vivo*. *Sci Transl Med* 1: 5ra13.

24. Mold, C., H. D. Gresham, and T. W. Du Clos. 2001. Serum amyloid P component and C-reactive protein mediate phagocytosis through murine Fc gamma Rs. *J Immunol* 166: 1200-1205.

25. Bharadwaj, D., C. Mold, E. Markham, and T. W. Du Clos. 2001. Serum amyloid P component binds to Fc gamma receptors and opsonizes particles for phagocytosis. *J Immunol* 166: 6735-6741.

26. Bruhns, P., B. Iannascoli, P. England, D. A. Mancardi, N. Fernandez, S. Jorieux, and M. Daeron. 2009. Specificity and affinity of human Fcgamma receptors and their polymorphic variants for human IgG subclasses. *Blood* 113: 3716-3725.

27. Nimmerjahn, F., and J. V. Ravetch. 2006. Fcgamma receptors: old friends and new family members. *Immunity* 24: 19-28.

28. Chi, M., S. Tridandapani, W. Zhong, K. M. Coggeshall, and R. F. Mortensen. 2002. C-reactive protein induces signaling through Fc gamma RIIa on HL-60 granulocytes. *J Immunol* 168: 1413-1418.

29. Abram, C. L., and C. A. Lowell. 2009. The ins and outs of leukocyte integrin signaling. *Annu Rev Immunol* 27: 339-362.

30. Dewitt, S., R. J. Francis, and M. B. Hallett. 2013. Ca(2)(+) and calpain control membrane expansion during the rapid cell spreading of neutrophils. *J Cell Sci* 126: 4627-4635.

31. Ley, K., C. Laudanna, M. I. Cybulsky, and S. Nourshargh. 2007. Getting to the site of inflammation: the leukocyte adhesion cascade updated. *Nat Rev Immunol* 7: 678-689.

32. Sengupta, K., H. Aranda-Espinoza, L. Smith, P. Janmey, and D. Hammer. 2006. Spreading of neutrophils: from activation to migration. *Biophys J* 91: 4638-4648.

33. Lokuta, M. A., and A. Huttenlocher. 2005. TNF-alpha promotes a stop signal that inhibits neutrophil polarization and migration via a p38 MAPK pathway. *J Leukoc Biol* 78: 210-219.

34. van den Berg, J. M., F. P. Mul, E. Schippers, J. J. Weening, D. Roos, and T. W. Kuijpers. 2001. Beta1 integrin activation on human neutrophils promotes beta2 integrin-mediated adhesion to fibronectin. *Eur J Immunol* 31: 276-284.

35. Furie, M. B., M. C. Tancinco, and C. W. Smith. 1991. Monoclonal antibodies to leukocyte integrins CD11a/CD18 and CD11b/CD18 or intercellular adhesion molecule-1 inhibit chemoattractant-stimulated neutrophil transendothelial migration *in vitro*. *Blood* 78: 2089-2097.

36. Sandhaus, R. A., and G. Turino. 2013. Neutrophil elastase-mediated lung disease. *COPD* 10 Suppl 1: 60-63.

37. Vachino, G., L. W. Heck, J. A. Gelfand, M. M. Kaplan, J. F. Burke, R. W. Berninger, and K. P. McAdam. 1988. Inhibition of human neutrophil and Pseudomonas elastases by the amyloid P-component: a constituent of elastic fibers and amyloid deposits. *J Leukoc Biol* 44: 529-534.

38. Takai, S., K. Kimura, M. Nagaki, S. Satake, K. Kakimi, and H. Moriwaki. 2005. Blockade of neutrophil elastase attenuates severe liver injury in hepatitis B transgenic mice. *J Virol* 79: 15142-15150.

39. Korkmaz, B., M. S. Horwitz, D. E. Jenne, and F. Gauthier. 2010. Neutrophil elastase, proteinase 3, and cathepsin G as therapeutic targets in human diseases. *Pharma Reviews* 62: 726-759.

40. Takemasa, A., Y. Ishii, and T. Fukuda. 2012. A neutrophil elastase inhibitor prevents bleomycin-induced pulmonary fibrosis in mice. *The Eur Res J* 40: 1475-1482.

41. Wertheim, W. A., S. L. Kunkel, T. J. Standiford, M. D. Burdick, F. S. Becker, C. A. Wilke, A. R. Gilbert, and R. M. Strieter. 1993. Regulation of neutrophil-derived IL-8: the role of prostaglandin E2, dexamethasone, and IL-4. *J Immunol* 151: 2166-2175.

42. Tryzmel, J., V. Miskolci, S. Castro-Alcaraz, I. Vancurova, and D. Davidson. 2003. Interleukin-10 inhibits proinflammatory chemokine release by neutrophils of the newborn without suppression of nuclear factor-kappa B. *Pediatric Research* 54: 382-386.

43. Shanley, T. P., N. Vasi, and A. Denenberg. 2000. Regulation of chemokine expression by IL-10 in lung inflammation. *Cytokine* 12: 1054-1064.

44. Geissmann, F., M. G. Manz, S. Jung, M. H. Sieweke, M. Merad, and K. Ley. 2010. Development of monocytes, macrophages, and dendritic cells. *Sci* 327: 656-661.

45. Reilkoff, R. A., R. Bucala, and E. L. Herzog. 2011. Fibrocytes: emerging effector cells in chronic inflammation. *Nat Rev Immunol* 11: 427-435.

46. Schmidt, M., G. Sun, M. A. Stacey, L. Mori, and S. Mattoli. 2003. Identification of circulating fibrocytes as precursors of bronchial myofibroblasts in asthma. *J Immunol* 171: 380-389.

47. Sakai, N., K. Furuichi, Y. Shinozaki, H. Yamauchi, T. Toyama, S. Kitajima, T. Okumura, S. Kokubo, M. Kobayashi, K. Takasawa, S. Takeda, M. Yoshimura, S. Kaneko, and T. Wada. 2010. Fibrocytes are involved in the pathogenesis of human chronic kidney disease. *Hum Pathol* 41: 672-678.

48. Aiba, S., and H. Tagami. 1997. Inverse correlation between CD34 expression and proline-4-hydroxylase immunoreactivity on spindle cells noted in hypertrophic scars and keloids. *J Cutan Pathol* 24: 65-69.

49. Cowper, S. E. 2003. Nephrogenic fibrosing dermopathy: the first 6 years. *Current Opinion in Rheumatology* 15: 785-790.

50. Wang, J. F., H. Jiao, T. L. Stewart, H. A. Shankowsky, P. G. Scott, and E. E. Tredget. 2007. Fibrocytes from burn patients regulate the activities of fibroblasts. *Wound Repair Regen* 15: 113-121.

51. Shao, D. D., R. Suresh, V. Vakil, R. H. Gomer, and D. Pilling. 2008. Pivotal advance: Th-1 cytokines inhibit, and Th-2 cytokines promote fibrocyte differentiation. *J Leukoc Biol* 83: 1323-1333.

52. Maharjan, A. S., D. Pilling, and R. H. Gomer. 2011. High and low molecular weight hyaluronic acid differentially regulate human fibrocyte differentiation. *PloS one* 6: e26078.

53. Maharjan, A. S., D. Pilling, and R. H. Gomer. 2010. Toll-like receptor 2 agonists inhibit human fibrocyte differentiation. *Fibro Tissue Repair* 3: 23.

54. Pilling, D., C. D. Buckley, M. Salmon, and R. H. Gomer. 2003. Inhibition of fibrocyte differentiation by serum amyloid P. *J Immunol* 171: 5537-5546.

55. Gomer, R. H., D. Pilling, L. M. Kauvar, S. Ellsworth, S. D. Ronkainen, D. Roife, and S. C. Davis. 2009. A serum amyloid P-binding hydrogel speeds healing of partial thickness wounds in pigs. *Wound Repair Regen* 17: 397-404.

56. Pilling, D., D. Roife, M. Wang, S. D. Ronkainen, J. R. Crawford, E. L. Travis, and R. H. Gomer. 2007. Reduction of bleomycin-induced pulmonary fibrosis by serum amyloid P. *J Immunol* 179: 4035-4044.

57. Crawford, J. R., D. Pilling, and R. H. Gomer. 2012. FcgammaRI mediates serum amyloid P inhibition of fibrocyte differentiation. *J Leukoc Biol* 92: 699-711.

58. Pilling, D., N. M. Tucker, and R. H. Gomer. 2006. Aggregated IgG inhibits the differentiation of human fibrocytes. *J Leukoc Biol* 79: 1242-1251.

59. Haudek, S. B., J. Trial, Y. Xia, D. Gupta, D. Pilling, and M. L. Entman. 2008. Fc receptor engagement mediates differentiation of cardiac fibroblast precursor cells. *Proc Natl Acad Sci U S A* 105: 10179-10184.

60. Mosser, D. M., and J. P. Edwards. 2008. Exploring the full spectrum of macrophage activation. *Nat Rev Immunol* 8: 958-969.

61. Sica, A., and A. Mantovani. 2012. Macrophage plasticity and polarization: in vivo veritas. *J Clin Invest* 122: 787-795.

62. Sica, A. 2010. Role of tumour-associated macrophages in cancer-related inflammation. *Exp Onc* 32: 153-158.

63. Mantovani, A., A. Sica, S. Sozzani, P. Allavena, A. Vecchi, and M. Locati. 2004. The chemokine system in diverse forms of macrophage activation and polarization. *Trends Immunol* 25: 677-686.

64. Zhang, W., W. Xu, and S. Xiong. 2011. Macrophage differentiation and polarization via phosphatidylinositol 3-kinase/Akt-ERK signaling pathway conferred by serum amyloid P component. *J Immunol* 187: 1764-1777.

65. Gordon, S., and P. R. Taylor. 2005. Monocyte and macrophage heterogeneity. *Nat Rev Immunol* 5: 953-964.

66. Auffray, C., M. H. Sieweke, and F. Geissmann. 2009. Blood monocytes: development, heterogeneity, and relationship with dendritic cells. *Annu Rev Immunol* 27: 669-692.

67. Martinez, F. O., A. Sica, A. Mantovani, and M. Locati. 2008. Macrophage activation and polarization. *Front In Bioscie* 13: 453-461.

68. Quatromoni, J. G., and E. Eruslanov. 2012. Tumor-associated macrophages: function, phenotype, and link to prognosis in human lung cancer. *Amer J of Trans Res* 4: 376-389.

69. Balkwill, F. R., and A. Mantovani. 2012. Cancer-related inflammation: common themes and therapeutic opportunities. *Sem In Can Bio* 22: 33-40.

70. Murray, L. A., Q. Chen, M. S. Kramer, D. P. Hesson, R. L. Argentieri, X. Peng, M. Gulati, R. J. Homer, T. Russell, N. van Rooijen, J. A. Elias, C. M. Hogaboam, and E. L. Herzog. 2011. TGF-beta driven lung fibrosis is macrophage dependent and blocked by Serum amyloid P. *Int J Biochem Cell Biol* 43: 154-162.

71. Murray, L. A., R. Rosada, A. P. Moreira, A. Joshi, M. S. Kramer, D. P. Hesson, R. L. Argentieri, S. Mathai, M. Gulati, E. L. Herzog, and C. M. Hogaboam. 2010. Serum amyloid P therapeutically attenuates murine bleomycin-induced pulmonary fibrosis via its effects on macrophages. *PloS one* 5: e9683.

72. Moreira, A. P., K. A. Cavassani, R. Hullinger, R. S. Rosada, D. J. Fong, L. Murray, D. P. Hesson, and C. M. Hogaboam. 2010. Serum amyloid P attenuates M2 macrophage activation and protects against fungal spore-induced allergic airway disease. *J Allergy Clin Immunol* 126: 712-721 e717.

73. Wynn, T. A. 2004. Fibrotic disease and the T(H)1/T(H)2 paradigm. *Nat Rev Immunol* 4: 583-594.

74. Schuppan, D., and Y. O. Kim. 2013. Evolving therapies for liver fibrosis. *J Clin Invest* 123: 1887-1901.

75. Du Bois, R. M., S. D. Nathan, L. Richeldi, M. I. Schwarz, and P. W. Noble. 2012. Idiopathic pulmonary fibrosis: lung function is a clinically meaningful endpoint for phase III trials. *Am J Respir Crit Care Med* 186: 712-715.

76. Peisajovich, A., L. Marnell, C. Mold, and T. W. Du Clos. 2008. C-reactive protein at the interface between innate immunity and inflammation. *Exp Rev of Clin Immunol* 4: 379-390.

77. Haudek, S. B., Y. Xia, P. Huebener, J. M. Lee, S. Carlson, J. R. Crawford, D. Pilling, R. H. Gomer, J. Trial, N. G. Frangogiannis, and M. L. Entman. 2006. Bone marrow-derived fibroblast precursors mediate ischemic cardiomyopathy in mice. *Proc Natl Acad Sci U S A* 103: 18284-18289.

78. Dillingh, M. R., B. van den Blink, M. Moerland, M. G. van Dongen, M. Levi, A. Kleinjan, M. S. Wijsenbeek, M. L. Lupher, Jr., D. M. Harper, J. A. Getsy, H. C. Hoogsteden, and J. Burggraaf. 2013. Recombinant human serum amyloid P in healthy volunteers and patients with pulmonary fibrosis. *Pulm Pharmacol Ther* 26: 672-676.

79. Amulic, B., C. Cazalet, G. L. Hayes, K. D. Metzler, and A. Zychlinsky. 2012. Neutrophil function: from mechanisms to disease. *Annu Rev Immunol* 30: 459-489.

80. Stibenz, D., M. Gräfe, N. Debus, M. Hasbach, I. Bahr, K. Graf, E. Fleck, U. Thanabalasingam, and C. Bührer. 2006. Binding of human serum amyloid P componentto L-selectin. *Euro J of Immunol* 36: 446-456.

81. Bucala, R., L. A. Spiegel, J. Chesney, M. Hogan, and A. Cerami. 1994. Circulating fibrocytes define a new leukocyte subpopulation that mediates tissue repair. *Mol Med* 1: 71-81.

82. Quan, T. E., S. E. Cowper, and R. Bucala. 2006. The role of circulating fibrocytes in fibrosis. *Curr Rheumatol Rep* 8: 145-150.

83. Lu, J., L. L. Marnell, K. D. Marjon, C. Mold, T. W. Du Clos, and P. D. Sun. 2008. Structural recognition and functional activation of FcgammaR by innate pentraxins. *Nat* 456: 989-992.

84. Nimmerjahn, F., and J. V. Ravetch. 2008. Fcgamma receptors as regulators of immune responses. *Nat Rew. Immunology* 8: 34-47.

85. Lu, J., K. D. Marjon, L. L. Marnell, R. Wang, C. Mold, T. W. Du Clos, and P. Sun. 2011. Recognition and functional activation of the human IgA receptor (FcalphaRI) by C-reactive protein. *Proc Natl Acad Sci U S A* 108: 4974-4979.

86. Pilling, D., V. Vakil, and R. H. Gomer. 2009. Improved serum-free culture conditions for the differentiation of human and murine fibrocytes. *J Immunol Methods* 351: 62-70.

87. Cox, N., D. Pilling, and R. H. Gomer. 2012. NaCl potentiates human fibrocyte differentiation. *PloS one* 7: e45674.

88. Pilling, D., T. Fan, D. Huang, B. Kaul, and R. H. Gomer. 2009. Identification of markers that distinguish monocyte-derived fibrocytes from monocytes, macrophages, and fibroblasts. *PloS One* 4: e7475.

89. Herlihy, S. E., D. Pilling, A. S. Maharjan, and R. H. Gomer. 2013. Dipeptidyl peptidase IV is a human and murine neutrophil chemorepellent. *J Immunol* 190: 6468-6477.

90. Cormier, C. Y., J. G. Park, M. Fiacco, J. Steel, P. Hunter, J. Kramer, R. Singla, and J. LaBaer. 2011. PSI:Biology-materials repository: a biologist's resource for protein expression plasmids. *J of Strucl and Func Gen* 12: 55-62.

91. Witt, A. E., L. M. Hines, N. L. Collins, Y. Hu, R. N. Gunawardane, D. Moreira, J. Raphael, D. Jepson, M. Koundinya, A. Rolfs, B. Taron, S. J. Isakoff, J. S. Brugge, and J. LaBaer. 2006. Functional proteomics approach to investigate the biological activities of cDNAs implicated in breast cancer. *J Proteome Res* 5: 599-610.

92. Bang, R., L. Marnell, C. Mold, M. P. Stein, K. T. Clos, C. Chivington-Buck, and T. W. Clos. 2005. Analysis of binding sites in human C-reactive protein for Fc{gamma}RI, Fc{gamma}RIIA, and C1q by site-directed mutagenesis. *J Biol Chem* 280: 25095-25102.

93. Ruiz-Arguelles, A., and B. Perez-Romano. 2001. Immunophenotypic analysis of peripheral blood lymphocytes. *Cur Prot in Cytometry* Chapter 6: Unit 6 5.

94. Crawford, J. R., D. Pilling, and R. H. Gomer. 2010. Improved serum-free culture conditions for spleen-derived murine fibrocytes. *J of Immunol Met* 363: 9-20.

95. Anthony, R. M., F. Wermeling, and J. V. Ravetch. 2012. Novel roles for the IgG Fc glycan. *Ann N Y Acad Sci* 1253: 170-180.

96. Ravetch, J. V., and B. Perussia. 1989. Alternative membrane forms of Fc gamma RIII(CD16) on human natural killer cells and neutrophils. Cell type-specific expression of two genes that differ in single nucleotide substitutions. *J Exp Med* 170: 481-497.

97. Maxwell, K. F., M. S. Powell, M. D. Hulett, P. a. Barton, I. F. McKenzie, T. P. Garrett, and P. M. Hogarth. 1999. Crystal structure of the human leukocyte Fc receptor, Fc gammaRIIa. *Nat Struc Bio* 6: 437-442.

98. van Vugt, M. J., A. F. Heijnen, P. J. Capel, S. Y. Park, C. Ra, T. Saito, J. S. Verbeek, and J. G. van de Winkel. 1996. FcR gamma-chain is essential for both surface expression and function of human Fc gamma RI (CD64) *in vivo*. *Blood* 87: 3593-3599.

99. Shields, R. L., A. K. Namenuk, K. Hong, Y. G. Meng, J. Rae, J. Briggs, D. Xie, J. Lai, A. Stadlen, B. Li, J. A. Fox, and L. G. Presta. 2001. High resolution mapping of the binding site on human IgG1 for Fc gamma RI, Fc gamma RII, Fc gamma RIII, and FcRn and design of IgG1 variants with improved binding to the Fc gamma R. *J Biol Chem* 276: 6591-6604.

100. Pilling, D., C. D. Buckley, M. Salmon, and R. H. Gomer. 2003. Inhibition of fibrocyte differentiation by serum amyloid P. *J. Immunol.* 171: 5537-5546.

101. Pilling, D., N. M. Tucker, and R. H. Gomer. 2006. Aggregated IgG inhibits the differentiation of human fibrocytes fied the factor in serum , which inhibits fibrocyte (SAP). . *J Leukoc Bio* 79.

102. Kim, M. K., X. Q. Pan, Z. Y. Huang, S. Hunter, P. H. Hwang, Z. K. Indik, and A. D. Schreiber. 2001. Fc gamma receptors differ in their structural requirements for interaction with the tyrosine kinase Syk in the initial steps of signaling for phagocytosis. *Clin Immunol* 98: 125-132.

103. Huang, Z. Y., S. Hunter, M. K. Kim, P. Chien, R. G. Worth, Z. K. Indik, and A. D. Schreiber. 2004. The monocyte Fcgamma receptors FcgammaRI/gamma and FcgammaRIIA differ in their interaction with Syk and with Src-related tyrosine kinases. *J Leukoc Biol* 76: 491-499.

104. Hunter, S., N. Sato, M. K. Kim, Z. Y. Huang, D. H. Chu, J. G. Park, and A. D. Schreiber. 1999. Structural requirements of Syk kinase for Fcgamma receptor-mediated phagocytosis. *Exp Hemat* 27: 875-884.

105. Bellini, A., and S. Mattoli. 2007. The role of the fibrocyte, a bone marrow-derived mesenchymal progenitor, in reactive and reparative fibroses. *Lab Invest* 87: 858-870.

106. Strieter, R. M., E. C. Keeley, M. D. Burdick, and B. Mehrad. 2009. The role of circulating mesenchymal progenitor cells, fibrocytes, in promoting pulmonary fibrosis. *Trans Am Clin Climatol Assoc* 120: 49-59.

107. Cox, N., D. Pilling, and R. H. Gomer. 2014. Serum amyloid P: a systemic regulator of the innate immune response. *J Leukoc Biol* 96: 739-743.

108. Cox, N., D. Pilling, and R. H. Gomer. 2014. Distinct fcgamma receptors mediate the effect of serum amyloid p on neutrophil adhesion and fibrocyte differentiation. *J Immunol* 193: 1701-1708.

109. Verstovsek, S., R. A. Mesa, L. M. Foltz, V. Gupta, J. O. Mascarenhas, E. K. Ritchie, R. Hoffman, R. T. Silver, M. Kremyanskaya, O. Pozdnyakova, R. P. Hasserjian, E. Trehu, H. M. Kantarjian, and J. R. Gotlib. 2014. Phase 2 Trial of PRM-151, an Anti-Fibrotic Agent, in Patients with Myelofibrosis: Stage 1 Results. *Blood* 124: 713-713.

110. Devaraj, S., and I. Jialal. 2011. C-reactive protein polarizes human macrophages to an M1 phenotype and inhibits transformation to the M2 phenotype. *Arteriosclerosis, thrombosis, and vascular biology* 31: 1397-1402.

111. Pegues, M. A., M. A. McCrory, A. Zarjou, and A. J. Szalai. 2013. C-reactive protein exacerbates renal ischemia-reperfusion injury. *Amer J of Physio Rena Physio* 304: F1358-1365.

112. Li, Z. I., A. C. Chung, L. Zhou, X. R. Huang, F. Liu, P. Fu, J. M. Fan, A. J. Szalai, and H. Y. Lan. 2011. C-reactive protein promotes acute renal inflammation and fibrosis in unilateral ureteral obstructive nephropathy in mice. *Lab Invest* 91: 837-851.

113. Glover, G. I., P. S. Mariano, and J. R. Petersen. 1976. Reinvestigation of the phenacyl bromide modification of alpha-chymotrypsin. *Biochemistry* 15: 3754-3760.

114. Hu, X. Z., T. T. Wright, N. R. Jones, T. N. Ramos, G. A. Skibinski, M. A. McCrory, S. R. Barnum, and A. J. Szalai. 2011. Inhibition of experimental autoimmune encephalomyelitis in human C-reactive protein transgenic mice is FcgammaRIIB dependent. *Autoimmune Disea* 2011: 484936.

115. Mantovani, A., S. Valentino, S. Gentile, A. Inforzato, B. Bottazzi, and C. Garlanda. 2013. The long pentraxin PTX3: a paradigm for humoral pattern recognition molecules. *Ann N Y Acad Sci* 1285: 1-14.

116. van Kooyk, Y., and T. B. Geijtenbeek. 2003. DC-SIGN: escape mechanism for pathogens. *Nat Rev Immunol* 3: 697-709.

117. Anthony, R. M., F. Wermeling, M. C. I. Karlsson, and J. V. Ravetch. 2008. Identification of a receptor required for the anti-inflammatory activity of IVIG. *Proc Natl Acad Sci U S A* 105: 19571-19578.

118. Garcia-Vallejo, J. J., and Y. van Kooyk. 2013. The physiological role of DC-SIGN: a tale of mice and men. *Trends Immunol* 34: 482-486.

119. Pepys, M. B., T. W. Rademacher, S. Amatayakul-Chantler, P. Williams, G. E. Noble, W. L. Hutchinson, P. N. Hawkins, S. R. Nelson, J. R. Gallimore, J. Herbert, and et al. 1994. Human serum amyloid P component is an invariant constituent of amyloid deposits and has a uniquely homogeneous glycostructure. *Proc Natl Acad Sci U S A* 91: 5602-5606.

120. Kuhn, R., J. Lohler, D. Rennick, K. Rajewsky, and W. Muller. 1993. Interleukin-10-deficient mice develop chronic enterocolitis. *Cell* 75: 263-274.

121. Smith, P., D. J. DiLillo, S. Bournazos, F. Li, and J. V. Ravetch. 2012. Mouse model recapitulating human Fcgamma receptor structural and functional diversity. *Proc Natl Acad Sci U S A* 109: 6181-6186.

122. Pilling, D., and R. H. Gomer. 2014. Persistent lung inflammation and fibrosis in serum amyloid P component (APCs-/-) knockout mice. *PloS one* 9: e93730.

123. Martinez, F. O., L. Helming, R. Milde, A. Varin, B. N. Melgert, C. Draijer, B. Thomas, M. Fabbri, A. Crawshaw, L. P. Ho, N. H. Ten Hacken, V. Cobos Jimenez, N. A. Kootstra, J. Hamann, D. R. Greaves, M. Locati, A. Mantovani, and S. Gordon. 2013. Genetic programs expressed in resting and IL-4 alternatively activated mouse and human macrophages: similarities and differences. *Blood* 121: e57-69.

124. Borrok, M. J., and L. L. Kiessling. 2007. Non-carbohydrate inhibitors of the lectin DC-SIGN. *J Am Chem Soc* 129: 12780-12785.

125. Prost, L. R., J. C. Grim, M. Tonelli, and L. L. Kiessling. 2012. Noncarbohydrate glycomimetics and glycoprotein surrogates as DC-SIGN antagonists and agonists. *ACS Chem Biol* 7: 1603-1608.

126. Deban, L., R. C. Russo, M. Sironi, F. Moalli, M. Scanziani, V. Zambelli, I. Cuccovillo, A. Bastone, M. Gobbi, S. Valentino, A. Doni, C. Garlanda, S. Danese, G. Salvatori, M. Sassano, V. Evangelista, B. Rossi, E. Zenaro, G. Constantin, C. Laudanna, B. Bottazzi, and A. Mantovani. 2010. Regulation of leukocyte recruitment by the long pentraxin PTX3. *Nat Immunol* 11: 328-334.

127. Wynn, T. A., and L. Barron. 2010. Macrophages: master regulators of inflammation and fibrosis. *Sem In Liver Dise* 30: 245-257.

128. Geijtenbeek, T. B., and S. I. Gringhuis. 2009. Signalling through C-type lectin receptors: shaping immune responses. *Nat Rev Immunol* 9: 465-479.

129. Bharhani, M. S., R. Borojevic, S. Basak, E. Ho, P. Zhou, and K. Croitoru. 2006. IL-10 protects mouse intestinal epithelial cells from Fas-induced apoptosis via modulating Fas expression and altering caspase-8 and FLIP expression. *Amer J of Physio* 291: G820-829.

130. Xu, W., A. Roos, N. Schlagwein, A. M. Woltman, M. R. Daha, and C. van Kooten. 2006. IL-10-producing macrophages preferentially clear early apoptotic cells. *Blood* 107: 4930-4937.

131. Olszak, T., J. F. Neves, C. M. Dowds, K. Baker, J. Glickman, N. O. Davidson, C. S. Lin, C. Jobin, S. Brand, K. Sotlar, K. Wada, K. Katayama, A. Nakajima, H. Mizuguchi, K. Kawasaki, K. Nagata, W. Muller, S. B. Snapper, S. Schreiber, A.

Kaser, S. Zeissig, and R. S. Blumberg. 2014. Protective mucosal immunity mediated by epithelial CD1d and IL-10. *Nat* 509: 497-502.

132. Nimmerjahn, F., and J. V. Ravetch. 2008. Fcgamma receptors as regulators of immune responses. *Nat Rev Immunol* 8: 34-47.

133. Uhlen, M., L. Fagerberg, B. M. Hallstrom, C. Lindskog, P. Oksvold, A. Mardinoglu, A. Sivertsson, C. Kampf, E. Sjostedt, A. Asplund, I. Olsson, K. Edlund, E. Lundberg, S. Navani, C. A. Szigyarto, J. Odeberg, D. Djureinovic, J. O. Takanen, S. Hober, T. Alm, P. H. Edqvist, H. Berling, H. Tegel, J. Mulder, J. Rockberg, P. Nilsson, J. M. Schwenk, M. Hamsten, K. von Feilitzen, M. Forsberg, L. Persson, F. Johansson, M. Zwahlen, G. von Heijne, J. Nielsen, and F. Ponten. 2015. Proteomics. Tissue-based map of the human proteome. *Sci* 347: 1260419.

134. Whitsett, J. A., and T. Alenghat. 2014. Respiratory epithelial cells orchestrate pulmonary innate immunity. *Nat Immunol* 16: 27-35.

135. Sakai, N., T. Wada, H. Yokoyama, M. Lipp, S. Ueha, K. Matsushima, and S. Kaneko. 2006. Secondary lymphoid tissue chemokine (SLC/CCL21)/CCR7 signaling regulates fibrocytes in renal fibrosis. *Proc Natl Acad Sci U S A* 103: 14098-14103.

136. Moeller, A., S. E. Gilpin, K. Ask, G. Cox, D. Cook, J. Gauldie, P. J. Margetts, L. Farkas, J. Dobranowski, C. Boylan, P. M. O'Byrne, R. M. Strieter, and M. Kolb. 2009. Circulating fibrocytes are an indicator of poor prognosis in idiopathic pulmonary fibrosis. *Am J Respir Crit Care Med* 179: 588-594.

137. McAnulty, R. J. 2007. Fibroblasts and myofibroblasts: their source, function and role in disease. *Int J Biochem Cell Biol* 39: 666-671.

138. Abe, R., S. C. Donnelly, T. Peng, R. Bucala, and C. N. Metz. 2001. Peripheral blood fibrocytes: differentiation pathway and migration to wound sites. *J Immunol* 166: 7556-7562.

139. Hamilton, J. A., E. R. Stanley, A. W. Burgess, and R. K. Shadduck. 1980. Stimulation of macrophage plasminogen activator activity by colony-stimulating factors. *J Cell Physiol* 103: 435-445.

140. Wynn, T. A., and T. R. Ramalingam. 2012. Mechanisms of fibrosis: therapeutic translation for fibrotic disease. *Nat Med* 18: 1028-1040.

141. Hamilton, J. A. 2008. Colony-stimulating factors in inflammation and autoimmunity. *Nat Rev Immunol* 8: 533-544.

142. Shi, C., and D. I. Simon. 2006. Integrin signals, transcription factors, and monocyte differentiation. *Trends in Cardio Med*16: 146-152.

143. Shi, C., X. B. Zhang, Z. P. Chen, K. Sulaiman, M. W. Feinberg, C. M. Ballantyne, M. K. Jain, and D. I. Simon. 2004. Integrin engagement regulates monocyte differentiation through the forkhead transcription factor Foxp1. *J Clin Invest* 114: 408-418.

144. Hogg, N., I. Patzak, and F. Willenbrock. 2011. The insider's guide to leukocyte integrin signalling and function. *Nat Rev Immunol* 11: 416-426.

145. Hynes, R. O. 1992. Integrins: versatility, modulation, and signaling in cell adhesion. *Cell* 69: 11-25.

146. Sudhakaran, P. R., A. Radhika, and S. S. Jacob. 2007. Monocyte macrophage differentiation *in vitro*: Fibronectin-dependent upregulation of certain macrophage-specific activities. *Glycoconj J* 24: 49-55.

147. He, F. J., and G. A. MacGregor. 2009. A comprehensive review on salt and health and current experience of worldwide salt reduction programmes. *J Hum Hypertens* 23: 363-384.

148. Susic, D., and E. D. Frohlich. 2012. Salt consumption and cardiovascular, renal, and hypertensive diseases: clinical and mechanistic aspects. *Curr Opin Lipidol* 23: 11-16.

149. Yuan, B. X., and F. H. Leenen. 1991. Dietary sodium intake and left ventricular hypertrophy in normotensive rats. *Am J Physiol* 261: H1397-1401.

150. Yu, H. C., L. M. Burrell, M. J. Black, L. L. Wu, R. J. Dilley, M. E. Cooper, and C. I. Johnston. 1998. Salt induces myocardial and renal fibrosis in normotensive and hypertensive rats. *Cir* 98: 2621-2628.

151. Kagiyama, S., K. Matsumura, M. Fukuhara, K. Sakagami, K. Fujii, and M. Iida. 2007. Aldosterone-and-salt-induced cardiac fibrosis is independent from angiotensin II type 1a receptor signaling in mice. *Hyper Res* 30: 979-989.

152. Munck, L. K. 1995. Chloride dependent amino acid transport in the human small intestine. *Gut* 36: 215-219.

153. Broer, S. 2008. Amino acid transport across mammalian intestinal and renal epithelia. *Physiol Rev* 88: 249-286.

154. Frohlich, E. D., Y. Chien, S. Sesoko, and B. L. Pegram. 1993. Relationship between dietary sodium intake, hemodynamics, and cardiac mass in SHR and WKY rats. *Am J Physiol* 264: R30-34.

155. Perry, I. J., and D. G. Beevers. 1992. Salt intake and stroke: a possible direct effect. *J Hum Hypertens* 6: 23-25.

156. Strazzullo, P., L. D'Elia, N. B. Kandala, and F. P. Cappuccio. 2009. Salt intake, stroke, and cardiovascular disease: meta-analysis of prospective studies. *BMJ* 339: b4567.

157. He, F. J., M. Burnier, and G. A. Macgregor. 2011. Nutrition in cardiovascular disease: salt in hypertension and heart failure. *Eur Heart J* 32: 3073-3080.

158. Colden-Stanfield, M., and E. K. Gallin. 1998. Modulation of K+ currents in monocytes by VCAM-1 and E-selectin on activated human endothelium. *Am J Physiol* 275: C267-277.

159. Arcangeli, A., M. Carla, M. R. Del Bene, A. Becchetti, E. Wanke, and M. Olivotto. 1993. Polar/apolar compounds induce leukemia cell differentiation by modulating cell-surface potential. *Proc Natl Acad Sci U S A* 90: 5858-5862.

160. Lindinger, M. I., G. J. Heigenhauser, R. S. McKelvie, and N. L. Jones. 1992. Blood ion regulation during repeated maximal exercise and recovery in humans. *Am J Physiol* 262: R126-136.

161. Farquhar, W. B., E. E. Paul, A. V. Prettyman, and M. E. Stillabower. 2005. Blood pressure and hemodynamic responses to an acute sodium load in humans. *Journal of applied physiology* 99: 1545-1551.

162. Tobias, J. W., M. M. Bern, P. A. Netland, and B. R. Zetter. 1987. Monocyte adhesion to subendothelial components. *Blood* 69: 1265-1268.

163. Springer, T. A. 1994. Traffic signals for lymphocyte recirculation and leukocyte emigration: the multistep paradigm. *Cell* 76: 301-314.

164. Jentsch, T. J., V. Stein, F. Weinreich, and A. A. Zdebik. 2002. Molecular structure and physiological function of chloride channels. *Physiol Rev* 82: 503-568.

165. Fahlke, C. 2001. Ion permeation and selectivity in ClC-type chloride channels. *American journal of physiology. Renal physiology* 280: F748-757.

166. Qu, Z., and H. C. Hartzell. 2000. Anion permeation in Ca(2+)-activated Cl(-) channels. *J Gen Physiol* 116: 825-844.

167. Franciolini, F., and W. Nonner. 1987. Anion and cation permeability of a chloride channel in rat hippocampal neurons. *J Gen Physiol* 90: 453-478.

168. Ashton, N., B. E. Argent, and R. Green. 1991. Characteristics of fluid secretion from isolated rat pancreatic ducts stimulated with secretin and bombesin. *J Physiol* 435: 533-546.

169. Bellini, A., and S. Mattoli. 2007. The role of the fibrocyte, a bone marrow-derived mesenchymal progenitor, in reactive and reparative fibroses. *Lab Invest* 87: 858-870.

170. Kisseleva, T., H. Uchinami, N. Feirt, O. Quintana-Bustamante, J. C. Segovia, R. F. Schwabe, and D. A. Brenner. 2006. Bone marrow-derived fibrocytes participate in pathogenesis of liver fibrosis. *J Hepatol* 45: 429-438.

171. Oh, M. H., S. Y. Oh, J. Yu, A. C. Myers, W. J. Leonard, Y. J. Liu, Z. Zhu, and T. Zheng. 2011. IL-13 induces skin fibrosis in atopic dermatitis by thymic stromal lymphopoietin. *J Immunol* 186: 7232-7242.

172. Gill, G. V., P. H. Baylis, C. T. Flear, and J. Y. Lawson. 1985. Changes in plasma solutes after food. *J of The Royal Soc of Med* 78: 1009-1013.

173. Ciesla, D. J., E. E. Moore, G. Zallen, W. L. Biffl, and C. C. Silliman. 2000. Hypertonic saline attenuation of polymorphonuclear neutrophil cytotoxicity: timing is everything. *The J of Trauma* 48: 388-395.

174. Pascual, J. L., L. E. Ferri, A. J. Seely, G. Campisi, P. Chaudhury, B. Giannias, D. C. Evans, T. Razek, R. P. Michel, and N. V. Christou. 2002. Hypertonic saline resuscitation of hemorrhagic shock diminishes neutrophil rolling and adherence to endothelium and reduces *in vivo* vascular leakage. *Ann of Surg* 236: 634-642.

175. Junger, W. G., F. C. Liu, W. H. Loomis, and D. B. Hoyt. 1994. Hypertonic saline enhances cellular immune function. *Cir Shock* 42: 190-196.

176. Kolsen-Petersen, J. A. 2004. Immune effect of hypertonic saline: fact or fiction? *Acta anaesthesiologica Scan* 48: 667-678.

177. Shapiro, L., and C. A. Dinarello. 1995. Osmotic regulation of cytokine synthesis *in vitro*. *Proc Natl Acad Sci U S A* 92: 12230-12234.

178. Balgoma, D., A. M. Astudillo, G. Perez-Chacon, O. Montero, M. A. Balboa, and J. Balsinde. 2010. Markers of monocyte activation revealed by lipidomic profiling of arachidonic acid-containing phospholipids. *J Immunol* 184: 3857-3865.

179. Mantovani, A., P. Allavena, A. Vecchi, and S. Sozzani. 1998. Chemokines and chemokine receptors during activation and deactivation of monocytes and dendritic cells and in amplification of Th1 versus Th2 responses. *Int J Clin Lab Res* 28: 77-82.

180. Wang, H., Y. Mao, B. Zhang, T. Wang, F. Li, S. Fu, Y. Xue, T. Yang, X. Wen, Y. Ding, and X. Duan. 2010. Chloride channel ClC-3 promotion of osteogenic differentiation through Runx2. *J Cell Biochem* 111: 49-58.

181. Bikle, D. D., A. Ratnam, T. Mauro, J. Harris, and S. Pillai. 1996. Changes in calcium responsiveness and handling during keratinocyte differentiation. Potential role of the calcium receptor. *J Clin Invest* 97: 1085-1093.

182. Catanozi, S., J. C. Rocha, M. Passarelli, M. L. Guzzo, C. Alves, L. N. Furukawa, V. S. Nunes, E. R. Nakandakare, J. C. Heimann, and E. C. Quintao. 2003. Dietary sodium chloride restriction enhances aortic wall lipid storage and raises plasma lipid concentration in LDL receptor knockout mice. *J Lipid Res* 44: 727-732.

183. Reuter, S., E. Bussemaker, M. Hausberg, H. Pavenstadt, and U. Hillebrand. 2009. Effect of excessive salt intake: role of plasma sodium. *Curr Hypertens Rep* 11: 91-97.

APPENDIX I

NaCl POTENTIATES HUMAN FIBROCYTE DIFFERENTIATION*

Summary

Excessive NaCl intake is associated with a variety of fibrosing diseases such as renal and cardiac fibrosis. This association has been attributed to increased blood pressure as the result of high NaCl intake. However, studies in patients with high NaCl intake and fibrosis reveal a connection between NaCl intake and fibrosis that is independent of blood pressure. We find that increasing the extracellular concentration of NaCl to levels that may occur in human blood after high-salt intake can potentiate, in serum-free culture conditions, the differentiation of freshly-isolated human monocytes into fibroblast-like cells called fibrocytes. NaCl affects the monocytes directly during their adhesion. Potassium chloride and sodium nitrate also potentiate fibrocyte differentiation. The plasma protein Serum Amyloid P (SAP) inhibits fibrocyte differentiation. High levels of extracellular NaCl change the SAP Hill coefficient from 1.7 to 0.8, and cause a four-fold increase in the concentration of SAP needed to inhibit fibrocyte differentiation by 95%. Together, our data suggest that NaCl potentiates fibrocyte differentiation. NaCl-increased fibrocyte differentiation may thus contribute to NaCl-increased renal and cardiac fibrosis.

---

* Reprinted under the Creative Commons Attribution License *PLOS ONE*. Cox, N., D. Pilling, and R. H. Gomer. NaCl potentiates human fibrocyte differentiation. *PloS one*. 2012;7(9):e45674. Copyright © 2012 by the authors.

Introduction

Fibrosing diseases such as pulmonary fibrosis, congestive heart disease, and renal fibrosis involve the formation of unwanted scar tissue in internal organs (73, 135). The scar tissue in fibrosis leads to organ malfunction and subsequent organ failure (73). Fibrosis is associated with approximately 45% of deaths in the U.S (73). Fibrosis involves infiltration of blood leukocytes into the affected organs, activation and/or appearance of fibroblast-like cells, tissue remodeling, and deposition of extracellular matrix proteins such as collagen (45, 81, 82, 136-138). Fibrosis can be caused by factors such as environmental toxins, or aberrant healing events (45).

Fibrocytes are $CD45^+$, collagen I^+ fibroblast-like cells that have been implicated in scar tissue formation and fibrosis (45, 82, 88, 136, 138). These cells share similarities with both blood leukocytes and tissue resident cells (81, 88). Fibrocytes, depending on the environmental cues, can express extracellular proteases, or matrix proteins such as collagen (45, 106). Fibrocytes differentiate from $CD14^+$ monocytes (138). Following their recruitment to a specific tissue, monocytes can differentiate into macrophages, dendritic cells, or fibrocytes (45, 65, 66). Serum Amyloid P (SAP), a pentameric protein from the pentraxin family of proteins, interacts with Fc receptors on monocytes to inhibit fibrocyte differentiation (13, 23, 54, 58).

Monocytes leave the bone marrow and travel through the blood vessels until they are recruited into a specific tissue in response to chemokines. Afterward, they mature and differentiate under the influence of signaling molecules such as M-CSF, GM-CSF, IL-4, IL-13, and TGF-β1 (60, 139-141). One component of monocyte activation and

differentiation is a group of receptors belonging to the integrin family of proteins (142, 143). Integrins are composed of α and β subunits (144). These proteins aid in monocyte adhesion to components of extracellular matrices and are central to inflammation, immunity, and homeostasis (145). The adhesive properties of integrins contribute to different patterns of monocyte differentiation under various conditions (142, 143, 146).

Much remains to be understood about the mechanisms which trigger fibrosis and fibrocyte differentiation. Congestive heart disease and renal fibrosis have previously been linked to high NaCl intake in both humans and various animal models, but the exact mechanism underlying this connection is unknown (135, 147-151). Sodium and chloride ions contribute to the maintenance of electrical gradients across the membrane of many cells. In addition, sodium and chloride ions are used to absorb nutrients such as amino acids in the intestine, and regulate blood pressure and volume (147, 152, 153). The latter function of sodium and chloride ions has been the focus of many studies, since abnormalities in blood pressure have been associated with stroke, cardiac fibrosis, and renal fibrosis (148).

It is generally accepted that there is a direct correlation between high salt intake and high blood pressure which in turn increases the chances of heart disease, stroke and renal failure (148). Until recently, it was believed that high blood pressure is the main contributor to heart disease and renal failure. However, animal and clinical studies have shown the deleterious effects (i. e. stroke, cardiac and renal fibrosis) of salt in the absence of increased blood pressure (147, 150, 154, 155). For instance, Wistar or Wistar-Kyoto rats exposed to salt overload develop cardiac, vascular, and renal fibrosis

without exhibiting a significant increase in blood pressure (149, 150). In addition, a connection between salt intake and fibrosis that is independent of high blood pressure has been previously established (147, 156, 157).

A variety of studies indicate that different ions can modulate immune cell function. For instance, potassium channels and potassium transport affect the integrin-dependent activation of the monocytic-derived cell line, THP-1 (158). Altering cation transport in murine erythroleukemia cells can induce differentiation (159). This, combined with the increased instances of fibrosing diseases in patients with high dietary salt intake, caused us to investigate the role of NaCl in the activation of monocytes and their subsequent differentiation into fibrocytes. Our results suggest that high concentrations of NaCl potentiate fibrocyte formation.

Materials and Methods

PBMC and monocyte isolation, cell culture, and fibrocyte differentiation assay

Human blood was collected into heparin tubes (BD Bioscience, San Jose, CA) from adult volunteers who gave written consent and with specific approval from the Texas A&M University human subjects Institutional Review Board. Peripheral blood mononuclear cells (PBMCs) were isolated from the blood by Ficoll-Paque Plus (GE Healthcare Biosciences, Piscataway, NJ) and cultured in Fibrolife (LifeLine Cell Technology, Walkersville, MD) medium or where indicated in RPMI 1640 (SigmaAldrich, St. Louis, MO) as described previously (86). $CD14^+$ monocytes were isolated by negative selection using magnetic Dynabeads (Dynal Biotech, Milwaukee,

WI) as described previously (54). $CD14^+$ monocytes were plated in 96-well plates with $5x10^4$ cells in 200 µl per well. After 5 days, the plates were air dried, fixed with methanol and stained using a Hema 3 staining Kit (Thermo Fisher Scientific, Milwaukee, WI) (86). Fibrocytes were identified and counted based on their elongated spindle-shaped morphology in five different 900 µm-diameter fields of view per well.

Salt solutions and SAP purification

One molar solutions of sodium chloride, sodium gluconate, sodium nitrate, and other salts were prepared in Fibrolife (LifeLine Cell Technology) basal medium or RPMI-1640 (SigmaAldrich) where indicated. The 1 M solutions were then filter sterilized using Acrodisc 0.2µm syringe filters (Pall, Port Washington, NY). Prepared solutions were then added to the wells at the indicated concentrations. Human Serum Amyloid P was purified from human serum as described previously (56).

Immunohistochemistry

PBMCs were cultured for 5 days on eight-well glass microscope slides (Thermo Fisher) as described previously (88). The cells were then air dried before fixation in acetone for 10 minutes. The cells were stained for CD13, CD45, CD68, Pro-collagen I (Developmental Studies Hybridoma Bank, University of Iowa), CD90, and Prolyl 4-hydroxylase as described previously (88).

Adhesion Assay

96-well polystyrene plates (BD Biosciences) were coated with 15 ug/mL of bovine plasma fibronectin (SigmaAldrich) or bovine collagen I (SigmaAldrich) for 1 hour at 37˚C. The plate was then washed 3 times with PBS and then blocked with 4% BSA (SigmaAldrich, cat # A3059) in PBS for 1 hour at 37°C. Afterward, the plate was washed with serum-free medium, and peripheral blood mononuclear cells were incubated on the plate for 1 hour at 37˚C. The plates were then washed 3 times with PBS and adherent cells were counted in five 900 μm-diameter fields of view per well.

PBMC/monocyte pulse experiment

PBMCs or monocytes were incubated with additional concentrations of NaCl for the indicated times at 37˚C to determine the effect of additional of NaCl on fibrocyte differentiation during adhesion. Then, approximately 95% of the medium was gently removed, so as not to disturb the cells, and replaced with fresh medium. The cells were left to differentiate for 5 days. To determine the effect of NaCl on adherent cells, PBMCs or monocytes were incubated in 96-well plates for 1 hour at 37˚C, and the medium was then replaced with medium containing additional NaCl. The cells were left for 1 hour at 37˚C, and subsequently the medium was replaced with fresh medium with no additional NaCl. These cells were then left to differentiate for 5 days. To elucidate the effect of NaCl on PBMCs or monocytes before their adhesion to the plate, cells were placed in BSA-coated Eppendorf tubes for 1 hour in medium with additional NaCl at 4˚C. The cells were then collected by centrifugation for 5 minutes at 300 x g. The

pelleted cells were resuspended in fresh medium and incubated in a 96-well plate for 5 days at 37˚C to differentiate.

Adhesion molecules and flow cytometry

96-well polystyrene plates (BD Biosciences) were coated with 20 µg/mL of plasma fibronectin (SigmaAldrich) overnight at 4°C. The following day the coated wells were washed 3 x with PBS and blocked with 2% BSA in PBS. After blocking, the wells were washed 3 x with PBS and then the PBMCs were plated with $2x10^5$ cells per well in the presence or absence of 25 mM additional NaCl for 1 hour at 37°C. After the incubation, the medium was replaced with PBS/ 10 mM EDTA and the plate was left at 4°C for 15 minutes to detach the cells from the wells. The detached cells were then pelleted by centrifugation at 300 x g for 5 minutes and resuspended in 2% BSA in PBS. Following centrifugation, the cells were stained for CD11a (BioLegend, San Diego, CA), CD11b (BioLegend), CD11c (BioLegend), CD11b activation epitope (BioLegend), CD18 (BioLegend), CD18 activation epitope (Abd Serotec), CD31 (BioLegend), CD45 (BioLegend), CD49d (BioLegend) and, CD62L (BioLegend) as described previously (88).

Statistical analysis

Data was analyzed by ANOVA (with Dunnett's post test) or t-test when appropriate using Prism software (GraphPad software, San Diego, CA). Normality was tested using Shapiro-Wilk and D'Agostino-Pearson omnibus tests.

Results

Additional NaCl can potentiate fibrocyte formation without influencing cell viability

Since fibrocytes are implicated in fibrosing diseases, and NaCl may promote fibrosis, we examined the hypothesis that NaCl might affect fibrocyte differentiation. Using PBMCs from a variety of donors, we observed 600 to 2800 fibrocytes per 10^5 PBMCs in both Fibrolife and RPMI 1640 medium. For all donors, additional NaCl significantly potentiated fibrocyte differentiation, when compared to the control with no added NaCl (Fig. 21A and B). In Fibrolife medium, NaCl caused a maximum potentiation of fibrocyte differentiation at 30 mM additional NaCl. The $[Na^+]$ and $[Cl^-]$ concentrations in Fibrolife medium are 126 mM and 119 mM, respectively. At 30 mM additional NaCl, both the sodium and the chloride concentration of Fibrolife medium ($[Na^+]$ =156 mM, $[Cl^-]$=144 mM) are in excess when compared to human blood ($[Na^+]$=137 mM, $[Cl^-]$=102 mM) (160, 161). The $[Na^+]$ and $[Cl^-]$ concentrations in RPMI 1640 medium are 134 mM and 107 mM, respectively. In RPMI 1640 medium, NaCl caused a maximum potentiation of fibrocyte differentiation at 20 mM additional NaCl, making $[Na^+]$ =154 mM, and $[Cl^-]$=127 mM, again in excess when compared to human blood.

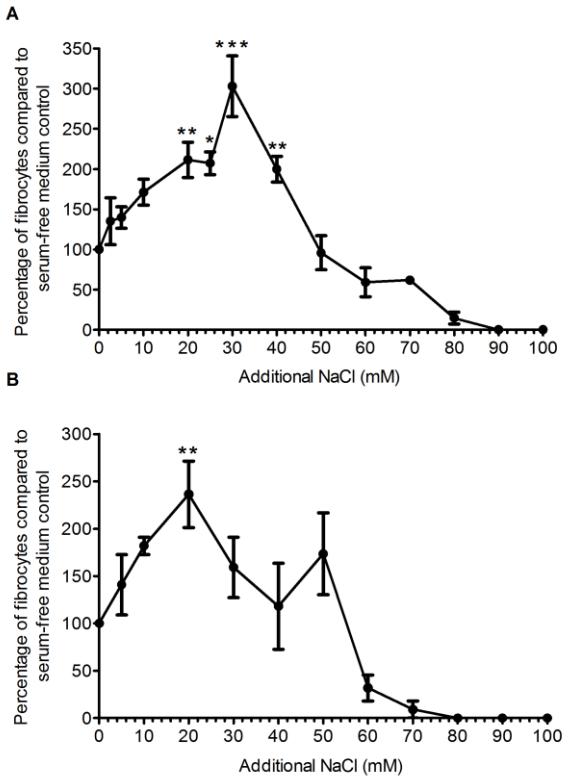

Figure 21: Addition of NaCl to Fibrolife or RPMI based-medium increases fibrocyte differentiation.

Human PBMCs were cultured for 5 days in serum-free medium in the presence of the indicated concentrations of additional NaCl in either Fibrolife (A) or RPMI (B) medium. Results are expressed as mean ± SEM, n=8. * indicates statistical significance with $p < 0.05$, ** indicates $P < 0.01$, and *** indicates $p < 0.001$ by ANOVA compared to the no additional NaCl control.

To verify that the NaCl-induced spindle-shaped cells are fibrocytes, we stained PBMCs after 5 days of incubation with or without 25 mM additional NaCl in Fibrolife for fibrocyte markers. In the presence or absence of added NaCl, the elongated cells were positive for the fibrocyte markers CD13, CD45, CD68, pro-collagen I, and prolyl 4-hydroxylase, and showed no observable staining for the fibroblast marker CD90, indicating that the elongated cells are fibrocytes, and that NaCl thus is increasing the number of fibrocytes (Fig. 22).

An increase in the total number of adherent cells in our assay plates could account for the increased fibrocyte count. To address this possibility, we counted the number of adherent cells after 5 days of incubation with additional NaCl. At 30 mM additional NaCl and below, we observed no significant change in the number of adherent cells as the result of additional NaCl (Fig. 23). The addition of 60 mM additional NaCl did however decrease the number of adherent cells, indicating reduced cell viability.

25 mM additional NaCl does not influence PBMC adhesion

Fibrocytes differentiate from $CD14^+$ monocytes (45, 138). Monocytes are activated in response to adhesion to extracellular matrix proteins as well as tissue culture plates (65, 66). To understand the mechanism behind the potentiation of fibrocyte formation by NaCl, we investigated the influence of NaCl on the initial adhesion of PBMCs to plates, since such changes could influence PBMC activation and therefore differentiation. PBMC adhesion to collagen I-coated, fibronectin-coated, or un-coated tissue culture plates was not influenced by increasing NaCl concentrations (Fig. 24).

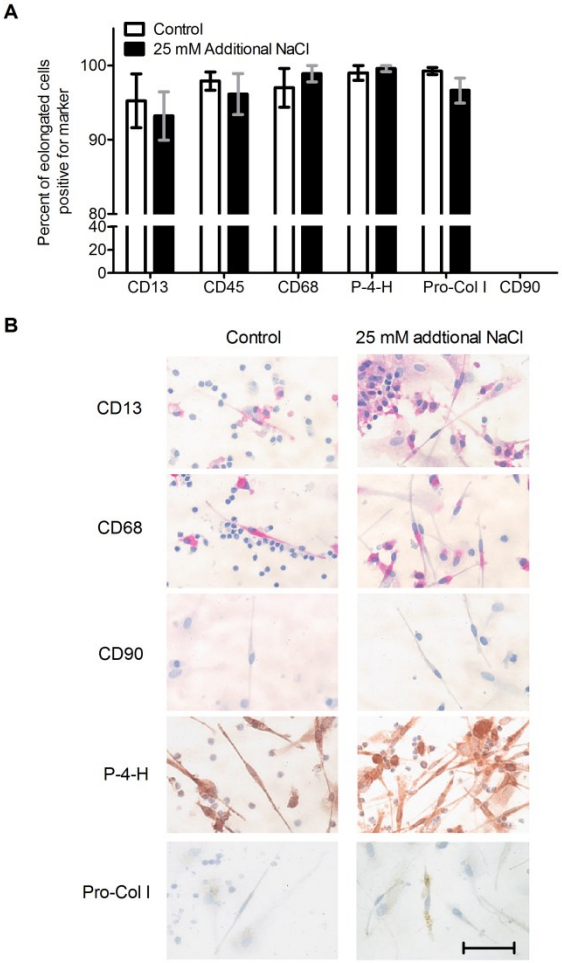

Figure 22: The elongated cells are fibrocytes.
PBMCs were cultured in Fibrolife medium for five days in the presence or absence of 25 mM additional NaCl. Cells were fixed and stained for the indicated markers. (A) The elongated spindle-shaped cells in the wells stained positive for CD13, CD45, CD68, Prolyl 4-hydroxylase (P-4-H), Pro-Collagen I (Pro-Col I) and had no apparent staining for the fibroblast marker CD90. Results are expressed as mean ± SEM, n=3. (B) Cells were stained with the indicated antibodies. Positive staining was identified by red for alkaline phosphatase staining and brown for peroxidase staining. Cells were counterstained blue with hematoxylin to identify nuclei. Size bar is 50 μm.

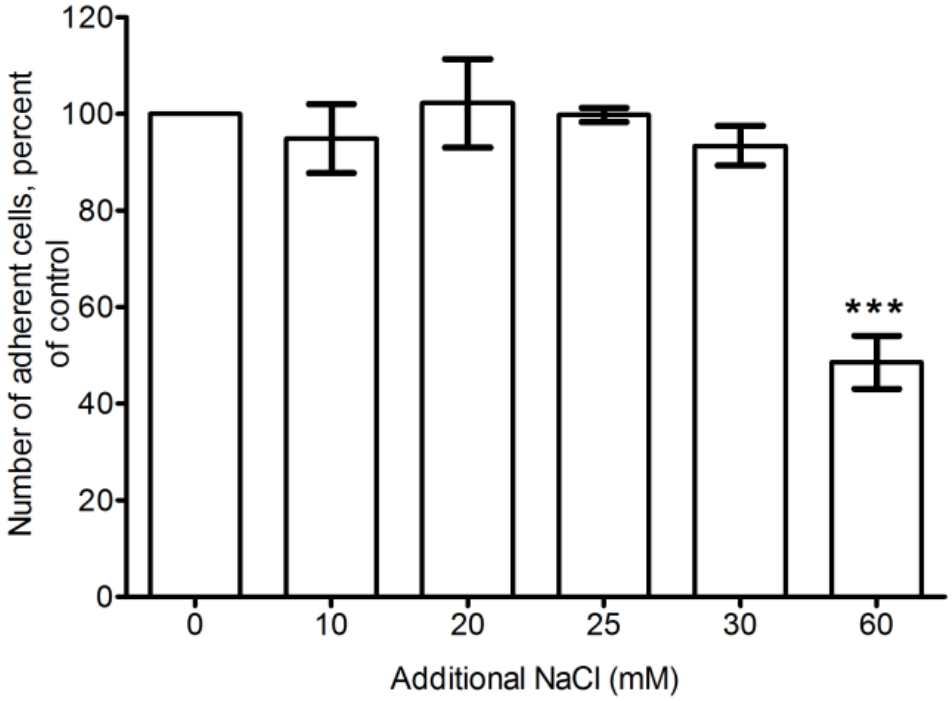

Figure 23: The effect of NaCl on adherent cells after 5 days.
PBMCs were incubated with the indicated concentrations of added NaCl, and the number of adherent cells was counted after 5 days. Counts were then normalized to the control with no added NaCl (0). Values are mean ± SEM, n=3. *** indicates statistical significance by ANOVA compared to the control ($p < 0.001$).

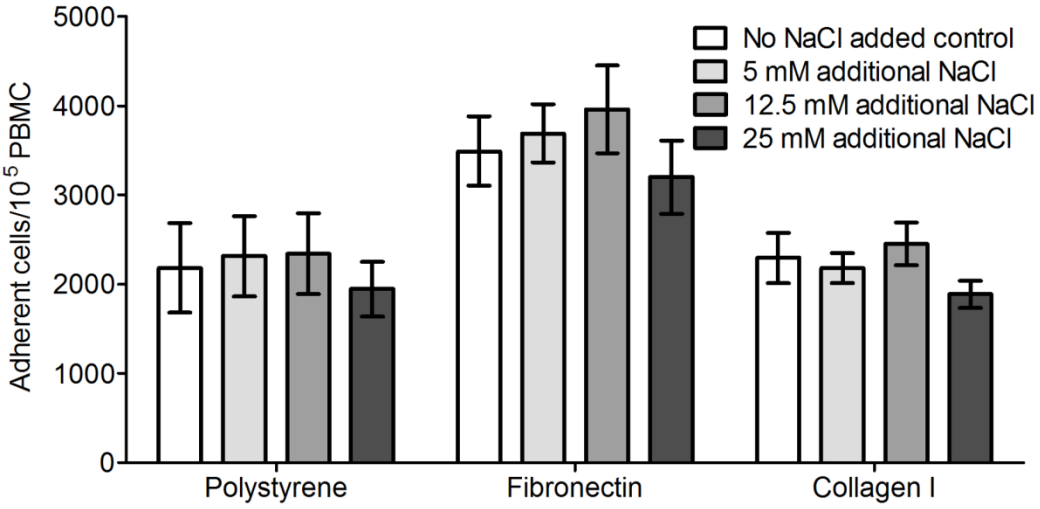

Figure 24: NaCl does not influence the adhesion of PBMCs to plastic, plasma fibronectin or collagen I.
PBMCs were incubated on uncoated polystyrene plates, fibronectin coated plates, or bovine collagen I coated plates for one hour in the indicated concentrations of additional NaCl. The non-adhered cells were then rinsed off and the number of adherent cells were counted. Values are mean ± SEM, n=4.

However, as previously observed, more PBMCs adhered to fibronectin-coated plates than un-coated plates ((162) and Fig. 24). These results suggest that the observed increase in fibrocyte differentiation is not caused by changes in the ability of PBMCs to initially adhere to extracellular matrix proteins or tissue culture plates.

Monocyte to fibrocyte differentiation is potentiated by additional NaCl

The NaCl-induced increase in fibrocyte formation from PBMCs could be due to either secretion of a fibrocyte stimulating factor by non-monocytic cells, or via direct effect of NaCl on monocytes. To distinguish between these two possibilities, we isolated $CD14^+$ cells and examined their differentiation into fibrocytes in the presence of increasing NaCl concentrations. We observed 1400 to 9200 fibrocytes per 10^5 monocytes from 3 different donors. When fibrocyte counts were compared to the no NaCl added control, fibrocyte differentiation was significantly increased by 20 mM to 30 mM additional NaCl (Fig. 25). This suggests that monocytes are directly influenced by the additional NaCl, and not through a secreted factor from CD14-negative cells.

PBMCs and monocytes are influenced during their adhesion by additional NaCl

PBMCs are activated by their adhesion to extracellular matrix proteins and tissue culture plates (163). To elucidate the mechanism behind the NaCl-induced increase in fibrocyte formation, we incubated PBMCs with additional NaCl before, during, and after their adhesion (Fig. 26). We observed that incubation of PBMCs with additional NaCl for one hour during their adhesion potentiated fibrocyte formation (Fig. 26). Incubation

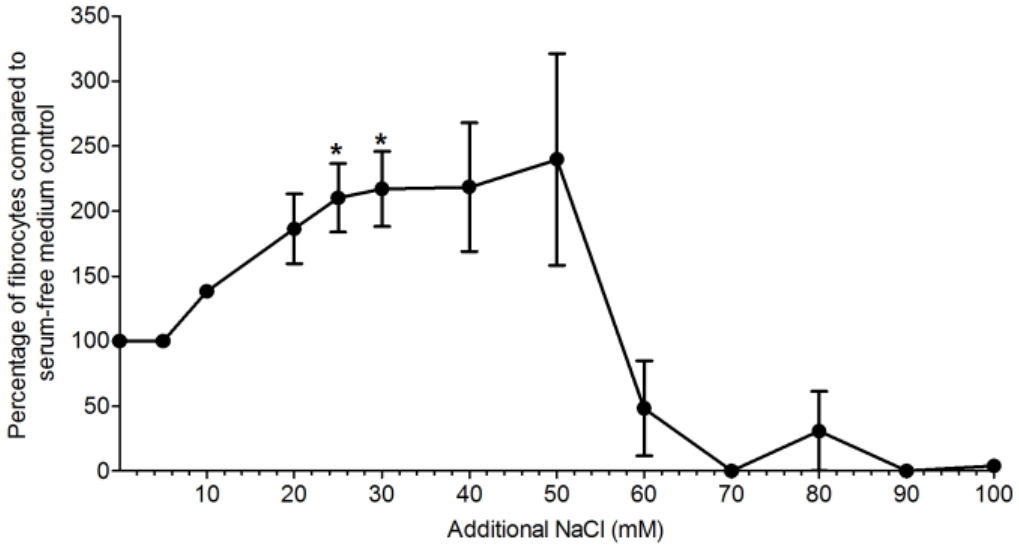

Figure 25: NaCl directly potentiates the differentiation of monocytes into fibrocytes.
$CD14^+$ monocytes were incubated with the indicated additional concentrations of NaCl. After 5 days, fibrocytes were counted. Values are mean ± SEM, n=3. * indicates $p < 0.05$ compared to control (ANOVA). The absence of error bars indicate that error was smaller than the plot symbol.

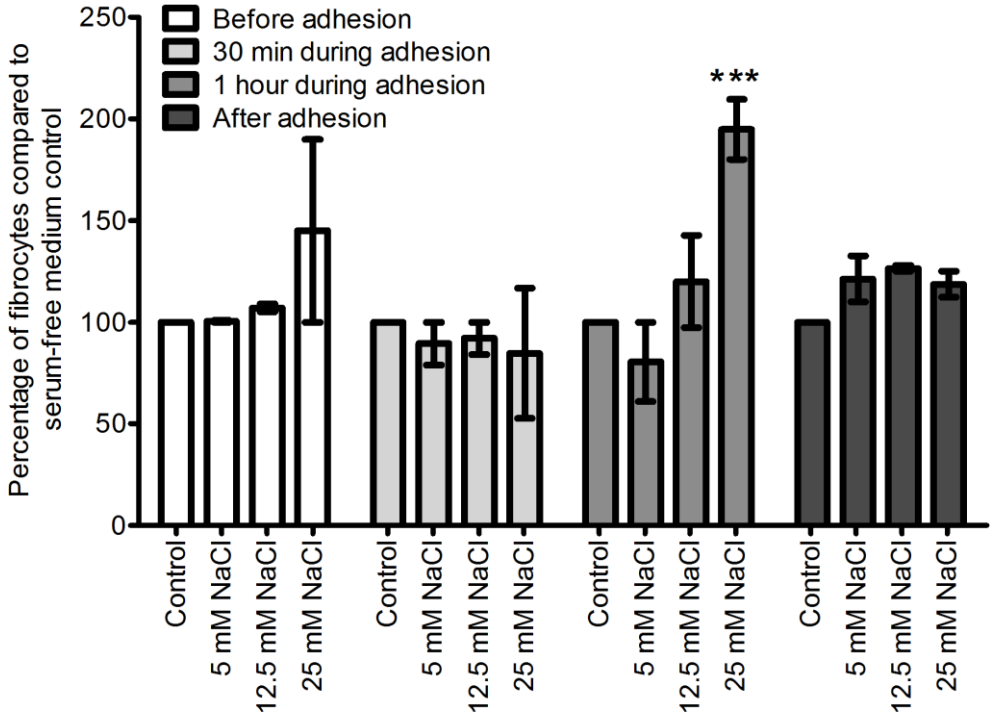

Figure 26: The presence of additional NaCl during PBMC adhesion increases fibrocyte differentiation.
PBMCs were incubated with additional NaCl , before, during, before, and after their adhesion to tissue culture treated plates. Values are mean ± SEM, n=6. *** indicates $p < 0.001$ compared to control (t-test). The absence of an error bar indicates that the error was smaller than the line thickness.

of PBMCs with additional NaCl before or after their adhesion, or for 30 minutes during their adhesion, had no significant effect on fibrocyte formation (Fig. 26). These data suggest that NaCl influences fibrocyte precursors during adhesion. $CD14^+$ monocytes were also incubated with additional NaCl before, during, and after adhesion. Similar to the results with PBMCs, incubation of monocytes with additional NaCl during their adhesion resulted in increased fibrocyte formation (Fig. 27). A 30-minute incubation of monocytes with 25 mM additional NaCl was sufficient for this potentiation.

Since additional NaCl potentiates fibrocyte differentiation by influencing monocytes during their initial adhesion to the plate, we examined the effects of 25 mM additional NaCl on different adhesion molecules. We incubated PBMCs in the presence or absence of 25 mM additional NaCl for 1 hour at 37°C. Following incubation, the cells were stained for CD11a, CD11b, CD11c, CD11b activation epitope, CD18, CD18 activation epitope, CD31, CD49d, and CD62L. The stained cells were subjected to flow cytometry and the $CD14^+$ monocytes were investigated for any change in the mentioned adhesion molecules. We observed no change in the studied adhesion molecules as the result of additional NaCl (Fig. 28).

Sodium nitrate but not sodium gluconate potentiates fibrocyte differentiation

Sodium nitrate and sodium gluconate are two classical sodium chloride substitutes used to probe chloride transport (164). Nitrate can bind and cross chloride channels (164-167). Gluconate only mimics the electrical charge of chloride while being unable to cross the majority of chloride channels (164-168). Sodium nitrate but not

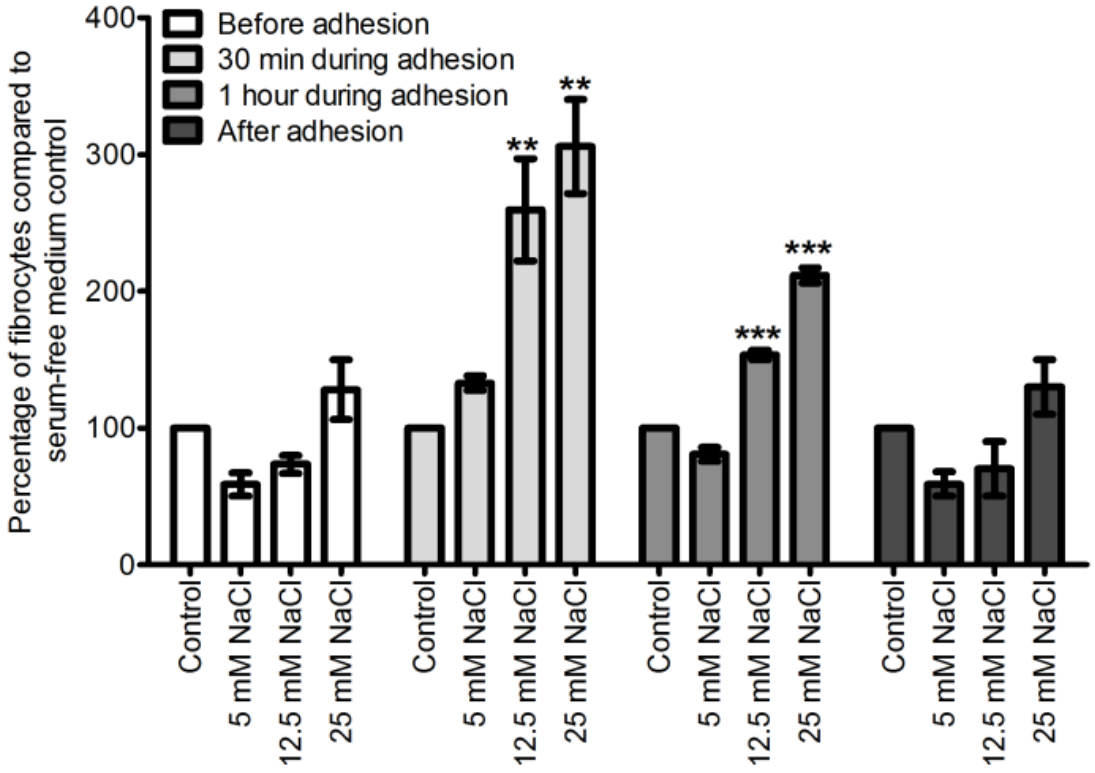

Figure 27: The presence of additional NaCl during CD14$^+$ monocyte adhesion increases fibrocyte formation.
Isolated monocytes were incubated with additional NaCl before, during, and after their adhesion to tissue culture treated plates. Values are mean ± SEM, n=4, ** indicates $p < 0.01$, and *** indicates $p < 0.001$ compared to control (ANOVA).

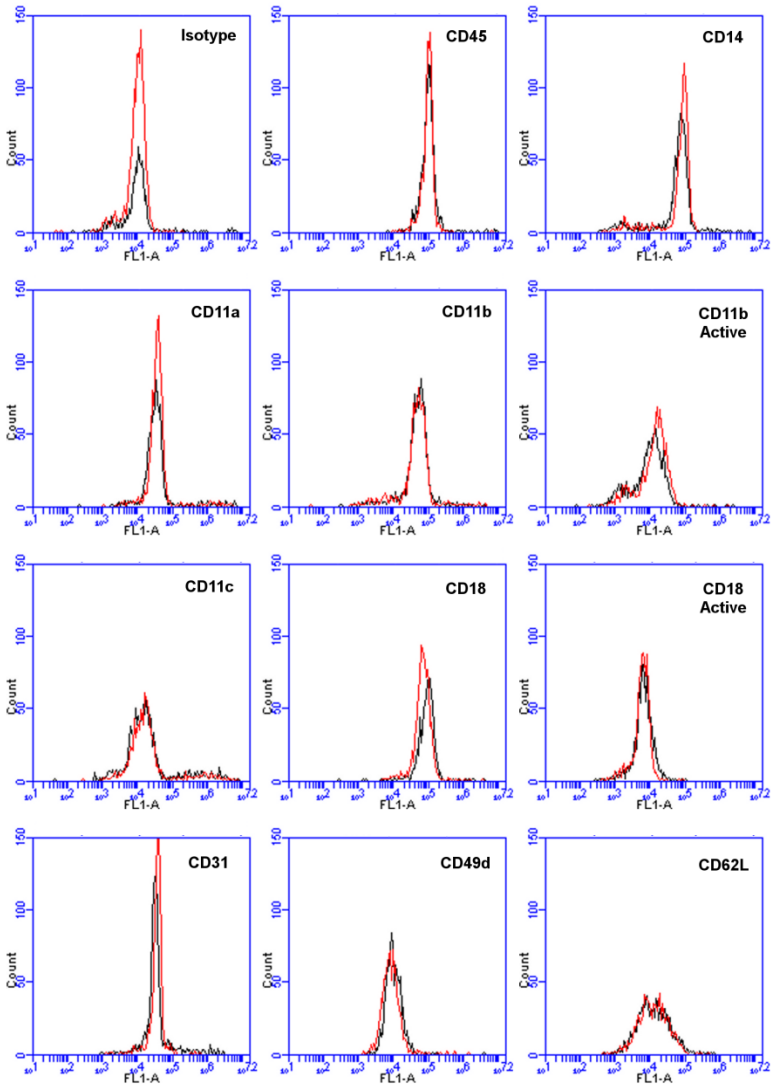

Figure 28: Incubation of PBMCs with additional NaCl does not influence the cell-surface levels of several adhesion molecules.
PBMCs were incubated in the presence or absence of 25 mM additional NaCl for 1 hour at 37 °C and then stained for the indicated adhesion molecules. Monocytes were identified by their forward and side scatter characteristics and the expression of CD14. Flow cytometry plots are representative results from three separate donors. Histograms represent fluorescence intensity of the indicated marker in control cells (Black line) and NaCl treated Cells (Red line).

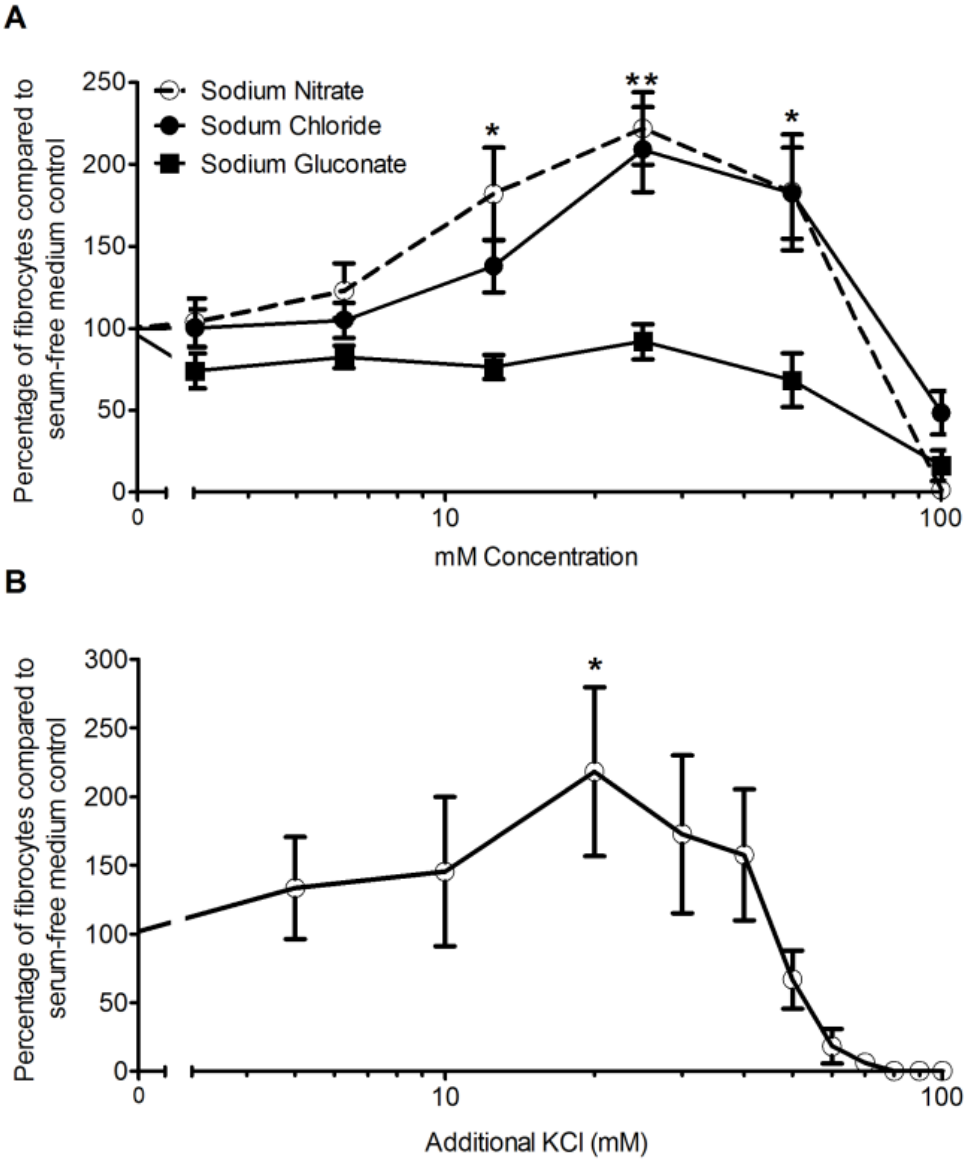

Figure 29: Sodium nitrate and potassium chloride potentiate fibrocyte differentiation.

PBMCs were cultured with the indicated concentrations of additional (A) sodium chloride, sodium nitrate, or sodium gluconate, or (B) potassium chloride. Values are mean ± SEM, n=6. * indicates $p < 0.05$, and ** indicated $p < 0.01$ compared to control by ANOVA.

sodium gluconate potentiated fibrocyte differentiation (Fig. 29A). The response of PBMCs to sodium nitrate was similar to that of NaCl. This suggests that chloride transport across the membrane is a requirement for potentiation of fibrocyte differentiation by additional NaCl. In addition to sodium nitrate and sodium gluconate, we investigated other compounds such as potassium chloride, rubidium chloride, cesium chloride, choline chloride, tetraethyl ammonium chloride, and monosodium glutamate. Adding 25 mM potassium chloride potentiated fibrocyte differentiation (Fig. 29B). Monosodium glutamate had no effect of fibrocyte differentiation but was toxic when added in excess of 50 mM. Choline chloride and rubidium chloride were toxic at concentrations higher than 4 mM, while cesium chloride and tetraethyl ammonium chloride were toxic at 2 mM (data not shown).

NaCl interferes with the ability of Serum Amyloid P to inhibit fibrocyte differentiation

Human Serum Amyloid P (hSAP) is a pentameric protein secreted from the liver that inhibits fibrocyte differentiation (54, 56, 77). The addition of 25 mM NaCl to the medium changed the Hill coefficient for the inhibition of fibrocyte differentiation by hSAP from 1.7 ± 0.1 to 0.7 ± 0.1 (mean ± SEM, $n=5$, $p < 0.05$ by t-test) (Fig. 30). In addition, adding 25 mM to the medium significantly inhibited the ability of high concentrations of hSAP to inhibit fibrocyte differentiation (Fig. 30). The data indicate that NaCl, in addition to potentiating fibrocyte differentiation, influences how hSAP inhibits fibrocyte differentiation.

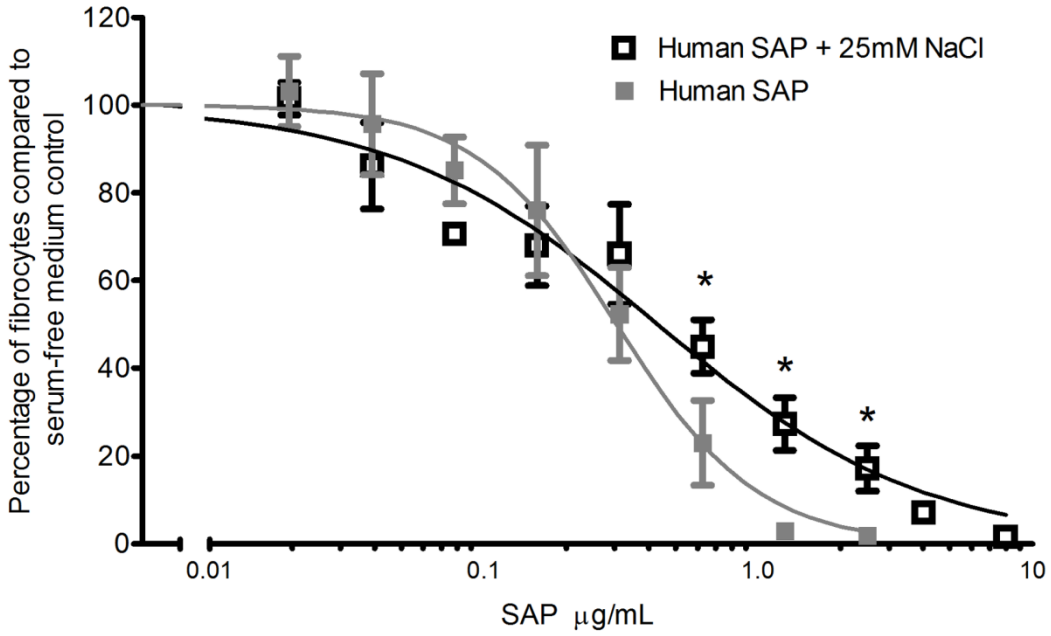

Figure 30: NaCl interferes with the ability of hSAP to inhibit fibrocyte differentiation.
PBMCs were incubated with or without additional 25 mM NaCl with the indicated concentrations of human SAP (hSAP). After 5 days, fibrocytes were counted. Values are mean ± SEM, n=5. * indicates $p < 0.05$ compared to SAP alone control (dashed line) by ANOVA. The absence of error bars indicate that error was smaller than the plot symbol. Lines are sigmoidal dose-response curves with variable Hill coefficient fit to the data.

Discussion

Monocyte-derived fibrocytes are found in fibrotic lesions, skin wounds, and tumors (45, 47, 81, 82, 136, 169-171). We have shown here that the differentiation of human monocytes into fibrocytes in serum-free culture is potentiated by NaCl. This increase appears to be a direct effect of NaCl on monocytes. In patients with long-term elevated salt intake, there is a 5% increase in serum NaCl, raising [Na^+] from 137 mM to 144 mM (161). In addition, food intake increases the blood sodium chloride level for ~4 hours (172). We observed that 155 mM [Na^+] and 130 [Cl-] potentiates fibrocyte differentiation, and we hypothesize that this [Na^+] and [Cl-] concentration could occur in the serum or tissues of some individuals, at least for a few hours after eating a high-salt meal. However short, this transient increase could be sufficient to increase fibrocyte differentiation.

In animal models and humans, increasing the extracellular osmolarity suppresses neutrophil functions such as cellular cytotoxicity and migration (173, 174). In addition, when tested on PBMCs *in vitro*, high salt increases the secretion of the pro-inflammatory cytokines IL-8 and TNF-α (175-177). These studies indicate that extracellular osmolarity can affect cells of the immune system. The increase in fibrocyte differentiation in response to increased NaCl could thus be due to increased osmolarity. However, we observed that adding up to 50 mM sodium gluconate or monosodium glutamate to the medium, which would also increase osmolarity, did not affect fibrocyte differentiation. Alternatively, an increase in cell proliferation as the result of additional NaCl could explain the increase in fibrocyte count. However, previous studies on the proliferation of

fibrocytes and fibrocyte precursors revealed no appreciable proliferation (51). Thus, the observed increase in fibrocyte differentiation is probably not related to the medium osmolarity or cell proliferation in our *in vitro* assay and most likely involves a direct effect of NaCl on monocytes.

When monocytes are activated following their recruitment into the tissue and adhesion to extracellular matrices, they undergo changes in gene expression and receptor levels (163, 178, 179). Following adhesion, monocytes are activated through a series of intracellular signaling events. We found that NaCl was most effective at increasing fibrocyte differentiation during monocyte adhesion. This was not accompanied by any changes in the expression of adhesion molecules CD11a, CD11b, CD11c, CD18, CD31, CD49d, and CD62L. In agreement with this, the additional NaCl did not influence the adhesive properties of monocytes to plasma fibronectin, collagen I, or un-coated tissue culture plates. Membrane potential and ion transport affect the activation of the monocyte-derived cell line THP-1 (158). It is thus possible that the effect of NaCl on fibrocyte differentiation is largely due to the increased NaCl affecting membrane potential and ion transport during the adhesion stage of monocyte activation.

Ion channels, especially chloride channels, appear to affect cellular activation and differentiation. In osteoblasts, the chloride channel ClC-3 regulates osteo-differentiation (180). The development and differentiation of keratinocytes is regulated in part by calcium-gated chloride channels (181). We observed that sodium nitrate but not sodium gluconate potentiated fibrocyte differentiation. Nitrate can pass through chloride channels, while gluconate cannot (164, 167). Combined with the observation

that KCl potentates fibrocyte differentiation, this suggests that chloride ions might play a role in the NaCl-induced potentiation of fibrocyte differentiation.

Monocyte activation and the subsequent differentiation into fibrocyte is influenced by variety factors such as SAP, M-CSF, GM-CSF, IL-4, IL-13 and, TGF-β1 (51, 54, 138). These regulators of the immune system each use distinct and sometimes overlapping signaling transduction pathways making it difficult to identify the exact pathway responsible for the NaCl-induced increase in fibrocyte formation.

Excessive intake of NaCl has been associated with high blood pressure, stroke, heart disease, and kidney disease (147, 148, 182, 183). The correlation between high salt intake and these diseases has generally been attributed to high blood pressure (148). However, studies in rats have questioned this correlation (149, 150). In addition, two independent studies on cohorts of patients with high salt intake and fibrosis showed a connection between these two factors that was independent of high blood pressure (156, 157). Here we have shown that fibrocyte differentiation can be potentiated by increasing extracellular NaCl levels *in vitro*. An intriguing possibility is that the link between high sodium chloride intake and fibrosis involves NaCl potentiating fibrocyte differentiation.

In addition to participating in fibrosis, fibrocytes participate in wound healing (45, 55, 81). Our observations suggest that having ~155 mM [Na^+] and ~ 130 mM [Cl^-] in wound dressings could not only potentiate fibrocyte differentiation but also influence the ability of hSAP to inhibit fibrocyte differentiation, and thus potentiate wound healing.

APPENDIX II

SUPPLEMENTAL FIGURES

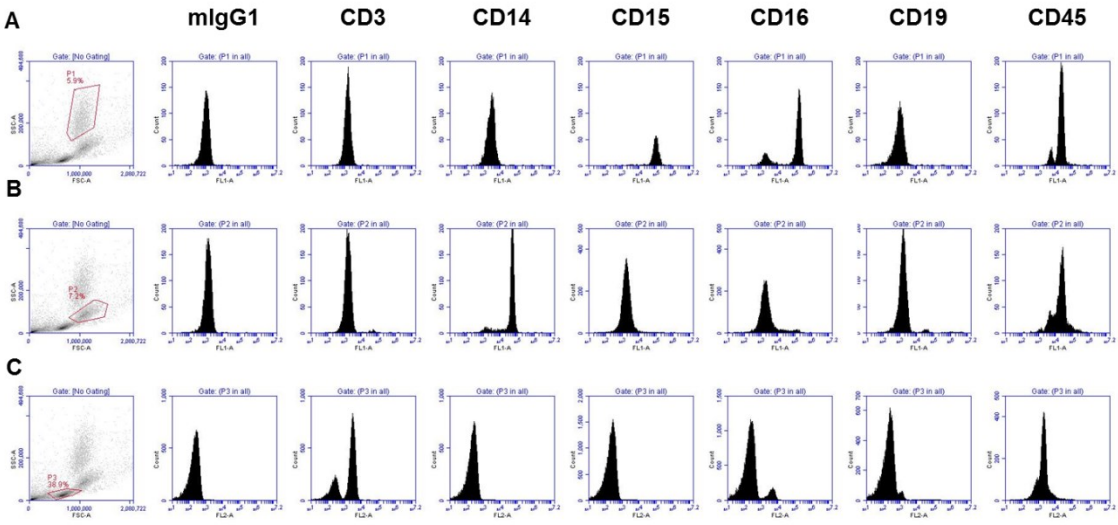

Figure S 1: Identification of neutrophils, monocytes, and lymphocytes.
Peripheral blood cells were isolated by density centrifugation and then stained for CD3, CD14, CD15, CD16, CD19, and CD45. Mouse IgG1 was used as the isotype control. Plots are representative of 3 independent experiments. Following staining, the cells were subjected to flow cytometry. (A) Neutrophils were positive for CD15, CD16, and CD45, (B) monocytes were positive for CD14, CD45, and some for CD16. (C) ~65-78% of lymphocytes were positive for CD3, ~5-10% for CD16, ~3-8% for CD19, and all for CD45. The cell distribution match previously published data.

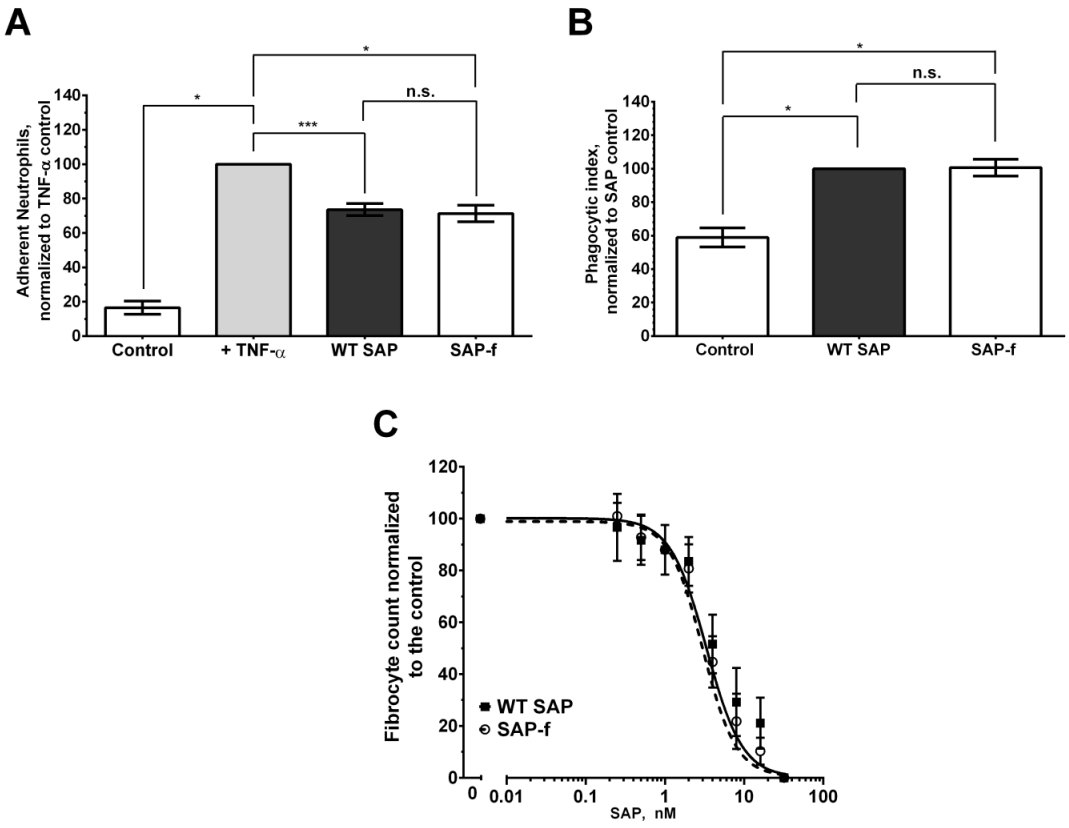

Figure S 2: Alexa Fluor 647-labeled SAP (SAP-f) has no detectable functional defects.

WT SAP was labeled with Alexa Fluor 647 and then tested for its effects on (**A**) neutrophil adhesion, (**B**) phagocytosis of Zymosan A, and (**C**) inhibition of fibrocyte differentiation. In (**C**) the data are fit to sigmoidal dose response curves with a variable Hill coefficient. Values are mean ± SEM, n=3. * represents $p<0.05$ and *** represents $p<0.001$ by t-test; n.s. indicates not significant. The absence of error bars indicates that the error was smaller than the line or plot symbol.

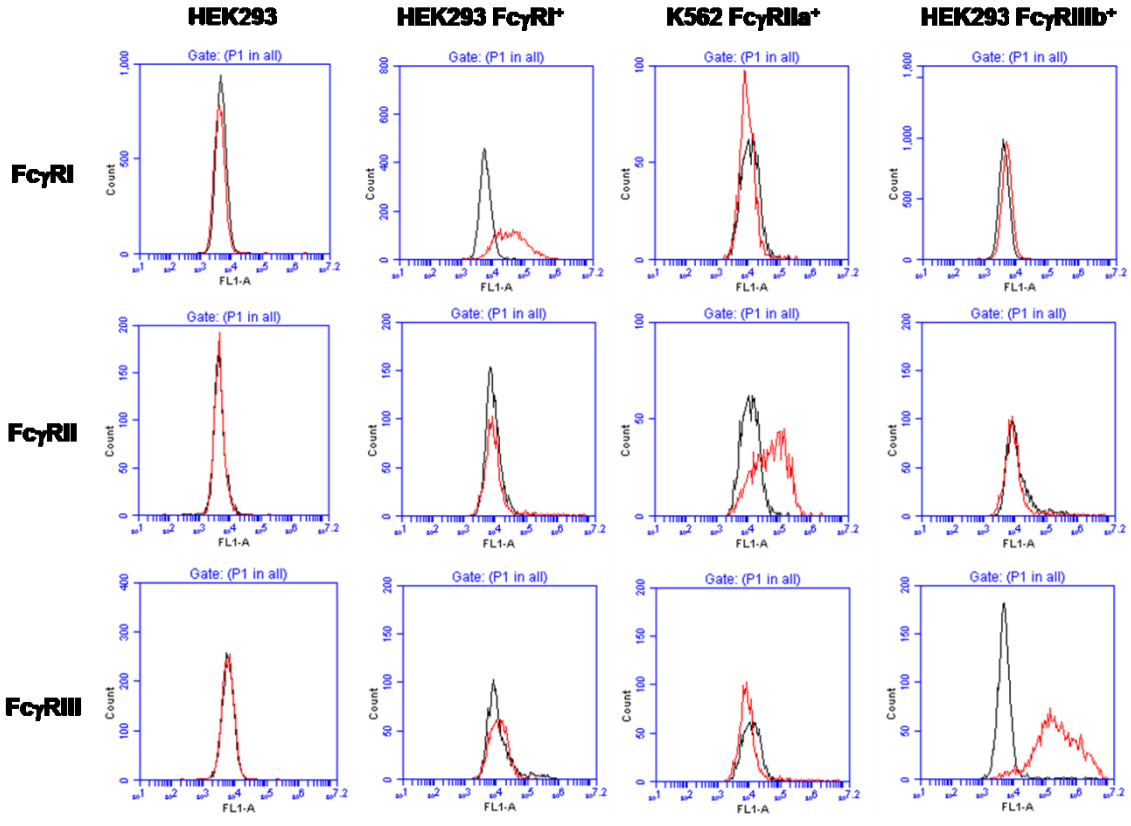

Figure S 3: The expression of Fcγ receptors on K562 cells and HEK293 cells. K562 cells, HEK293 or HEK293 cells expressing FcγRI or FcγRIIIb were gated on based on their forward scatter and side scatter characteristics and then stained for FcγRI, FcγRII, or FcγRIII. Staining was measured by flow cytometry. Mouse IgG1 (black line) was used as the isotype control for all the antibodies used (red line). Plots are representative of 3 independent experiments.

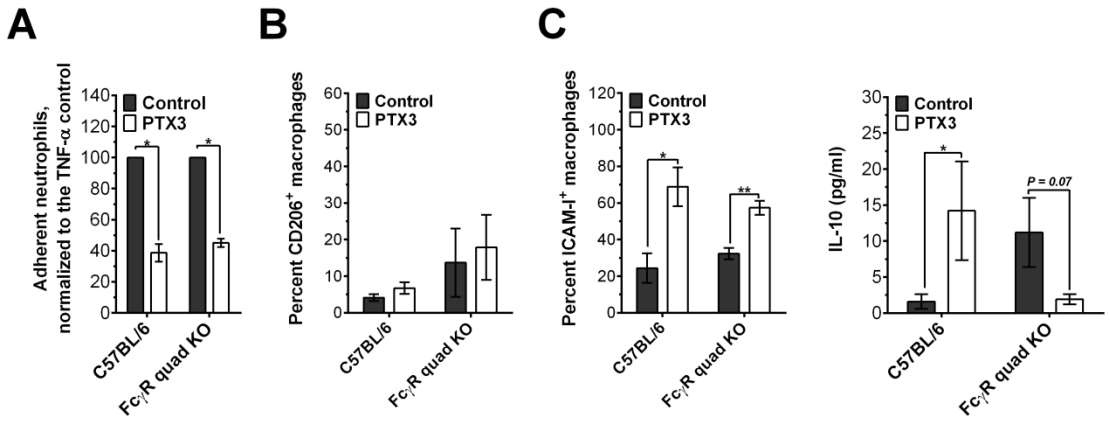

Figure S 4: Fcγ receptors are not necessary for some PTX3 effects on neutrophils and macrophages.

A) Mouse neutrophils were incubated with 0 (control) or 1 μg/ml of PTX3, transferred to a fibronectin-coated plate, and then activated with TNF-α. After 30 minutes, neutrophils bound to the plate were stained and counted, n=3. **B,C**) Mouse bone marrow-derived macrophages from C57BL/6 or FcγR deficient mice were polarized for 3 days in serum-free medium containing 0 (control) or 1 μg/ml of PTX3. Cells were then fixed and stained for CD206 and ICAM-1, n=3. **D**) C57BL/6 or FcγR deficient macrophages were polarized and then soluble IL-10 levels in supernatants were measured by ELISA, n=3. **P*<0.05,***P*<0.01 (*t*-test). (**A-D**) Values are ± SEM.

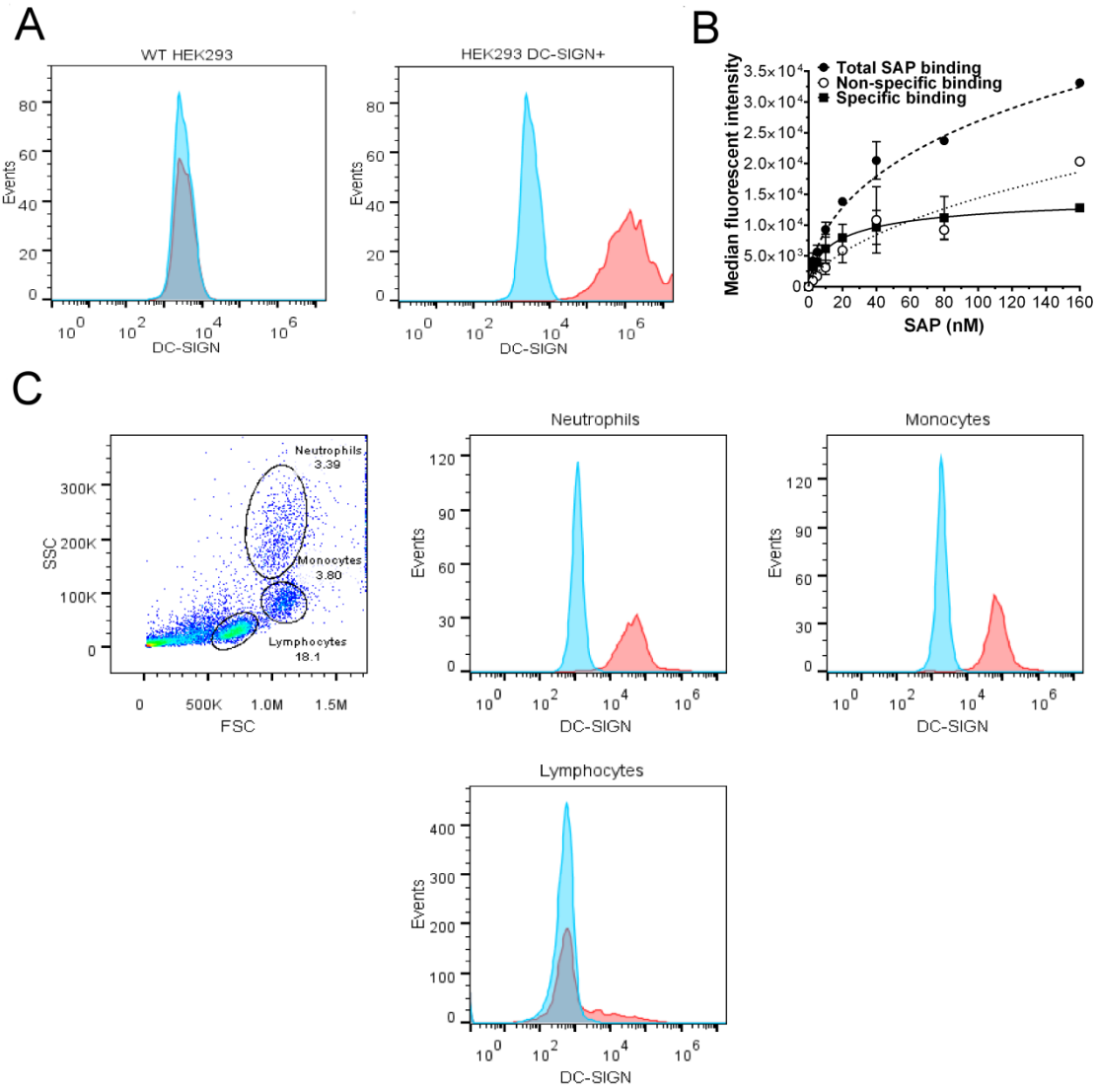

Figure S 5: SAP binding to DC-SIGN$^+$ HEK293 cells.
A) The expression of DC-SIGN (red line) on a) HEK293 cells and HEK293 cells expressing DC-SIGN was determined by flow cytometry. Mouse IgG1 (blue line) was used as the isotype control. Plots are representative of 3 independent experiments. **B**) HEK293 cells expressing DC-SIGN were incubated with fluorescently-labeled SAP. The cells were then washed and the binding of the labeled SAP to the cells was measured by flow cytometry. Mock transfected cells were used to estimate the non-specific binding, n=3. **C**) The expression of DC-SIGN (red) on human leukocytes was determined by flow cytometry. Plots are representative of 3 individual experiments. (**B**) Values are mean ± SEM. (**B**) Curves are fits to models of one-site binding with variable Hill coefficient.

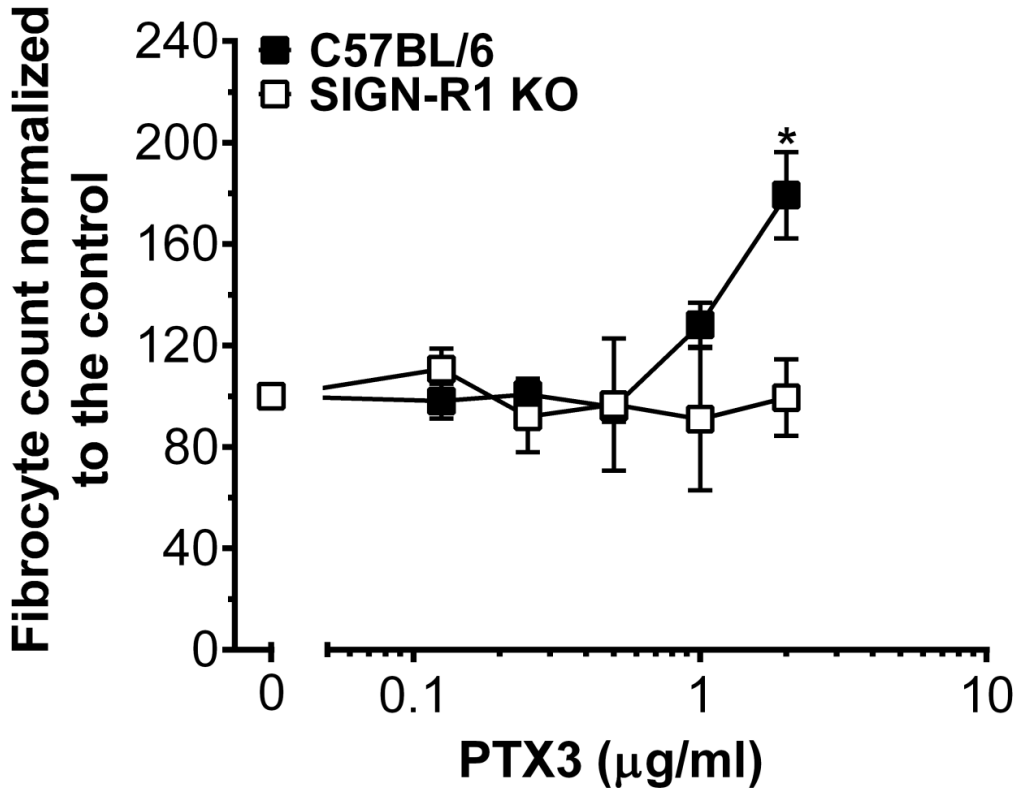

Figure S 6: SIGN-R1 is necessary for the effect of PTX3 on fibrocyte differentiation.

Spleen cells from SIGN-R1 null mice were incubated with the indicated concentrations of PTX3. After 5 days, cells were fixed, stained, and fibrocytes were counted, n=3. **P*<0.05 (*t*-test). Values are mean ± SEM.

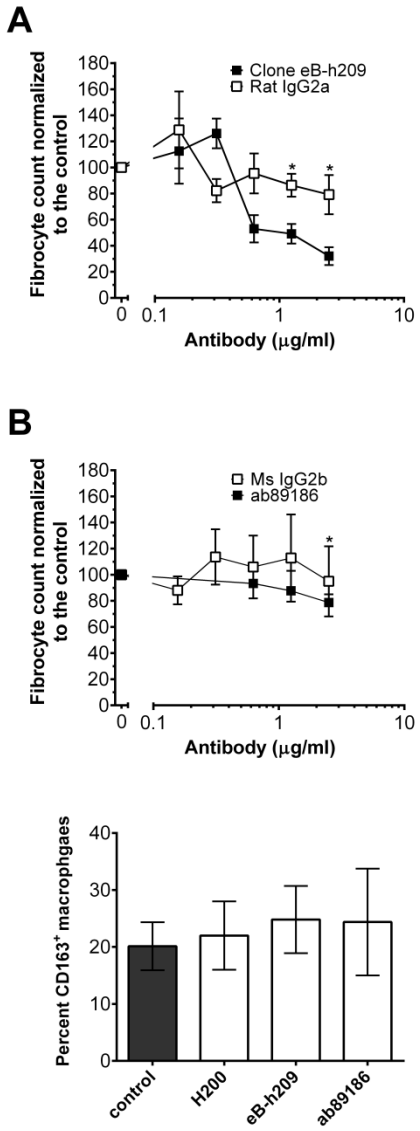

Figure S 7: The effect of anti-human DC-SIGN antibodies on fibrocyte differentiation and macrophage polarization.
A-B) Human PBMCs were incubated with the indicated concentrations of anti-DC-SIGN antibodies or isotype controls. After 5 days, fibrocytes were counted, n=3. **C**) Human monocyte-derived macrophages were polarized for 3 days in serum-free medium with 1 μg/ml of the indicated antibody. Macrophages were then fixed and stained for CD163, n=3. **P*<0.05 (*t*-test, relative to isotype control). (**A-C**) Values are mean ± SEM.

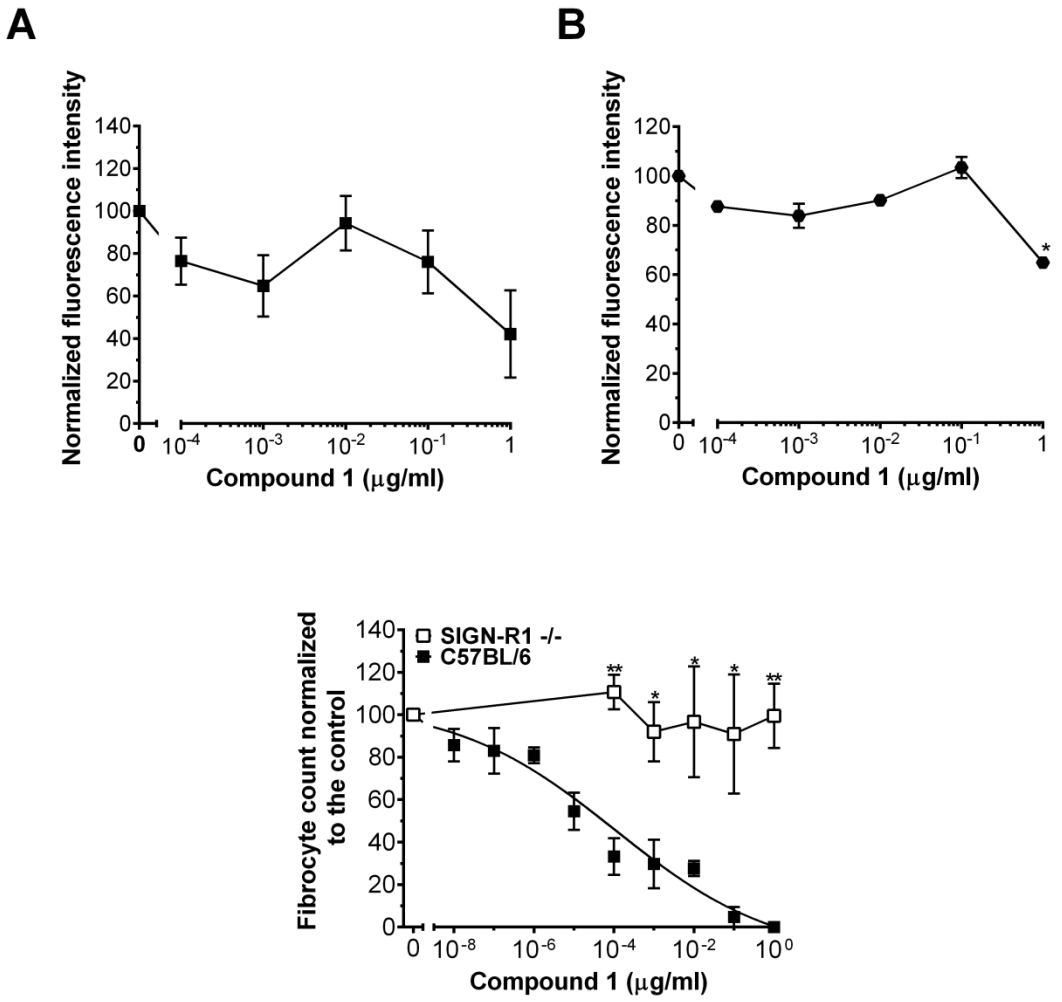

Figure S 8: Compound 1 inhibits fibrocyte differentiation through SIGN-R1 without causing extensive cell death.

A) Human PBMCs or **B**) C57Bl/6 mouse spleen cells were incubated with the indicated concentrations of compound 1. After 5 days, Alamar blue was used to estimate cell viability, n=3. **C**) Mouse spleen cells were incubated with increasing concentrations of compound 1. After 5 days, cells were fixed, stained, and fibrocytes were counted, n=4. Compound 1 inhibited murine fibrocyte differentiation with an IC_{50} of 91±47 pg/ml. **P*<0.05, ***P*<0.01 (*t*-test). (**A-C**) Values are mean ± SEM. (**C**) C57BL/6 data were fit to a sigmoidal dose response curve with a variable Hill coefficient.

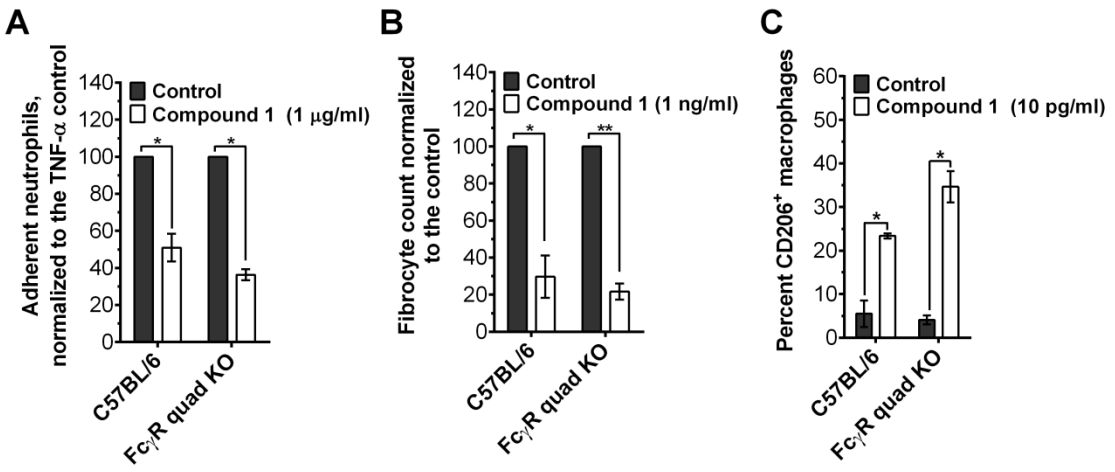

Figure S 9: Compound 1 inhibits neutrophil adhesion and fibrocyte differentiation and promotes M2 macrophages in absence of FcγR.

A) Mouse neutrophils were incubated with 0 (control) or 1 μg/ml of compound 1, transferred to a fibronectin coated plate, and then activated with TNF-α. After 30 minutes, neutrophils bound to the plate were stained and counted, n=3. **B**) Mouse spleen cells were incubated with 0 or 1 ng/ml of compound 1. After 5 days, cells were fixed, stained, and fibrocytes were counted. **C**) Murine bone marrow-derived macrophages were polarized for 3 days in serum-free medium containing 0 or 10 pg/ml of compound 1. Cells were then stained for CD206, n=3.*P<0.05, **P<0.01 (t-test). (**A-C**)Values are mean ± SEM.

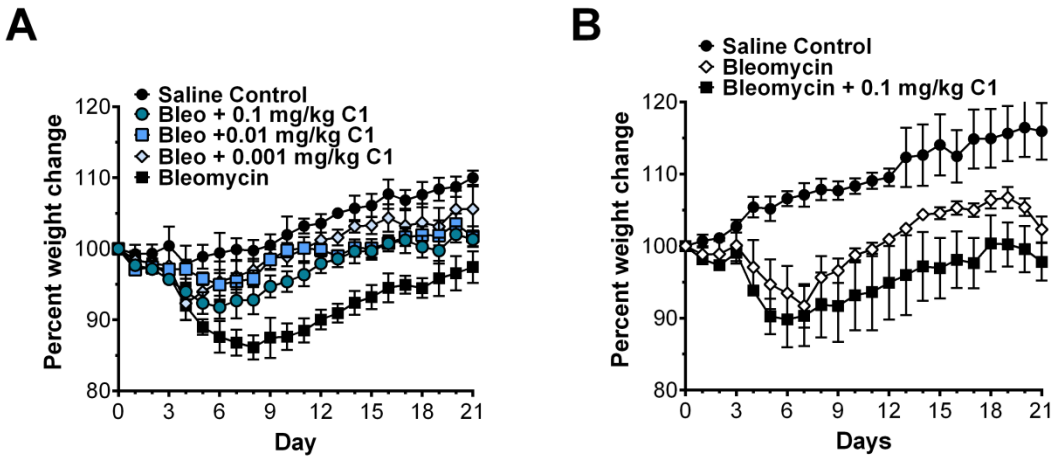

Figure S 10: The effect of compound 1 on mouse weights.
A) Mice in Figure 5 were weighed daily, n=3. **B**) IL-10 deficient mice were weighted daily, n=3. (**A-B**) Values are mean ± SEM.